UNIVERSITY OF SANNIO

Department of Science and Technology

Ph.D. candidate

Danijela D. Smiljanić

Surfactant modified natural zeolites as adsorbents for contaminants of emerging concern:

Non-Steroidal Anti-Inflammatory drugs

Ph.D. thesis in Science and Technology for Health and Environment

(XXXIII Cycle)

Tutor

Prof. Alessio Langella

Coordinator of the Doctorate

Prof. Francesco Maria Guadagno

Benevento, 2020

Acknowledgments

I am deeply grateful to Dr. Francesco Izzo for helping me accommodate when I have just arrived in Italy, and for many other technical issues, also for introducing me to the instrumental techniques in the Mineralogical laboratory. Next, I would like to thank Dr. Chiara Germinario and Prof. Celestino Grifa for all their help during the course of my Ph.D. study.

I would like to express my sincere gratitude to Prof. Mariano Mercurio for following my research, and for all help, insightful advice, and patience.

Additionally, I would like to express gratitude to Prof. Bruno de Gennaro for his treasured support which was influential in shaping my experiment methods and critiquing my results. I would also like to thank other members of DICMaPI for a pleasant time spent together in the lab.

I would like to thank Prof. George E. Rottinghaus and all the members of his laboratory. It is their kind help and support that have made my research and life in the USA a wonderful time.

I would like to offer my special thanks to Dr. Aleksandra Daković and her team for their useful comments and suggestions, as well as their assistance in the experimental research.

Last but not least, I am extremely grateful to my supervisor, Prof. Alessio Langella for his invaluable advice, continuous support, and patience during my Ph.D. study.

My appreciation also goes out to my family and friends for their encouragement and support all through my studies.

Abstract

In this study, composites of two zeolite-rich rocks were modified with cationic surfactants cetylpyridinium chloride (containing one hydrophobic tail) and Arquad® 2HT-75 (having two hydrophobic tails) and tested for the adsorption of contaminants of emerging concern – diclofenac, ibuprofen, naproxen, and ketoprofen.

Modifying a clinoptilolite- and phillipsite-rich tuffs with different amounts of selected surfactants resulted in the preparation of composites with monolayer or bilayer of each surfactant at zeolitic surfaces. Starting materials and prepared composites were characterized by ATR–FTIR and STA coupled with EGA. The point of the zero charge was determined for starting materials and composites, providing the information of materials surface properties and their buffering capacities. Zeta potential measurements confirmed that the negative charge of the natural zeolites was compensated and close to zero when surfactants formed monolayers at the zeolitic surface or reversed to positive when bilayers of surfactants are present at the zeolitic surface. Extensive washing of the composites and repeated zeta potential measurements have shown that surfactants were unstable at the zeolite surface, especially in bilayer formation. However, composites with bilayers prepared using the two-tailed surfactant Arquad® 2HT-75 had excellent stability. These results suggested that SMNZs could be tailored for safe applications for water treatment purposes.

The capabilities of the prepared sorbents to adsorb four drugs were estimated by the determination of adsorption isotherms and kinetic runs. Maximum adsorption capacities, obtained from the Langmuir model, were in the range from 1-35 mg/g, where the best results were achieved with composites containing bilayers of surfactants at the zeolitic surfaces. Physicochemical properties (pKa and log K_{ow}) of investigated drugs helped explain the mechanism of their adsorption by SMNZs. Between the two used zeolite-rich tuffs, composites prepared using clinoptilolite-rich tuff had the better performance. As far as the two surfactants are considered, composites with cetylpyridinium chloride gave better results. Using the best performing adsorbent, drug adsorption isotherms were conducted in the natural water collected from Grindstone creek (Columbia, Missouri, USA) to have a more realistic system.

Consequently, a slight decrease in diclofenac and ibuprofen adsorption was observed, while adsorption of NAP and KET was quite similar. Kinetic runs were performed in distilled water as well as in the presence of inorganic ions (sulfates and bicarbonates), and these interfering agents have caused an adsorption decrease for bilayer composites. For comparison reasons, kinetic runs for each drug were performed using activated carbon under similar experimental conditions. ATR-FTIR analysis and zeta potential measurements were performed on composites after adsorption of drugs, confirming the presence of drugs at zeolitic surfaces without any change of structures of composites.

Keywords

Surfactant modified natural zeolites (SMNZs), contaminants of emerging concern, diclofenac, ketoprofen, naproxen, ibuprofen, cationic surfactants, Arquad® 2HT-75, cetylpyridinium chloride, zeta potential, surfactant stability

Abbreviations

AC	Activated carbon
ACN	Acetonitrile
AOPs	Advanced Oxidation Processes
ARQ	Arquad® 2HT-75
ASA	Acetylsalicylic acid
ATR–FTIR	Attenuated Total Reflectance – Fourier Transform Infrared spectroscopy
BTEX group	Benzene, toluen, ethylbenzene and xylenes
C-A-B	Clinoptilolite-Arquad® 2HT-75-Bilayer
C-A-M	Clinoptilolite-Arquad® 2HT-75-Monolayer
C-C-B	Clinoptilolite-Cetylpyridinium chloride-Bilayer
C-C-M	Clinoptilolite-Cetylpyridinium chloride-Monolayer
CEC	Cationic Exchange Capacity
CoEC	Contaminants of Emerging Concern

CPyCl	Cetylpyridinium chloride
DCF	Diclofenac
DSC	Differential Scanning Calorimetry
ECEC	External Cationic Exchange Capacity
EGA	Evolved Gas Analysis
FDA	Food and Drug Administration
HDTMA	Hexadecyltrimethylammonium
HPLC	High-Performance Liquid Chromatography
IBU	Ibuprofen
ICP–OES	Inductively Coupled Plasma – Optical Emission Spectrometry
IZ CLI	Clinoptilolite-rich tuff
KET	Ketoprofen
NAP	Naproxen
NSAIDs	Non-Steroidal Anti-Inflammatory Drugs
NZs	Natural zeolites
ODTMA	Octadecyltrimethylammonium
PHIL75	Phillipsite-rich tuff
P-A-B	Phillipsite-Arquad® 2HT-75-Bilayer
P-A-M	Phillipsite-Arquad® 2HT-75-Monolayer
P-C-B	Phillipsite-Cetylpyridinium chloride-Bilayer
P-C-M	Phillipsite-Cetylpyridinium chloride-Monolayer
RE	Removal Efficiency
SA	Salicylic acid
SMNZs	Surface Modified Natural Zeolites
STA	Simultaneous Thermal Analysis
TG	Thermogravimetry

UV–VIS	Ultraviolet-Visible spectroscopy
WWTPs	Wastewater treatment plants

Table of Contents

1 Introduction

1.1 Contaminants of Emerging Concern

With industrial and technological development, the number of xenobiotic molecules present in the environment has drastically increased. More than 100,000 chemicals have been registered in the European Union, with an estimate that about 30,000-70,000 are in daily use (Loos et al., 2009). With still not well-known effects on the environment, these numerous potential contaminants are commonly called Emerging Contaminants or Contaminants of Emerging Concern (Loos et al., 2013; Petrovic et al., 2004). Sauvé and Desrosiers (2014), in the review article, recommended differentiation between these two terms considering as Emerging Contaminants only contaminants which have appeared recently and as Contaminants of Emerging Concern (CoEC) substances already present for a while in the environment but for which concerns have been raised recently (Sauvé and Desrosiers, 2014).

They have also given a definition of CoEC: *"as naturally occurring, manufactured or manmade chemicals or materials which have now been discovered or are suspected present in various environmental compartments and whose toxicity or persistence are likely to significantly alter the metabolism of a living being."* Also, the recommendation is that potential CoEC should remain "emerging" as long as there is no enough information in the scientific literature or until it is proven that is harmful or not (Sauvé and Desrosiers, 2014).

Within the CoEC, we include pharmaceuticals, steroid hormones, personal care products, pesticides, surfactants, fragrances, plasticizers, flame retardants, nanoparticles, perfluoroalkyl compounds, algal toxins, various trace elements such as rare earths and radionuclides, etc.

The development of analytical techniques has also improved the ability to detect a wide range of these compounds at low concentrations. Especially concerning are human or veterinary pharmaceuticals present in surface waters (Loos et al., 2013, 2010, 2009; Sousa et al., 2018). Since water is needed for all living beings, it is crucial to understand the impact of CoEC on water quality; thus, in 2000 European Union published the Water Framework Directive (WFD/2000/60/EC), suggesting several strategies against water pollution (Sousa et al., 2018; Tiedeken et al., 2017). One of the strategies was the formation of the first Watch Lists of substances for Union-wide monitoring (2008) with three substances: diclofenac (DCF), 17-α-ethinylestradiol, 17-β-estradiol. In 2015, this list was updated (the second Watch List) with the

addition of the following molecules: 2,6-di-tert-butyl-4-methylphenol, 2-ethylhexyl 4-methoxycinnamate, macrolide antibiotics (erythromycin, clarithromycin, azithromycin), methiocarb, neonicotinoids (imidacloprid, acetamiprid, etc.). This measure has increased scientific interest in these compounds and, consequently, the number of published papers concerning their monitoring and possible negative effects.

As another countermeasure, the Network of reference laboratories, research centers, and related organizations for monitoring of emerging environmental substances (called NORMAN) was established to improve the exchange of information on emerging environmental substances between research teams from different countries and encourages the validation and harmonization of measurement methods and monitoring tools.

1.1.1 Pharmaceuticals as Contaminants of Emerging Concern

Pharmaceuticals, although being consumed for much longer, have emerged as CoEC only in the last two or three decades. Because of massive consumption, these contaminants have found different pathways into the water (non-treated effluents from pharmaceutical industry and hospitals, non-regular disposal of drugs from households, excretion of drugs and their metabolites – through urine and feces) (Płuciennik-Koropczuk, 2015; Rivera-Utrilla et al., 2013; Tiedeken et al., 2017; Vieno and Sillanpää, 2014). Probably the most important sources of pharmaceuticals are effluents from traditional wastewater treatment plants (WWTPs), which are not specialized in their removal (Płuciennik-Koropczuk, 2015) (Fig. 1).

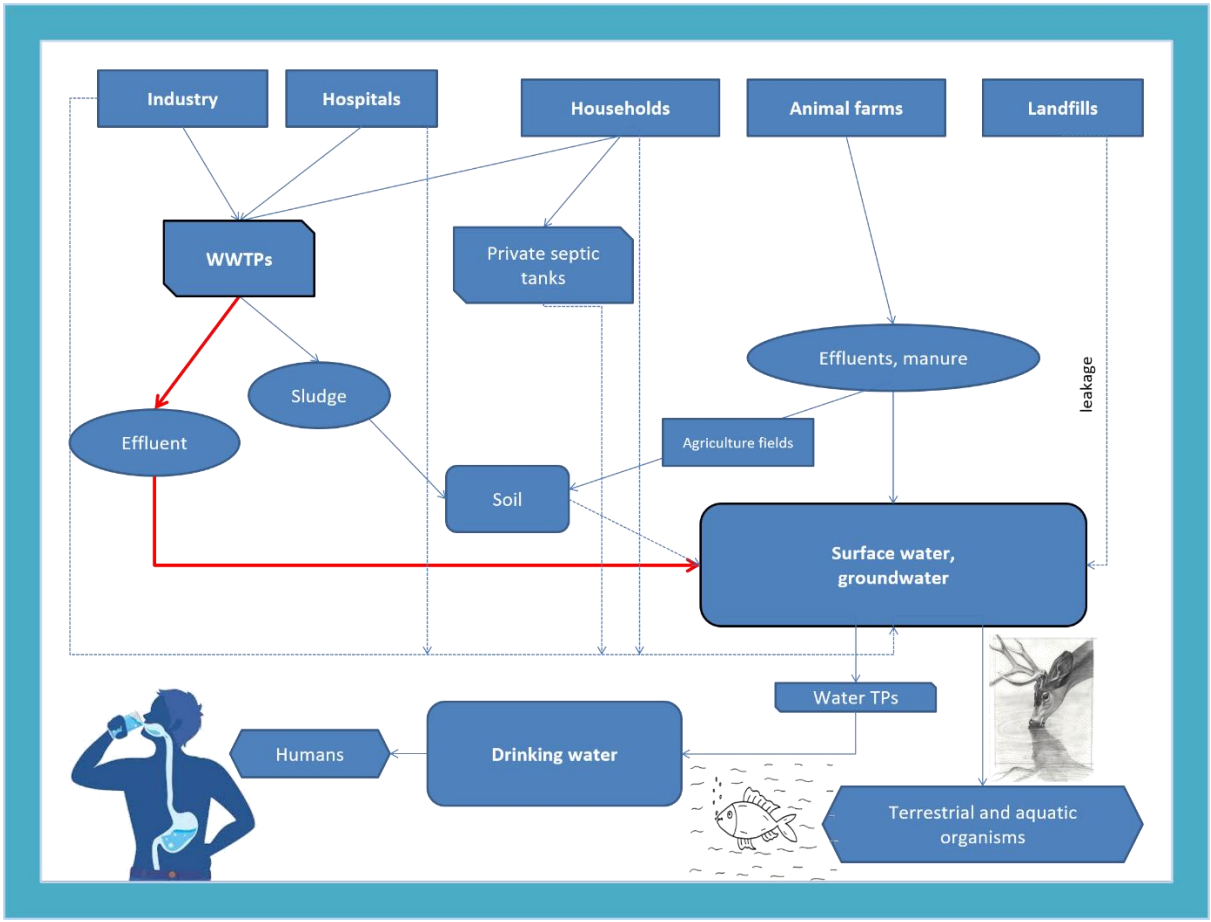

Fig. 1. *Possible pathways of CoEC, with specific attention on the wastewater treatment plants (WWTPs) effluents (poster presentation, Krakow,* Smiljanić et al., 2018).

Although acute toxicity of pharmaceuticals is not expected, chronic exposure can have negative consequences. For example, the presence of antibiotics in the environment can be a cause of bacteria resistance. Other examples are hormones, which can cause changes in the endocrine system even at very low concentrations (Cleuvers, 2004; Petrovic et al., 2004; Tiedeken et al., 2017). Several reviews and publications have shown that concentration of CoEC can vary drastically, from ng/L to µg/L, depending on the type of water (wastewater, surface water, groundwater, seawater, etc.), location of sampling, the season of the year, quality of wastewater treatment, development of a country, etc. (Bonnefille et al., 2018; Lolić et al., 2015; Loos et al., 2013, 2010, 2009; Sousa et al., 2018; Terzić et al., 2008; Yang et al., 2017).

1.1.1.1 Non-Steroidal Anti-Inflammatory Drugs - NSAIDs

Non-Steroidal Anti-Inflammatory Drugs (NSAIDs) are over-the-counter drugs used in the treatment of fever and different pain states (headache or toothache, rheumatic pain, etc.) (Burian and Geisslinger, 2005) that have found wide application in human and veterinary medicine and consequently are among the possible CoEC.

NSAIDs' mechanism of action is the inhibition of prostaglandin synthesis by inhibition of cyclooxygenase enzymes (COX-1 and/or COX-2). Prostaglandins are lipid compounds present in almost all tissues in a human and animal body, produced from arachidonic acid via cyclooxygenases (Ricciotti and Fitzgerald, 2011). They are made at the site where the cell is damaged and they promote inflammation that causes pain and fever. By inhibiting cyclooxygenase enzymes, NSAIDs inhibit the inflammatory response and, in this way, have analgesic and antipyretic properties.

COX-1 has a regulatory role in many physiological processes. For example, COX-1 is responsible for prostaglandins that protect stomach mucose from stomach acid, while COX-2 is connected only with inflammation (Zarghi and Arfaei, 2001). One of the classifications of NSAIDs is based on selectivity towards COX-1 and COX-2. Non-selective drugs inhibit both COX-1/COX-2 (acetylsalicylic acid, diclofenac, ibuprofen, ketoprofen, naproxen, indomethacin, etc.), but because of the inhibition of COX-1, these drugs can have adverse effects on the gastrointestinal tract (mostly in the stomach and upper duodenum), causing ulcers and ulcer perforations and bleeding erosions (Wongrakpanich et al., 2018).

Some of the COX-2 inhibiting drugs, popularly called coxibs, are celecoxib, rofecoxib, valdecoxib, etoricoxib, etc. (Sánchez-Borges et al., 2010). On the other side, non-selective NSAIDs can be further divided by the chemical structure:

- salicylates (acetylsalicylic acid);
- acetic acid derivatives (indomethacin, diclofenac, etc.);
- propanoic acid derivatives (ibuprofen, naproxen, ketoprofen, etc.);
- enolic acid derivatives - oxicams (piroxicam, meloxicam, etc.);
- anthranilic acid derivatives – fenamates (mefenamic acid, flufenamic acid, etc.);
- others (nimesulide, licofelone, etc.).

1.1.1.1.1 NSAIDs as Contaminants of Emerging Concern

NSAIDs are one of the most frequently detected pharmaceuticals in water (Gros et al., 2010; Loos et al., 2013; Yang et al., 2017). Being the largest group of over-the-counter drugs in the world (Sousa et al., 2018), it is hard to calculate actual annual consumption. Intercontinental Marketing Statistics (IMS) data collected from 86 countries showed that 1443±58 tons (only) of diclofenac (DCF) is annually consumed (Lonappan et al., 2016) and references therein). From now on, the focus will be only on four NSAIDs: **diclofenac (DCF), ibuprofen (IBU), naproxen (NAP), and ketoprofen (KET)**.

Diclofenac had caught worldwide attention as a contaminant in 2004 (Oaks et al., 2004) when it was discovered that its use for veterinary purposes had caused kidney failure and consequently a collapse of a population of three *Gyps vulture* species (Lonappan et al., 2016 and references therein). Therefore, DCF (together with two hormones) was placed on the first Watch List of CoEC (Directive 2013/39/EU (Article 8b)) to collect necessary information about them as potential pollutants and to suggest Environmental Quality Standards for them (Sousa et al., 2018).

Sousa et al. (2018) observed that other 28 organic contaminants, not listed in the EU legislation, are often monitored. Between them, NAP, KET, and IBU are some of the most frequently detected in rather high concentrations (Sousa et al., 2018). Detected concentrations of NSAIDs are dependent on several factors (especially the type of water body) and can vary from several ng/L (seawater) to even mg/L (effluents from the pharmaceutical industry) (Bonnefille et al., 2018; Coelho et al., 2010; Gros et al., 2010; Lolić et al., 2015; Loos et al., 2013, 2009; Płuciennik-Koropczuk, 2015; Terzić et al., 2008; Yang et al., 2017).

Acute effects of NSAIDs (DCF, IBU, NAP, and ASA) examined using biotests (on green alga and *Daphnia Magna*) have shown potential toxicity or no toxicity towards these organisms, with EC_{50} (half-maximal effective concentration – the concentration which causes a response halfway between the baseline and maximum) generally higher than 100 mg/L (only DCF had lower values), but in the case of *Daphnia Magna* experimentally measured mixture toxicity was higher than the predicted one (Cleuvers, 2004). According to the review of Bonnefille et al. (2018), prolonged exposure to DCF (even at concentrations in ng/L), depending on organisms studied and their growth stage, as a result, had various effects like the modification of critical biological functions (Bonnefille et al., 2018). Considering a possible increase in

toxicity of NSAIDs when they are mixed, but also the not well-known interaction with other pollutants, chronic exposure should not be easily disregarded.

Wastewater treatment plants (WWTPs) effluents represent major pharmaceuticals sources in the aquatic environment since many of them are not significantly removed in WWTPs and flow into receiving water bodies (Dordio et al., 2009; Rivera-Utrilla et al., 2013). Removal efficiencies (RE) of NSAIDs in WWTPs have shown a wide range of values even for the same drug, confirming that conventional WWTPs are not specialized enough in their removal (Gros et al., 2010; Lolić et al., 2015; Loos et al., 2013; Płuciennik-Koropczuk, 2015; Sousa et al., 2018; Tiedeken et al., 2017). Depending on the WWTPs examined, these usually consist of a primary (mechanical treatment and/or primary sludge) and a secondary (active sludge – biological) treatment; tertiary treatment (Advanced Oxidation Processes – AOPs, membrane techniques, adsorption of activated carbon and constructed wetlands), on the other hand, are rarely applied. Acidic pharmaceuticals, like NSAIDs, at neutral pH, are anions and thus not easily absorbed in the activated sludge and remain in the liquid phase (Bolong et al., 2009; Płuciennik-Koropczuk, 2015).

According to the data for the conventional WWTPs (primary and secondary treatment), Gros et al. (2010), reported ranges of removal efficiencies (REs) and average efficiency for NSAIDs: DCF (30-100%, 58%), KET (40-100%, 69%), IBU (65-100%, 91%); SA (82-99%, 96%), (Gros et al., 2010). Margot et al. (2013), in a pilot experiment, showed that removal efficiency of NSAIDs in conventional WWTP were 9±14 %, 57±46 %, 32±21 %, and 41±23 % for DCF, IBU, KET, and NAP, respectively, while tertiary treatment showed the higher efficiency (Margot et al., 2013). Although it is hard to compare REs between different WWTPs, this is in agreement with the literature concluding that DCF and KET are not easily removed from the water, while IBU is removed in higher percent (Coelho et al., 2010; Dordio et al., 2009; Lolić et al., 2015; Terzić et al., 2008; Tiedeken et al., 2017; Vieno and Sillanpää, 2014).

As a direct consequence of DCF being on the Watch Lists of CoEC, literature about this molecule rapidly increased and pointed that DCF is an especially persistent molecule. Diclofenac has shown low removal efficiency in secondary treatment (conventional activated sludge plants). In contrast, tertiary treatment gave promising results, especially AOPs (RE are 95-100%) (Tiedeken et al. (2017), and references therein). Still, the main drawback is the potential formation of equally or more toxic and persistent by-products. For diclofenac, 18 intermediates were identified in the process of ozonation, although the increase in toxicity was

not detected (Coelho et al., 2010). This problem can be solved with a combination of AOPs with adsorption techniques; in that case, the problem is the accumulation of DCF onto the adsorbent. These combined systems can be useful for all CoEC. An additional issue can be the formation of complexes between diclofenac and metals usually present in the polluted waters like Pb^{2+} (complex has antibacterial activity) or Cu^{2+} (complex can cleave DNA) (Lonappan et al., 2016), and references therein). Membrane techniques such as nanofiltration and reverse osmosis gave promising results, contrary to microfiltration and ultrafiltration. At the same time, constructed wetlands had poor removal efficiency for DCF (Tiedeken et al., 2017, and references therein).

Except for the unknown toxicity of produced intermediates, the additional drawback when using AOPs is that these processes are costly and operationally complex (Kyzas et al., 2015). Therefore physical technique, like adsorption, is the most promising due to its simple design, no toxicity, and low cost (Apreutesei et al., 2008; Kyzas et al., 2015). Reeve and Fallowfield (2018), in the review article, stated that *"the affordability of water treatment is an important consideration since water could be treated to the highest standards but be out of reach to certain segments of society, worsening health outcomes (WHO, 2008). Thus, any solutions that may reduce the cost of water treatment could play an important role in not only improving water quality itself but improving access to water treatment."* (Reeve and Fallowfield, 2018).

Concerning adsorbents, the essential property is their adsorption capacity and based on this, different materials (various types of activated carbons, clays, polymers, zeolites, composite materials) have been suggested for the removal of pharmaceuticals from water (Kyzas et al., 2015). Other parameters (pH, temperature and ionic strength of the solution, the concentration of pollutants, contact time, agitation speed) also play an important role in the adsorption process, making it impossible to compare the efficiency of two adsorbents, even for the same molecule, unless they are studied under the same conditions (Kyzas et al., 2015). Due to its high surface area and adsorption capacity, the most tested adsorbent is activated carbon, but it also has some limitations connected to the high costs for its production and regeneration, and that regeneration process itself is a source of pollution (Torabian et al., 2010). These problems encouraged the quest for new, readily available low-cost adsorbents (Apreutesei et al., 2008).

1.2 Natural zeolites and their modifications

1.2.1 Natural zeolites (NZ)

1.2.1.1 General properties

Natural zeolites, as main component of numerous volcanic tuffs, had been used since ancient times as dimensional blocks for buildings, as well as in pozzolanic cement. But as minerals, zeolites were discovered in 1756 by Alex Frederic Cronstedt, a Swedish mineralogist. The name zeolite is a combination of two Greek words ζέω meaning to boil and λίθος meaning stone. When heated, this stone was "boiling" because of the loss of water molecules from the zeolite structure (Mumpton, 1977). The next significant discoveries on zeolites were in the 1850s: their dehydration-rehydration behavior and ion exchange properties. In 1930 the first cristal structure was determined, and it was concluded that zeolites possess aluminosilicate frameworks with loosely bound alkaline, alkaline-earth cations, or both (Inglezakis and Zorpas, 2012).

Zeolites are defined as aluminosilicate minerals, with a three-dimensional framework consisting of SiO_4 and AlO_4 tetrahedra linked through shared oxygen atoms in a regular way, thus producing cavities and channels which can be occupied by cations, water molecules and/or small molecules (Inglezakis and Zorpas, 2012; Smith, 1984). Due to the three-dimensional structure and silicon: oxygen ratio of 1:2 (since all corners of tetrahedra are shared), zeolites, together with quartz, feldspars, and feldspathoids, belong to the group of tectosilicate minerals.

Zeolites can be represented by the empirical formula (Payra and Dutta, 2003):

$$M_{n/v}^{+v} \cdot \left[Si_{(1-n)}Al_n O_2\right] \cdot yH_2O \qquad \text{(Eq. 1)}$$

Extraframework cations — Aluminosilicate framework — Water molecules

and their structure can be derived into three components: the **aluminosilicate framework**, **interconnected void spaces in the framework** that contain **metal cations and water molecules** (Flanigen, 1977). In Formula (Eq. 1), the portion in square brackets represents the tetrahedral framework with an overall negative charge, which increases as the Si/Al ratio decreases (Passaglia and Sheppard, 2001). M^{+v} represents exchangeable cations (monovalent

and/or divalent, usually Na^{+}, K^{+}, Ca^{2+}, Mg^{2+}), necessary to compensate the negative charge that originates from the isomorphic substitution of Si^{4+} with Al^{3+} (the structural cations), and are placed inside of zeolite channels together with water molecules. The number of water molecules usually is not higher than half of the oxygen atoms in the framework (Pabalan and Bertetti, 2001).

The ratio Si/Al can vary but, according to Löwenstein's rule –Al–O–Al– linkages are not allowed; thus, the Si/Al ratio in zeolites must be at least ≥ 1, but it can go to ∞ (Inglezakis and Zorpas, 2012). The lower Si/Al ratio (more Si was substituted with Al) indicates that the zeolite framework is hydrophilic and "likes" metal cations. Usually, natural zeolites have a lower Si/Al ratio comparing to synthetic zeolites. Another property that depends on this ratio is thermal stability. The explanation for this is that Si – O bond is shorter (1.60 Å) than Al – O (1.75 Å); thus, more energy is needed to break this bond, and a higher Si/Al ratio (more Si – O bonds) indicates that the zeolite framework is stable at higher temperatures (Cruciani, 2006; Derouane and Fripiat, 1987). Zeolites with Si/Al > 3.80 are very stable upon heating, zeolites with Si/Al < 1.28 are always quite unstable, while the stability of zeolites with intermediate Si/Al range can`t be directly predicted from the Si/Al ratio (Cruciani, 2006).

Isomorphic substitution of Si with Al makes that the zeolitic framework has a net negative charge, which is compensated with extraframework cations, giving zeolites an ability to exchange ions. Extraframwork cations already present in the zeolite can be exchanged for more desirable cations (e.g., cationic surfactants) or cations that we want to remove from some systems (e.g., heavy metals).

Two parameters are used to quantify the ability of natural zeolite to exchange cations. The first one is Cationic Exchange Capacity (CEC) – the amount of cations that zeolite can exchange, which can be determined by using different methods (de Gennaro et al., 2007a; Langella et al., 2000). Usually, CEC is between 0.6 and 2.3 mEq/g (Wang and Peng, 2010). The second parameter is called External Cationic Exchange Capacity (ECEC) and determines the amount of cations that can be exchanged on the zeolitic surface. The procedure to determine this parameter involves the exchange of bigger organic cations that can't enter the internal channels – for example, t-butylammonium (Ming and Dixon, 1987) or cationic surfactants like hexadecyltrimethylammonium (HDTMA) (Cappelletti et al., 2017; Haggerty and Bowman, 1994). This parameter is of great importance when surface modifications of zeolites are

performed. In this work, clinoptilolite- and phillipsite-rich tuffs were used, and their detailed characterization is given in section 3.1.1.

1.2.1.2 Global production and some applications

Naturally occurring zeolites usually are not pure and contain accessory minerals (like quartz, feldspar, clays, carbonates, etc.); thus, whenever a high degree of uniformity and purity is required, synthetic zeolites are preferred. Since natural zeolites are easily exploited, and treatment costs are usually low, they are more applicable when there are enormous demands and fewer quality requirements (Inglezakis and Zorpas, 2012, chapter 5).

More than 50 natural zeolites are known so far. Clinoptilolite is the most used zeolite available in many parts of the world and in relatively large mineable sedimentary deposits of sufficiently high purity. Other abundant zeolites are mordenite, ferrierite, chabazite, erionite, phillipsite, and analcime (Sarioglu, 2005).

Because of previously mentioned properties, such as cation exchange capacity and an open framework with internal channels of specific sizes, natural zeolites can be used as **ion exchangers, adsorbents, and molecular sieves**. Some applications are: in water treatment processes (ammonia filters, removal of heavy metals and other cations from contaminated water), in pozzolanic cement, in agriculture, for odor control, as pet litters, in the livestock industry as food additives, etc. (Inglezakis and Zorpas, 2012, chapters 1 and 2).

Interestingly, 80% of natural zeolite consumption in the USA market goes on animal nutrition, pet litter, water purification, and odor control. A Brasilian zeolite company reported that their main uses are: pet food market (38%), replacement of phosphates in laundry washing powders – as water softeners (38%), and water treatment (15%) (Inglezakis and Zorpas, 2012, chapter 2 and references therein).

The estimated global production of natural zeolites in the world is 2.5 to 3 metric tons per year, and China, Jordan, the Republic of Korea, Japan, the USA, and Turkey are some of the biggest producers. The current goal is to increase the production and consumption of natural zeolites and to focus on products of high added value (Inglezakis and Zorpas, 2012, chapter 2 and references therein).

The price of zeolites depends on the cost of processing and ranges between $55 and $267 per metric ton. On the other hand, synthetic zeolites are much more expensive: detergent grade (from $500 to $600/t) and catalyst-grade (up to US $45/kg). Depending on the application, natural zeolites are differently processed and this determines their prices: lower for industrial and agricultural applications ($30 to $120 per ton, where price increases for the finer products) and higher for products used as pet litter and odor control ($0.50 to $4.50 per kg) ((Inglezakis and Zorpas, 2012), and references therein).

Natural zeolites as abundant, inexpensive, eco-friendly adsorbents, with high cation exchange capacity, physicochemical stability, and superior hydraulic characteristics, ability to modestly adjust the pH of the medium, were investigated for water treatment (Delkash et al., 2015; Lemić et al., 2007; Misaelides, 2011). Therefore their application for water remediation has been extensively studied, and it is a promising technique in environmental cleaning processes (Wang and Peng, 2010).

Natural zeolites were tested for: the adsorption of ammonium (review of Wang and Peng, 2010, and references therein), removal of heavy metal cations from different systems (wastewaters, acid mine drainage, contaminated soils, etc.) and their selectivity order (Erdem et al., 2004; Misaelides, 2011), removal of radioactive cations such as Cs^{+}, Sr^{2+} (after the Three Miles Island and Chernobyl nuclear accidents) and exploring regions rich in natural zeolites as possible nuclear waste storages (e.g., Yucca Mountains, USA). Another application is for the trace-gas separation, where clinoptilolite and chabazite have outperformed commercially available synthetics in N_2O removal from the air (Ackley et al., 2003).

If natural zeolites do not contain fibrous minerals, they may be considered harmless to humans and animals (Colella, 2011; Inglezakis and Zorpas, 2012; Krajišnik et al., 2018). High oral doses of clinoptilolite (up to 6000 mg/mouse) and exposure for a longer period have shown no toxicity (Krajišnik et al., 2018; Pavelić et al., 2000; Pavelić and Hadžija, 2003). For this reason, natural zeolites are investigated for applications in human and veterinary medicine as dietary additives, antibacterial, antiviral and antimicrobial agents, drug carriers, adjuvants in anticancer therapy, vaccine adjuvants, detoxicants, hypocholesterolemic agents, etc. (Andronikashvili et al., 2009; Colella, 2011).

Clinoptilolite incorporated in the swine, cattle, and poultry diets improved not only productivity but also reduced diarrhea, mortality, the incidence of stomach ulcers and pneumonia cases. The topical application of zeolite on skin injuries in horses and cattle

improved the healing process. Clinoptilolite treatment of mice and dogs with different tumor types led to the improvement in the overall health status, prolongation of the life-span, and decrease of the tumor size (Andronikashvili et al., 2009; Colella, 2011).

Natural zeolite application in gastroenterology is especially interesting since they have been studied as buffers to reduce stomach acidity and to treat stomach ulcers. Consequently, a natural zeolite-based commercial antidiarrheal drug – “Enterex” and food additive “Litovit” are available in Cuba (Andronikashvili et al., 2009). Natural zeolite enriched with Ag^{+}, Cu^{2+} or Zn^{2+} were effective against bacteria and some fungi (Colella (2011) and references therein).

However, these materials have a relevant drawback that somehow limits their applications, namely their low or no affinity for anionic species, as well as for low polar molecules. To overcome this limitation, zeolites can be modified with iron, cationic surfactants, chitosan, polymers, etc. (de Gennaro, 2018). The aspect concerning the modification of zeolites with cationic surfactants and their potential applications is of particular relevance to the purposes of the present research thesis; therefore, more information about these modifications will be given in Section 1.2.3.

1.2.2 Surfactants

The word SURFACTANTs is an abbreviation from SURFace ACTive AgeNTs. Surfactants are amphiphilic compounds with a hydrophilic part (polar group usually called "head") and a hydrophobic part (in most cases hydrocarbon chain, thus often called "tails"). Almost all human activity requires surfactants, and they are significant ingredients in many formulations and processes (Pletnev, 2001).

The amphiphilic properties are causing them to concentrate at interfaces and to aggregate into various supramolecular structures in solution (micelles, cylindrical rods, bilayers, etc.). Based on the polar group's nature, surfactants are classified into non-ionic (they have no charge in the predominant working range of pH-anionic and neutral) and ionic. Among ionic surfactants, anionic, cationic, and amphoteric (zwitterionic) types exist. Some of the properties of anionic surfactants are dispersing ability, high foaming, sensitivity to water hardness, and protein denaturation. Thus these surfactants are often called "detergents" to emphasize their importance in cleaning products. Amphoteric surfactants possess both anionic and cationic

charges and show pH-dependent amphoteric properties. If both anionic and cationic properties are independent of the pH, this specific group is called zwitterionic surfactants (Pletnev, 2001).

A cationic surfactant can dissociate in solution forming a surface-active cation and anion. Compared to anionic surfactants, cationic ones are not effective in cleaning and, therefore, are not used as detergents. Cationic surfactants have found application as bactericides, fungicides, herbicides, textile auxiliaries, fabric softeners, hair conditioners, antistatics, corrosion inhibitors, anticaking agents in fertilizers, flotation agents, precursors for the synthesis of other surfactants, etc. Special attention is paid to their use for the modification of zeolites and clays in order to obtain surfactant modified minerals (Bowman et al., 1995; Daković et al., 2007a; Haggerty and Bowman, 1994; Li et al., 1998a; Li and Bowman, 2001; Marković et al., 2017b; Schulze-Makuch et al., 2002). Quaternary ammonium compounds ("quaternaries") are the most significant class of cationic surfactants (around 90%). Their structure characteristic is to have at least one nitrogen atom covalently bonded to four alkyl/aryl substituents.

Cationic surfactants used in this thesis are cetylpyridinium chloride monohydrate and Arquad® 2HT-75 (di(hydrogenated tallow alkyl)dimethyl ammonium chloride). Both surfactants are quaternary ammonium compounds, and their structures are given in Fig. 2.

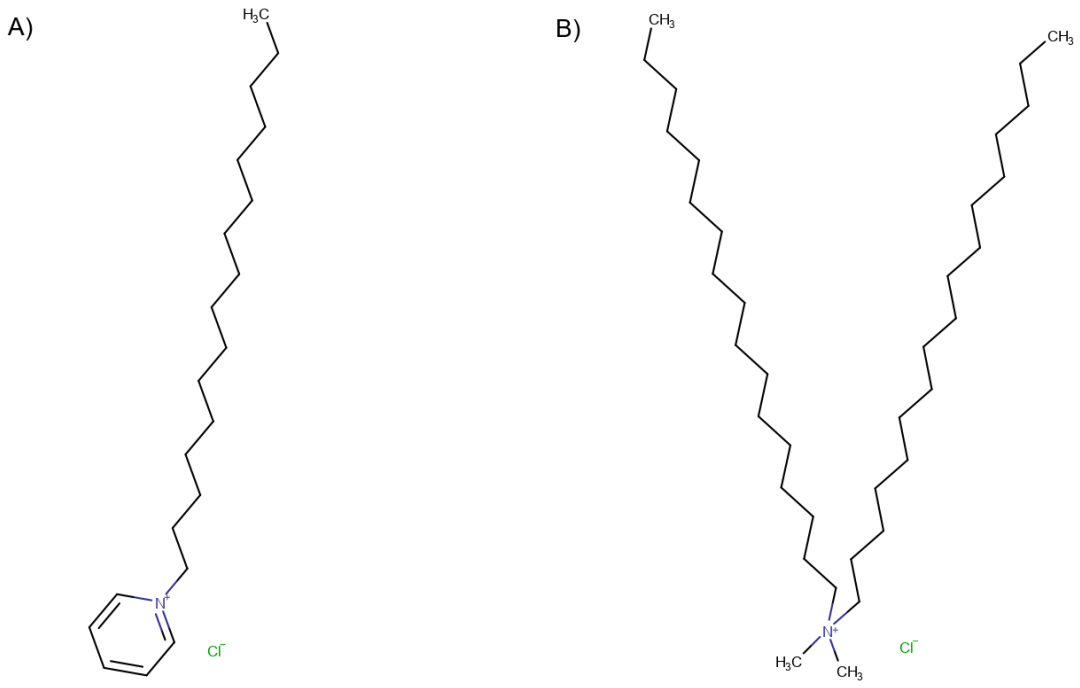

Fig. 2*. Structural formulas of A) Cetylpyridinium chloride; B) Arquad® 2HT-75 (Hydrocarbon chains were drawn with 18 C atoms. However, this surfactant is a mixture of surfactant with a*

chain length from 14-18 C atoms, with the highest percent of hydrophobic chains with 18 C atoms). Structures were drawn in the free software Marvin Sketch 20.1.

1.2.2.1 Cetylpyridinium chloride

Cetylpyridinium chloride monohydrate is a white crystalline solid, with formula $C_{21}H_{38}ClN\ H_2O$ (Fig. 2. A)). It is a secondary direct food additive permitted in food for human consumption approved by the U.S. FDA (2007) as an antimicrobial agent for surface treatment of raw poultry carcasses, at a level not exceeding 0.3 gram per pound of the carcass (FDA Web page, 2007). It is used in some mouthwashes, lozenges, toothpaste, throat/breath/nasal sprays, as an antiseptic for bacteria (especially effective against Gram-positive bacteria) (Rowe et al., 2006) and other microorganisms, to prevent dental plaque, to reduce gingivitis, and as an ingredient in certain pesticides (Bhattarai et al., 2013). The length of the hydrocarbon chain is around 20.93 Å, while the size pyridine head is 2.76 Å (Abezgauz et al., 2010). Additionally, log K_{ow} and solubility in water are 1.71 and 111 g/L (at 20˚C), respectively (Sigma-Aldrich CPyCl SDS, 2019). Its critical micellar concentration (CMC, a concentration above which supramolecular structures, like micelles, are formed) reported in the literature was around 0.8-0.9 mM (Bhattarai et al., 2013; Rowe et al., 2006) and it forms spherical micelles (Abezgauz et al., 2010). Reported LD_{50} (a lethal dose at which 50% of the test organism has died) for oral intake in rats and rabbits is 200 mg/kg and 400 mg/kg, respectively (Rowe et al., 2006), LC_{50} (a lethal concentration required to kill 50% of the test organism in a given time) for *Oncorhynchus mykiss* (rainbow trout) and *Cyprinus carpio* (carp) are 0.16 mg/L (96h) and, 0.01 mg/L (96h), respectively (CDH SDS, 2008; Jubilant SDS, 2012). EC_{50} for *Daphnia Magna* and *Selenastrum capricornutum* (algae) are 0.0041 mg/L (48h) and 0.0269 mg/L (72h), respectively (Jubilant SDS, 2012; Sigma-Aldrich CPyCl SDS, 2019). If the information given in section 1.1.1.1.1 about acute toxicity of NSAIDs is recalled – EC_{50} around 100 mg/L (bigger the value tested compound is less toxic), it is obvious that surfactant application for water treatment should be carefully approached.

1.2.2.2 Arquad® 2HT-75

Di(hydrogenated tallow alkyl)dimethyl ammonium chloride (DHTDMAC), commercially known as Arquad® 2HT-75 (the commercial name will be used through the thesis) is also a quaternary ammonium surfactant that has two long-hydrophobic chains on the one nitrogen atom (Fig. 2 B)). Arquad® 2HT-75 contains around 75% of active components (a mixture of surfactants with a different number of C atoms in the hydrocarbon chains: 14-18 carbons (James and Ogden, 1979) with the molar weight in the range 567-573.5 g/mol), around 15% of 2-propanol and 10% of water. This surfactant is used as a textile softener, conditioner, and dispersing agent, emulsifier, as a flocculant and antistatic agent. Some of the products in which this surfactant is present are inks and pigments, rinse aid, organoclays, paper chemicals, car rinse aid, textile and leather auxiliaries (Nouryon, 2020). Comparing to cetylpyridinium chloride, Arquad® 2HT-75 is in the form of a whitish paste and not soluble in the water, only dispersible. An interesting fact is that the type of supramolecular structure instead of the micelle is assumed to be bilayer (James and Ogden, 1979), or in the case of purified Arquad 2HT, the structure similar to multilayered liposomes (vesicles) characteristic of phospholipids (Okumura et al., 1983). These multilayered liposomes were visible under the transmission electron microscope (TEM) when the dispersion of 5 wt% of surfactant was used but also were present when further dilution to 0.1 wt% was performed. Again, the spherical liposome structure of multilayered bimolecular lamellas was present, but this time with a wider distance between lamellar layers (Okumura et al., 1983).

The use as softeners in the EU has been effectively discontinued due to concerns regarding slow biodegradation and potential effects on microbial processes during sewage treatment (Comber et al., 2008 and references therein). In the study of S.D.W. Comber et al. (2007), chronic toxicity of DODMAC (dimethyldioctadecylammonium chloride – the primary active component of DHTDMAC/Arquad® 2HT-75) was tested on several organisms, and their conclusion was that the overall tendency of DODMAC to bioaccumulate was low, which is in agreement with previous studies about DHTDMAC (Comber et al., 2008; Lewis and Wee, 1983). Reported LD_{50} for oral intake in rats was 5000 mg/kg, LC_{50} for fish 1 mg/L (96h), EC_{50} for *Daphnia Magna* was 0.35 mg/L (48h), and IC_{50} (half maximal inhibitory concentration) for algae was 0.012 mg/L (72h) (AkzoNobel SDS, 2009).

Both surfactants, in the respective material safety data sheets, are categorized (according to Regulation (EC) No 1272/2008) in H400 – very toxic to aquatic life. At the same time, Arquad® 2HT-75 also belongs to the category H410 – very toxic to aquatic life with long-lasting effects (Sigma-Aldrich ARQ SDS, 2019; Sigma-Aldrich CPyCl SDS, 2019). For this reason, in this thesis, the specific attention will be dedicated to surfactant stability at the zeolite surface.

1.2.3 Surfactant Modified Natural Zeolites – SMNZs

1.2.3.1 Preparation and general properties

Due to the hydrophilic surfaces (net negative charge of the framework) and hydrated inorganic cations, natural zeolites have no affinity for the adsorption of anionic species or hydrophobic molecules. Modification with cationic surfactants changes their surface, producing nanostructured composites well-known as Surfactant Modified Natural Zeolites (SMNZs) and enhancing adsorption of these molecules (de Gennaro et al., 2014; Esposito et al., 2015; Haggerty and Bowman, 1994; Sullivan et al., 1997). These modified zeolites in literature are also called Surface/Surfactant Modified Natural Zeolites or organozeolites. Although all terms are equally used, in this thesis, Surfactant Modified Natural Zeolites (SMNZs) will be preferred since it is more specific.

The net negative surface charge provides natural zeolites an affinity for adsorption of cationic species. Besides inorganic cations, adsorption of organic cations was also confirmed, but in this case, size of the zeolite channels is an important feature. Exchange of various alkyl ammonium cations was tested on Na-clinoptilolite (Barrer et al., 1967), and it was noticed that smaller molecules (like NH_4^+. $CH_3NH_3^+$, $(CH_3)_2NH_2^+$) could enter the 8- and 10-member rings (Table S1) and completely exchange Na^+ cations. In contrast, larger ions (i.e., tert-$C_4H_9NH_3^+$) remained at the zeolitic surface. Based on this, when zeolites are treated with long-chain cationic surfactants, these molecules could not enter the internal structure of the zeolite and surfactants can replace only cations at the zeolitic surface (up to ECEC value).

Different cationic surfactants were used for the modification of zeolite surface: hexadecyltrimethylammonium (HDTMA), octadecyltrimethylammonium (ODTMA),

cetylpyridinium (CPy), benzalkonium, etc. As counter anions for these surfactants, usually, chlorides and bromides are used (de Gennaro, 2018).

Depending on the amount of the surfactant used for the functionalization, it is possible to change the surface charge of the starting material from:

1. negative to neutral – monolayer formation (hemimicelle)
   This results in a hydrophobic surface due to the presence of hydrophobic surfactant tails. The amount of surfactant necessary for the preparation of complete monolayer corresponds to 100 % of the ECEC value of the starting material – zeolite.
2. negative to positive – bilayer formation (admicelle).
   As a result, the surface is hydrophilic (positively charged) due to the outer layer of cationic surfactant heads and has a hydrophobic organic phase made of intertwined surfactant tails. In this case, it is necessary to use the surfactant amount that corresponds to 200 % of ECEC of the starting zeolite.

Using the surfactant amounts below 100 % of ECEC will produce something like patchy monolayer, while the quantities between 100-200 % of ECEC will give patchy bilayer. When surfactants are present at the zeolitic surface, hydrophobic adsorbates can partition between hydrophobic surfactant tails. Simultaneously, patchy and complete bilayer will allow the adsorption of anionic species through ion exchange.

SMNZs have a possibility to be tailored, combining different natural zeolites and different cationic surfactants, for the specific application. As starting material, zeolite-rich rocks with a wide range of mineralogical compositions can be used. Consequently (due to different Si/Al ratios), cationic exchange capacity (CEC), external cationic exchange capacity (ECEC), hydrothermal stability, and hydrophobicity of the material can vary (Reeve and Fallowfield, 2018). An especially interesting research topic is the application of these adsorbents for environmental remediation.

Maintaining the cation exchange properties after modification, these nanocomposites of natural zeolites and surfactants may simultaneously remove different categories of pollutants: cations, anions, organic compounds (BETX – benzene, ethylbenzene, toluene and xylene – group, chlorophenol, perchloroethylene, dyes, pesticides, etc.) and even pathogens (Apreutesei et al., 2008; Hrenovic et al., 2008b; Reeve and Fallowfield, 2017; Wang and Peng, 2010).

The first SMNZs have appeared at the beginning of the 1990s following an idea previously successfully applied to clay minerals. Probably the most significant contributor and initiator of this modification is the scientific group from Socorro, New Mexico. Starting from 1994, they have performed a series of experiments and gradually suggested the mechanism of surface modification and a mechanism of adsorption of specific compounds by these modified minerals. Most of their experiments were performed on a clinoptilolite-rich tuff (74% of clinoptilolite). This starting material was modified with different amounts of hexadecyltrimethylammonium (HDTMA). In the following two sections, a short summary of their experiments will be given in order to explain the mechanism of the surface modification using surfactants and the adsorption mechanism of different types of adsorbates.

1.2.3.2 Formation of composites with monolayer and bilayer of surfactants

The effect of the surfactants` counterions was studied on clinoptilolite (100% ECEC value was around 100 mmol/kg) modified with the three surfactants that had the same cationic part - hexadecyltrimethylammonium (HDTMA) but different counter anions Br^-, Cl^- and HSO_4^-. The HDTMA sorption on the zeolite followed the trend HDTMA-Br > HDTMA-Cl > HDTMA-HSO_4, where Br^- has the smallest hydration sphere and could penetrate deeper into the Stern layer to neutralize the cationic head charge (Li and Bowman, 1997). The maximal amount of adsorbed HDTMA molecules was 208 mmol/kg (bilayer), 151 mmol/kg (patchy bilayer), and 132 mmol/kg (monolayer to patchy bilayer) for Br^-, Cl^-, HSO_4^- respectively. The conclusion of this work was that different surfactant counterions would affect the arrangement of HDTMA molecules, and in this way, the number of surfactant molecules adsorbed. To eliminate the influence of counterion, both surfactants used to modify natural zeolites in this thesis had chlorides as counterions.

Measurement of counterion concentration was used to distinguish the difference between monolayer (hemimicelle) sorption versus bilayer (admicelle) sorption, as the counterion should only be sorbed when bilayer is present at the zeolitic surface. The complete bilayer should have a ratio of sorbed surfactant to sorbed counterion around 0.5 (Li and Bowman, 1997; Sullivan et al., 1998a).

FT-Raman spectroscopy and Atomic Force Microscopy have shown that surfactant monomers and micelles are more disordered on the zeolite surface than in the solution. Additionally, the surfactant orientation on the zeolite surface will depend on the number of surfactant molecules, where the greater amounts will favor reducing disorder (Sullivan et al., 1998b, 1997).

Below critical micellar concentration (CMC), surfactant molecules exist as monomers in an aqueous solution; after this specific concentration is reached, surfactant monomers start to self-organize in the supramolecular structures – usually micelles. Modification of clinoptilolite-rich rock with HDTMA-Br was done under and above CMC, in amounts necessary to reach 50, 100, 150, and 200 mmol/kg. Above CMC, these loading levels were reached. However, below CMC, the actual loading levels were 50 mmol/kg. 68 mmol/kg, 82 mmol/kg and 89 mmol/kg. These results suggested that below CMC, monomers were not attaching on top of the first monolayer. On the other hand, above CMC, a mechanism was most likely based on the initial direct attachment of micelles to zeolite surfaces, suggesting that concentration above CMC is optimal for the bilayer preparation (Li et al., 1998a).

Finally, the conceptual model for the sorption of HDTMA onto clinoptilolite was suggested. For the monomer system (<CMC), the sorption below 100 % of the ECEC is in the form of individual monomers, which can differently interact with the surface, organize in patchy monolayer or even coil tail groups. If the amount of surfactant is increased, a monolayer is prepared (100% of ECEC). A further increase will lead to patchy bilayers (disperse admicelles). For the micellar system (>CMC) below the ECEC, sorption is in the form of admicelles that will later rearrange to a monolayer. Above the ECEC, micelles will form patchy bilayers or admicelles on the surface. At high loading levels, sorbed micelles are stable and give a complete bilayer (Sullivan et al., 1998a).

1.2.3.3 Adsorption mechanism

Series of experiments, including adsorption of chromates, have led to the definition of the adsorption mechanism of anionic species onto SMNZs with a suggestion that ion exchange with counterions dominates.

In the first experiments, was sorption of oxyanions (CrO_4^{2-}, SeO_4^{2-}, and SO_4^{2-}) onto prepared SMNZs (clinoptilolite-rich rock modified with HDTMA-Br) was studied. The stability of SMNZs has been tested: composites with surfactant amounts of 50% and 100% ECEC have shown that surfactant is irreversibly bound to zeolite surfaces. However, in the composite containing HDTMA in the amount of 200% ECEC, surfactant was easily removed from the surface. For this reason, the sorption of oxyanions was lower for 200% ECEC composite compared to 100% ECEC (Haggerty and Bowman, 1994).

After studying the influence of three different counterions (previously mentioned in section 1.2.3.2), prepared SMNZs were tested for the removal of chromates. The adsorption of chromates was following the order HDTMA-HSO_4 > HDTMA-Cl > HDTMA-Br. The simple explanation is that chromates will show the lowest exchange with the most stabile counterion – Br^- (Li and Bowman, 1997).

Bilayer composite was tested for the adsorption of nitrates and chromates from a binary mixture. Monovalent nitrates showed higher adsorption, most likely since they can be exchanged easier than chromates that require two cationic heads to balance the charge. Assuming that two divalent anions would have a similar sorption mechanism, a binary mixture of sulfates and chromates was used. An increase in sulfate concentration led to lower chromate sorption, especially for the highest sulfate concentration indicating that the two anions are competing for the same sorption sites (Li et al., 1998a).

The sorption of a non-polar hydrophobic organic compound – perchloroethylene (PCE) onto SMNZ was tested. Below monolayer, the PCE sorption coefficient onto the composite was proportional to the fractional organic carbon. However, above monolayer, the increase of PCE sorption coefficient was minimal. These results have suggested another adsorption mechanism – the PCE was partitioned between surfactant tails via hydrophobic interactions. When patchy bilayers or complete bilayers are formed, due to the hydrophobic bonding between surfactant molecules, the thickness of the bilayer is not double of monolayer thickness but less, resulting in a higher density of bilayer. The increased density reduced the partitioning of PCE, which has led to the conclusion that in the case of non-polar organic compounds, monolayer coverage is preferred (Li and Bowman, 1998).

The adsorption of non-ionic and ionizable organic compounds was also tested by SMNZs containing different amounts of surfactant (25-200 mmol/kg) (Li et al., 2000). The authors noticed that with the increase of surfactant loading above 100 % ECEC:

- adsorption of benzene (which was in neutral form at chosen pH) did not further increase. This confirms that partitioning is the main adsorption mechanism of neutral species like benzene, toluene, and xylene;
- adsorption of phenol (which was in the anionic form) increased due to additional ion exchange, previously confirmed as adsorption mechanism of inorganic anions;
- adsorption of aniline (which was in the cationic form) decreased due to the repulsion with positive cationic surfactant heads (Li et al., 2000).

This has led to the conclusion that SMNZs can be tailored for the specific target species/systems (knowing their pKa values) and solution characteristics (pH).

1.2.3.4 SMNZs applications and stability

Depending on the amount of the surfactant used for the functionalization, it is possible to change the surface chemistry of the starting material. When the monolayer is fully formed, the surface is hydrophobic and the surface charge is neutral, allowing the partition of hydrophobic molecules between hydrocarbon chains of the surfactant. In the case of a formed bilayer, the surface becomes again hydrophilic and has a positive charge and thus the ability to collect/adsorb anions and anionic molecules.

Among the possible applications of SMNZs, probably the most investigated are:

- removal of anionic species of metals such as chromates, selenates, arsenates, nitrates, perchlorates, etc. (Apreutesei et al., 2008; Bowman, 2003; de Gennaro, 2018; de Gennaro et al., 2020, 2014; Dimas Rivera et al., 2020; Haggerty and Bowman, 1994; Li et al., 1998a; Misaelides, 2011);
- removal of other organic water pollutants like BTEX group, bisphenol A, PCE, humic acid, dyes, bacteria, viruses, etc. (Bhatnagar and Sillanpää, 2017; J. Hrenovic et al., 2008; Li et al., 2014, 2000, 1999; Li and Bowman, 1998; Mirzaei et al., 2016; Schulze-Makuch et al., 2002; Zhan et al., 2011);
- adsorption of mycotoxins (Daković et al., 2007a, 2007b, 2005, 2003; Marković et al., 2017b; Tomašević-Čanović et al., 2003);

- as drug carriers for NSAIDs, doxorubicin, sulfamethoxazole, metronidazole, etc. (Cappelletti et al., 2017; Colella, 2011; de Gennaro et al., 2016; Izzo et al., 2019; Krajišnik et al., 2018, 2013b, 2011; Marković et al., 2016; Mercurio et al., 2018; Serri et al., 2016, 2017).

Even after functionalization SMNZs have great cation exchange capacity, opening the opportunity for simultaneous adsorption of different species: cations, anions, organic compounds, and even pathogens (Apreutesei et al., 2008; J. Hrenovic et al., 2008; Reeve and Fallowfield, 2018; Wang and Peng, 2010). This makes SMNZs very interesting adsorbents for environmental application.

The combination of the fact that SMNZs are extensively studied for water treatment purposes, as well as for pharmaceutical application, has led to the idea of using these adsorbents for the removal of NSAIDs as CoEC. Literature about the application of SMNZs for the removal of NSAIDs from water is rather scarce (Sun et al., 2017). Although experiments on the pharmaceutical application have confirmed the adsorption of NSAIDs onto SMNZs, for the application of these adsorbents for water treatment purposes, additional research is needed to understand the impact of complex matrixes (like wastewater) on the adsorption of the targeted drug, surfactant stability, and possible regeneration of used adsorbent.

Besides the ability of SMNZs to remove contaminants from water, a very important parameter is the long-term chemical and biological stability of these adsorbents. SMNZs with the bilayer formation have been reported to be especially unstable (Hrenovic et al., 2008a; Li et al., 1998b; Reeve and Fallowfield, 2017). The treatment of bilayer composite with 1 M CsCl has led to desorption of HDTMA and reduction of the surfactant amount to a monolayer coverage, while treatment with distilled water removed 10-15% of surfactant from this bilayer, probably due to the low ionic strength of the system that weakens the interaction between the cationic surfactant heads and the counterions (since the electric double layer expands). It was also concluded that the monolayer or the lower layer of the bilayer is held primarily via electrostatic forces, while the upper layer of the bilayer is held primarily via hydrophobic bonding and stabilized by counterions (Li et al., 1998b).

A surfactant leaching experiments (0.5 g of bilayer SMNZ in 50 mL of water) evidenced that hexadecyltrimethylammonium bromide (HDTMA-Br) was desorbing from the SMNZ surface. The final measured concentration of this surfactant in solution was 10^{-4} M (Reeve and

Fallowfield, 2017), which is significant when comparing to usual CoEC concentrations found in waters.

A review of Reeve et al. (2018) summarized that various studies confirmed surfactant desorption, especially when the bilayer was formed. It was also stated that when SNMZs are used in low-velocity conditions such as in permeable reactive barriers, desorption might not be an issue (Reeve and Fallowfield, 2018). To achieve better physicochemical stability of SMNZs, use of other surfactants, zeolites from different sources, and heat treatment were suggested (Bowman, 2003).

Additionally, the use of more eco-friendly cationic surfactants (like surfactants with two chains or Gemini surfactants prepared from natural amino acids and with cleavable ester bond) could open new possibilities for the application of these materials for environmental purposes (Pérez et al., 2014; Sarkar et al., 2010; Tehrani Bagha et al., 2007).

Another vital factor is the possible interference of other compounds present in wastewater and their adsorption instead of NSAIDs. The competition between anions was evident in the study on adsorption of chromates in the presence of sulfates and nitrates by clinoptilolite containing HDTMA-Br bilayer; when sulfates and nitrates reduced the adsorption of the target anion – chromate (Li et al., 1998a). Permeable membranes containing SMNZ removed viruses as the targeted species but also removed Br^- anions, again confirming that the targeted anion was not the only adsorbed species (Schulze-Makuch et al., 2002).

2 Aims of the work

Keeping in mind the significance of the water treatment, the main aim of this work is to investigate if specific SMNZs could be used as adsorbents to remove four NSAIDs – diclofenac, ketoprofen, ibuprofen, and naproxen considered as contaminants of emerging concern.

The main aim can be divided into smaller goals:

1) To prepare SMNZs by modifying the clinoptilolite- and phillipsite- rich rocks with Arquad® 2HT-75 (first time used for this purpose) or with commonly used cetylpyridinium chloride (for comparison reason). Clinoptilolite or phillipsite composites will be prepared with different amounts of each surfactant. Both surfactants have chlorides as counterions to eliminate the influence of counterion on the formation of SMNZs. ATR-FTIR analysis, STA with EGA, determination of pH_{pzc}, and measurements of zeta potential will be performed in order to characterize starting materials and composites. Additionally, the differences between these two surfactants (the number of hydrophobic tails attached to the cationic head – one for cetylpyridinium chloride, two for Arquad® 2HT-75) will be discussed, as well as how different amounts of surfactant are influencing the arrangments of surfactants into monolayer and bilayer at zeolitic surfaces.

2) To examine the stability of the surfactant molecules attached to the zeolite surface. For this purpose, zeta potential will be used as a parameter that will give information about the possible removal of surfactant molecules after extensive washing with distilled water.

3) To determine the adsorption capacities of prepared composites for the adsorption of diclofenac, ketoprofen, ibuprofen, and naproxen. Equilibrium and kinetic runs will be performed and mathematically modeled. The obtained results will be discussed depending on the type of zeolite, type and the amount of surfactant used for modification as well as on physicochemical properties of investigated drugs (pKa, and $\log K_{ow}$). ATR-FTIR and zeta potential measurements will be performed on composite+drug systems, collected after kinetic runs.

4) To estimate the influence of a more realistic medium on drug adsorption, the best performing adsorbent will be used to perform equilibrium runs in the Grindstone creek water (Columbia, MO). On the other hand, the influence of inorganic anions will be tested by adding the bicarbonates and sulfates in the batch system when performing kinetic runs.

5) Additionally, kinetic runs will be performed using the activated carbon as adsorbent (under similar experimental conditions), and the removal efficiency of each drug will be compared with the removal rates reached with SMNZs. This experiment aims to understand if the prepared composites can compete with a commercially most used adsorbent for water purification.

3 Materials and Methods

3.1 Materials

3.1.1 Clinoptilolite-rich tuff (IZ CLI) and phillipsite-rich tuff (PHIL75)

The geomaterials used in this study for the preparation of composites with surfactants were a phillipsite-rich tuff from Campanian region (Marano of Naples, Italy, trade name PHIL75) and a clinoptilolite-rich tuff from Eskişehir (Anatolia, Turkey, trade name IZ CLI), both commercialized in Italy from Italiana Zeoliti – CBC Group. Detailed mineralogical and chemical characterizations for the two materials were previously carried out (de Gennaro et al., 2007b, 2005; de Gennaro et al., 2009).

Clinoptilolite-rich tuff contained 79 wt% of clinoptilolite mineral, while phillipsite-rich tuff had 58 wt% of zeolitic content (44 wt%, 4 wt% and 10 wt% for phillipsite, chabazite and, analcime) (Table 1 a). Based on chemical composition (determined both on the single crystal (IZ CLI) and in bulk (PHIL75)), the Si/Al ratio was calculated to be 4.89 and 2.45 for IZ CLI and PHIL75, respectively (Table 1 b).

Table 1. a) *Mineralogical compositions of the investigated tuffs*

Starting material	**Mineral content (%)**							
	Phillipsite	*Chabazite*	*Analcime*	*Clinoptilolite*	*Quartz*	*Feldspar*	*Opal-CT*	*Smectite*
IZ CLI	*/*	*/*	*/*	*79*	*1*	*5*	*15*	*/*
PHIL75	*44*	*4*	*10*	*/*	*/*	*32*	*/*	*11*

Table 1. b) *Chemical compositions of the investigated tuffs*

Starting material	**Oxides (%)**										
	SiO_2	*Al_2O_3*	*TiO_2*	*Fe_2O_3*	*MnO*	*MgO*	*CaO*	*Na_2O*	*K_2O*	*P_2O_5*	*H_2O*
IZ CLI	*69.71*	*11.74*	*/*	*1.21*	*/*	*0.31*	*2.30*	*0.76*	*4.14*	*/*	*9.81*
PHIL75	*62.18*	*17.45*	*0.48*	*4.50*	*0.16*	*0.90*	*2.66*	*2.47*	*8.97*	*0.23*	*/*

3.1.2 Surfactants Arquad® 2HT-75 (ARQ) and cetylpyridinium chloride monohydrate (CPyCl)

For modification of the zeolitic surface, and based on obtained ECEC values for the two starting materials, two cationic surfactants were used in two different amounts 100% of ECEC (monolayer formation) and 200% of ECEC (bilayer formation). The first surfactant is cetylpyridinium chloride monohydrate (CPyCl) [CAS: 6004-24-6, M = 358.00 g/mol, Sigma Aldrich, assay: 98.0–102.0%] (Fig. 2 A)). Second surfactant was di(hydrogenated tallow) dimethylammonium chloride commercially known under the name Arquad® 2HT-75 (ARQ) [CAS:61789-80-8, M = 567–573 g/mol, Sigma Aldrich, assay: 98.0%] (Fig. 2 B))

3.1.3 Non-Steroidal Anti-Inflammatory Drugs (NSAIDs)

Non-Steroidal Anti-Inflammatory Drugs (NSAIDs) used in this study were: diclofenac sodium salt (DCF) (Fig. 3 a) [CAS:15307-79-6, Sigma Aldrich, ≥99.5%], ketoprofen (KET) (Fig. 3 b) [CAS: 22071-15-4, Sigma Aldrich, ≥98.0], ibuprofen sodium salt (IBU) (Fig. 3 c) [CAS: 31121-93-4, Sigma Aldrich, ≥98.0%] and naproxen sodium salt (NAP) (Fig. 3 d) [CAS: 26159-34-2, Sigma Aldrich, ≥98.0%]. Drug solutions for equilibrium experiments were prepared in phosphate buffer [CAS:7758-11-4, M = 174.18 g/mol, Fisher Chemical, ≥99.4%]. In kinetic runs, aimed at investigating the influence of inorganic anions, two salts were used: $MgSO_4$ x $7H_2O$ [CAS: 10034-99-8, M = 246,47 g/mol, Sigma Aldrich, ≥99.5%, pH = 5.87] and $NaHCO_3$ [CAS: 144-55-8, M = 84,01 g/mol, Sigma Aldrich, ≥99.7%, pH = 7.9].

Chemical structures of used drugs are given in Fig. 3, while some physicochemical properties are listed in Table 2.

Table 2. *Physicochemical properties of the investigated drugs*

NSAIDs	[1]M (g/mol)	[2]pKa	[2,4] log K_{ow}
Diclofenac sodium	318.13	[3]3.99; [4]4.24	4.51
Ketoprofen	254.28	[3]3.98; [4]4.07	3.12
Ibuprofen sodium	228.26	[3]4.42; [4]4.38	3.97
Naproxen sodium	252.24	[3]4.18; [4]4.15	3.18

[1]Sigma Aldrich Safety Data Sheets; [2]Turk Sekulic et al., 2019; [3]Avdeef et al., 2000; [4]Landry et al., 2015.

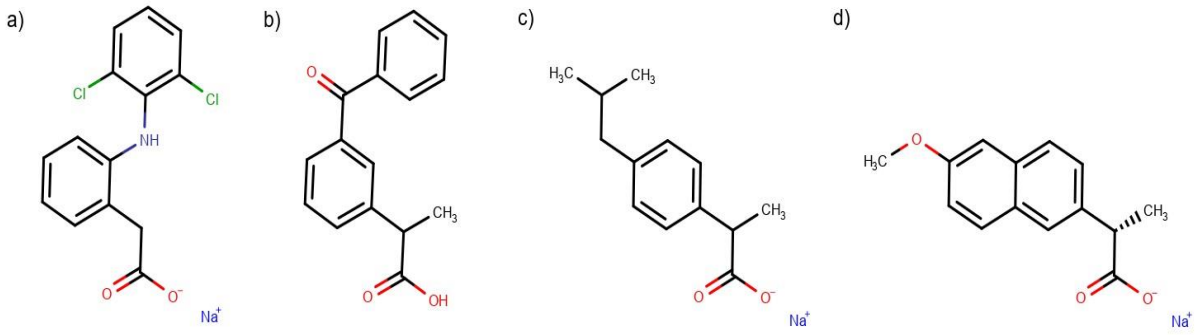

***Fig. 3**. Structural formulas of a) diclofenac sodium; b) ketoprofen; c) ibuprofen sodium, and d) naproxen sodium. Structures were drawn in the free software Marvin Sketch 20.1.*

3.2 Methods

3.2.1 External cationic exchange capacities (ECEC) determination

The external cationic exchange capacities (ECECs) were determined by treating 0.5 g of the starting material and 50 mL of surfactant solution (100 mM) under continuous stirring. The ECEC was measured using the modified Ming and Dixon method (Ming and Dixon, 1987), when instead of recommended t-butylammonium, a cationic surfactant: cetylpyridinium chloride (CPyCl) was used. This modification was in agreement with the literature where it was shown that both t-butylammonium and cationic surfactants are positively charged and too large to enter the internal zeolite structure and thus had the same result for ECEC (Haggerty and Bowman, 1994). All experiments were performed in triplicate. For five days, every 24 h the exhausted surfactant solution was replaced with a fresh one. Collected supernatants were analyzed for the exchanged cations (Na, K, Ca, and Mg) using ICP–OES (Perkin–Elmer Optima 2100 DV).

3.2.2 Functionalization of zeolite-rich tuffs

Surface modification of the starting materials was carried out by using the fast functionalization method previously reported in literature (de Gennaro et al., 2016). Combining two zeolite-rich tuffs (IZ CLI or PHIL75) with CPyCl or ARQ in amounts equal to 100% of ECEC value (monolayer formation) or 200 % of ECEC value (bilayer formation), eight composites were prepared. The suspensions of each zeolite-rich tuff and different concentrations of surfactants were prepared and mixed at 13,000 rpm using a high-speed dispenser (IKA T25 digital Ultra Turrax). The chosen solid-to-liquid ratio was 0.5 (100 g of zeolite-rich tuff and 200 mL of distilled water) with contact time between 30 min (monolayer composites) and 60 min (bilayer composites) due to different flow characteristics of the prepared systems. After the reaction time, the suspensions were filtered, washed with small amounts of distilled water, and air-dried at room temperature (25-30 ˚C).

Using IZ CLI as starting material, four composites were prepared: IZ CLI CPyCl monolayer (C-C-M); IZ CLI CPyCl bilayer (C-C-B); IZ CLI ARQ monolayer (C-A-M), and IZ CLI ARQ bilayer (C-A-B). Modifying PHIL75, the following composites were obtained: PHIL75 CPyCl monolayer (P-C-M); PHIL75 CPyCl bilayer (P-C-B); PHIL75 ARQ monolayer (P-A-M) and PHIL75 ARQ bilayer (P-A-B). For an easy overview, all composites are given in Table 3 with their detailed composition and respective abbreviations.

Table 3. *Surface modified natural zeolites used in this study as adsorbents*

Starting material	Surfactant	Surfactant amount	Abbreviation
IZ **C**LI	**C**etylpyridinium chloride	**M**onolayer	**C-C-M**
		Bilayer	**C-C-B**
	Arquad® 2HT-75	**M**onolayer	**C-A-M**
		Bilayer	**C-A-B**
PHIL75	**C**etylpyridinium chloride	**M**onolayer	**P-C-M**
		Bilayer	**P-C-B**
	Arquad® 2HT-75	**M**onolayer	**P-A-M**
		Bilayer	**P-A-B**

3.2.3 Characterization of NZ and SMNZs

3.2.3.1 Simultaneous Thermal Analysis

For simultaneous thermal analysis – STA (combined thermogravimetry – TG and Differential Scanning Calorimetry – DSC) NETZSCH STA 449 F3 Jupiter instrument was used. Experiments were carried out in alumina crucibles, in the temperature range 50-1100 ˚C with a heating rate of 10˚C/min in ultra-pure air (N_2/O_2 = 80/20) atmosphere (flow 100 mL/min). At the same time, Evolved Gases Analysis (EGA) was performed for starting materials and all composites (FTIR Bruker Tensor 27 instrument connected to STA device, 4000-600 cm^{-1}). Data were processed in Netzsch Proteus 6.1.0 (NETZSCH – Gerätebau GmbH) and Opus 7.2 software (Bruker Optik GmbH, Leipzig, Germany).

3.2.3.2 Attenuated Total Reflectance – Fourier Transform Infrared spectroscopy

Attenuated Total Reflectance – Fourier Transform Infrared (ATR–FTIR) spectroscopy was used to collect spectra of starting materials as well as composites in the spectral range 4000-400 cm^{-1} with resolution 2 cm^{-1} and 64 scans (Bruker Alpha; Opus 7.2 software – Bruker Optik GmbH, Leipzig, Germany).

3.2.3.3 Determination of the point of the zero charge

The point of the zero charge (pH_{pzc}) was determined for both starting materials (zeolite-rich tuffs) and all prepared composites according to the procedure given in the literature (Kragović et al., 2019). For each material, experiments were done using KNO_3, as an inert background electrolyte, at three different concentrations of 0.001 M, 0.01 M, and 0.1 M. Briefly, in 10 beakers, 50 mL of the 0.001 M KNO_3 was added, and the initial pH (pH_i) was adjusted in the range 1-12 by the addition of small amounts of either 0.1 M HNO_3 or 0.1 M KOH. The pH was measured on a pH/ion meter (Metrohm 781). After pH adjustment, the experiment was initiated by transferring each solution (10 different pH_i values) in 200 mL Erlenmeyer flasks containing 0.1 g of each zeolitic sample or composites. Flasks were shaken at 300 rpm for 24 h at room temperature (shaker Heidolph Unimax 1010), filtered using

qualitative very slow filter paper (LLG Labware, 7970267), and the final pH of each supernatant was measured (pH_f). The pH_{pzc} of the samples is represented by the plateau of the curve $pH_f = f(pH_i)$. The same procedure was repeated for the other two concentrations of KNO_3.

3.2.3.4 Zeta potential measurements and surfactant stability

The success of the surface modification was estimated using zeta potential measurement; additionally, this method was used to test surfactant stability on the zeolite surface. To remove any excess of surfactant and to check the stability of the products, 1.0 g of each composite was extensively washed with distilled water until chlorides were no longer detected. Absence of chlorides was confirmed with 0.1 M $AgNO_3$ solution [CAS: 7761-88-8, M = 169.87 g/mol, Merck, assay 98.0%]. Afterward, the zeta potentials of zeolite-rich tuffs and SMNZs before and after extensive washing were measured using a Zetasizer Nano ZS90, Malvern Instruments. Aqueous suspensions 0.1 mg/mL for each material were prepared, and the average value of 5 measurements was taken. Latex dispersion was used as a calibration standard.

3.2.4 Drug adsorption on SMNZs

3.2.4.1 Adsorption isotherms

Stock solutions (1000 mg/L) of DCF, KET, IBU, or NAP were prepared in methanol. Standard drug solutions were prepared by addition of appropriate amounts of methanolic stock solution of each drug to 0.01 M phosphate buffer solution adjusted at pH 6.5. This pH was chosen because the usually measured pH in WWTPs, is in the range 6-8; in addition, since the reported temperature in WWTPs is between 20 and 30 ˚C, experiments were carried out at room temperature (Çinar, 2005; Freitas et al., 2017; Zhao and Viraraghavan, 2004).

For the determination of adsorption isotherms, the initial drug concentrations were in the range of 2–100 mg/L. Experiments were done by mixing 5 mg of each SMNZ with 10 mL of each drug solution in 15 mL Falcon tubes. Each point has been made in duplicate. Falcon tubes were vortexed (to ensure maximal solid-liquid contact) and placed on a shaker for 60 min that,

according to literature, is the time sufficient to reach equilibrium (Krajišnik et al., 2011). After this period, tubes were centrifuged for 2 min at 3000 rpm, and the supernatant was collected in bullet tubes that were additionally centrifuged for 4 min at 13,500 rpm. Finally, 2 mL of each supernatant was transferred to HPLC autosample vials.

The experiments were performed using isocratic elution, at room temperature, with an injection volume of 20 µl and a flow rate of 1 mL/min. The mobile phase for the drugs was acetonitrile:water:acetic acid (ACN:H_2O:AA), at slightly different ratios in order to provide optimal retention times. For DCF and NAP (ACN:H_2O:AA) ratio was (50:50:0.2), for KET (45:55:0.2), while for IBU ratio was (55:45:0.2). The column was a Discovery® HS F5-5 (15 cm x 4.6 mm, Col:131403-05, BL: 7633, SUPELCO Analytical). HPLC analyses were performed on a Hitachi L-7100 pump with a Hitachi L-7200 autosampler, and UV detection with a Hitachi L-7400 UV spectrophotometer (λ=220 nm). Data were recorded and processed by Hitachi D-7000 data acquisition package with ConcertChrom software on a microcomputer.

3.2.4.1.1 Adsorption of NSAIDs in the Grindstone creek water

Adsorption of NSAIDs (DCF, KET, IBU, and NAP) by the adsorbent with the highest adsorption capacity was investigated on a real stream water sample from the Grindstone Nature Area in Columbia (Missouri, USA). The sample was filtered to remove visible impurities and then analyzed to confirm the absence of the peaks in the area of interest in chromatograms. Additionally, the pH was measured and was 7.1, while the chemical composition of the creek water remained unknown. The method used to determine NSAIDs` adsorption isotherms was the same as described in Section 3.2.4.1.

3.2.4.2 Kinetic runs

3.2.4.2.1 Kinetic runs performed in distilled water

Adsorption kinetic of drugs was studied by adding 0.5 g of each SMNZ to 1 L of DCF, KET, IBU, or NAP solution (C_0 = 20 mg/L) in distilled water (pH around 5), and followed over a time interval of 0-60 min. These suspensions were continuously mixed (around 500 rpm) at

room temperature, and pH was checked (pH meter Orion Star A211). At scheduled time intervals (2 min, 5 min, 10 min, 20 min, 30 min, 45 min, and 60 min), aliquots of the supernatant (5 mL) were withdrawn, microfiltered with HPLC filters (CHROMAFIL® Xtra CA – 20/25, 0.20 µm) and analyzed by UV-VIS (Spectrophotometer Shimadzu UV - 1900) with previously set calibration curves at λ = 275.5 nm, λ = 260 nm, λ = 221.7 nm and λ = 231.0 nm for DCF, KET, IBU and NAP, respectively.

3.2.4.2.2 The influence of inorganic anions on kinetic runs: the case of ibuprofen and naproxen

To study the possible influence of inorganic anions on the adsorption of drugs, kinetic experiments were also performed in salts solutions under the same conditions as described above (section 3.2.4.2.1). Two salts: $MgSO_4$ x $7H_2O$ and $NaHCO_3$, were used to provide the sulfate and bicarbonate anions. One gram of each salt was dissolved in 1 L of IBU or NAP solution (C_0 = 20 mg/L), and the experiment was initiated by adding 0.5 g of adsorbent. Kinetic runs were performed at a time interval of 0-60 min. At scheduled time intervals, 5 mL of IBU or NAP supernatant were withdrawn, microfiltered, and analyzed by UV-VIS.

3.2.4.2.3 Kinetic runs using competing adsorbent material – Activated Charcoal

For a better estimation of our composites, a comparison with commercial adsorbent – Activated Carbon/Charcoal (AC) (CAS:7440-44-0, Titolchimica) was made. Four kinetic runs were conducted in almost the same way as described in Section 3.2.4.2.1 using the same stock solutions, equipment, and initial concentrations. During each kinetic run, the pH value was frequently checked (pH meter Orion Star A211). Again, kinetic runs were conducted in batch conditions: 1 L of drug solution (initial concentration of 20 mg/L) and mixed with 0.25 g of AC. The amount of adsorbent was reduced from 0.5 g (used for SMNZ) to 0.25 g since preliminary experiments had shown that when 0.5 g of AC was used, kinetic runs were extremely fast, and the drug was completely removed after 2 min. Thus it was impossible to obtain a curve able to describe the adsorption performances of AC.

3.2.4.2.4 Characterization after adsorption: adsorbent+adsorbate systems

After kinetic runs, suspensions were filtered, and adsorbent+adsorbate systems were air-dried and stored. The zeta potential of these samples was measured under the same conditions as described in Section 3.2.3.4 and ATR-FTIR (Thermo Fisher Scientific 6700) was obtained for these systems and for pure crystalline NSAIDs in the range 4000-400 cm^{-1} and with the resolution of 2 cm^{-1} and 64 scans. Spectra were corrected (Omnic software) for the baseline and atmospheric influence (CO_2 and H_2O).

4 Results and Discussion

4.1 ECEC determination

The Cation Exchange Capacities (CEC) were previously evaluated using the Batch-Exchange Method (Cerri et al., 2002; Langella et al., 2003) and were 1.84 mEq/g and 2.44 mEq/g for IZ CLI and PHIL75, respectively (de Gennaro et al., 2007a, 2005). The ECEC of IZ CLI and PHIL75 was calculated as the average value of three measurements and is 0.09 mEq/g and 0.15 mEq/g, respectively.

The mass of surfactant necessary to prepare the clinoptilolite-monolayer is calculated by multiplying the ECEC value of clinoptilolite by the amount of clinoptilolite we want to modify and the molar mass of the surfactant (i.e., 358 g/mol for CPyCl). Thus, to modify 100 g of clinoptilolite-rich tuff by using CPyCl to get a monolayer coverage, it is necessary to use 3.222 g CPyCl; the double for a for bilayer coverage. The same applies to phillipsite-rich tuff and the other surfactant. The calculated surfactant mass divided by the amount of water used for the functionalization gives the concentration of surfactant at around 45 mM, which is above the critical micellar concentration (CMC) of CPyCl of around 0.9 mM (Bhattarai et al., 2013). For ARQ, CMC was not found, but supramolecular structures were confirmed at 0.1 wt%, again for preparation of SMNZs were used higher amounts of this surfactant. This corresponds to the conditions described in section 1.2.3.2 when the C > CMC, and the surfactant is attached to the surface in the micelle form, which benefits both monolayer and bilayer formation, especially the latter one. More information about prepared SMNZs will be given in the next section (4.2).

4.2 Characterization of NZs and SMNZs

4.2.1 Simultaneous Thermal Analysis

Thermal behavior of starting materials and SMNZs was investigated with STA (TG, DTG, and DSC) and EGA. The EGA plots (given in Supplementary material as Fig. S1) obtained for starting materials and composites were analyzed, as well as thermogravimetric curves and their derivative curves, and DSC curves in Figs. S2-S7. An example of a

threedimensional plot from EGA is given in Fig. 4, together with the peaks that correspond to vibrations that originate from H_2O, CO_2, CO, and surfactant molecules (CH_2 and CH_3 groups), and observations are listed in Table 3. In this table, the whole temperature range (50-1100 ˚C) was divided into four smaller, and for each region, peaks and evolved gasses (or specific IR vibrations) were summarized.

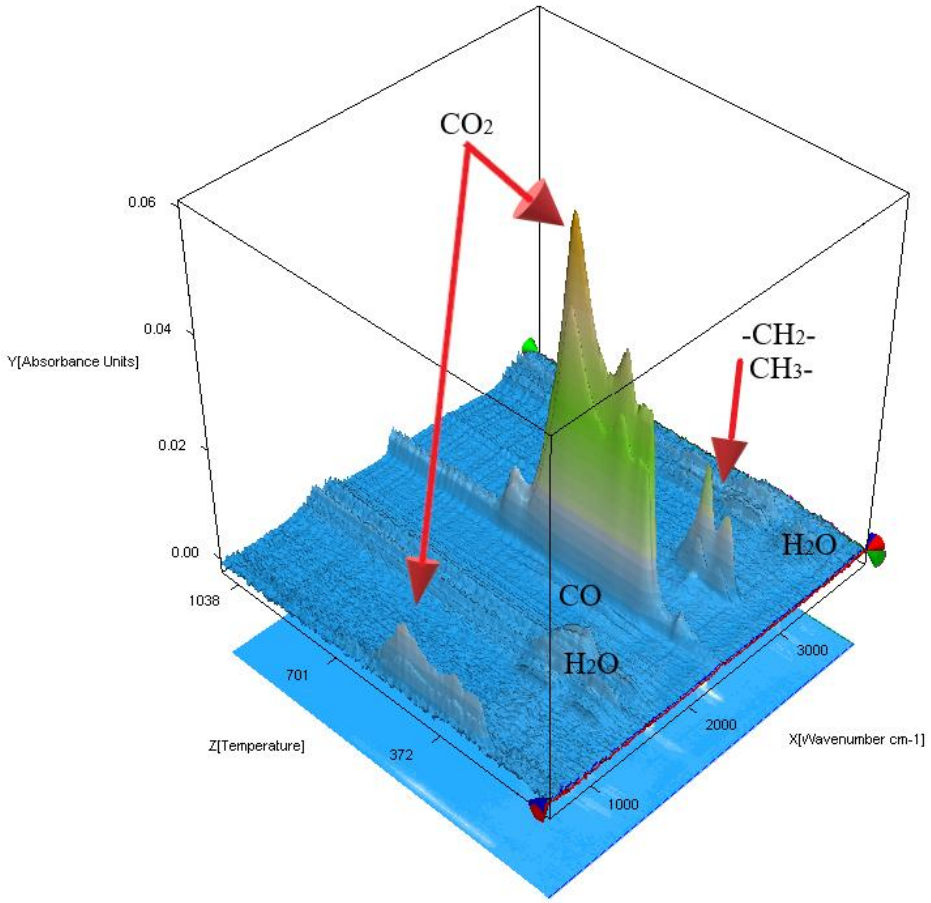

***Fig. 4**. An example of a threedimensional plot (wavenumber-temperature-absorbance units) from EGA.*

***Table 3.** Thermal behavior of starting materials and prepared composites*

	50-200 ˚C				**200-400 ˚C**				**400-700 ˚C**				**Total Δw (%)**
Sample	Δw (%)	DTG	DSC[a]	EGA	Δw (%)	DTG	DSC[b]	EGA	Δw (%)	DTG	DSC[b]	EGA	
IZ CLI	6.17	120	117	H_2O CO_2^{tr}	3.45			H_2O CO_2^{tr}	1.21			CO_2 H_2O^{tr}	**11.03**
C-C-M	5.63	120	119	H_2O	3.93	385	376	H_2O^{tr} CO_2 CO^{tr} ν(C-H)	2.99	542 657	552	CO_2 CO^{tr}	**12.78**
C-C-B	5.50	122	111	H_2O	5.56	235 365	277[a] 359	H_2O CO_2 CO ν(C-H) ν(C=O)^{tr} ν(arC-H)	3.58	532	544	CO_2 CO^{tr}	**15.01**
C-A-M	5.74	122	117	H_2O	4.96	260 376	354	H_2O^{tr} CO_2 CO^{tr} ν(C-H) ν(C=O)	3.01	525 658	446 522	CO_2 CO^{tr}	**13.92**
C-A-B	6.00	121	118	H_2O CO_2^{tr}	6.61	239	361	H_2O^{tr} CO_2 CO^{tr} ν(C-H) ν(C=O)	3.57	531	453	CO_2 CO^{tr}	**16.40**
PHIL75	5.32	149	156	H_2O CO_2^{tr}	2.75			CO_2 H_2O^{tr}	0.99	462 658		CO_2	**9.15**
P-C-M	5.01	157	124a	H_2O	4.32	336	329	H_2O CO_2 CO ν(C-H) ν(arC-H)	3.30	495 679	495	CO_2 CO	**12.82**
P-C-B	4.96	157	128	H_2O	5.31	240 341	243 336	ν(C-H) H_2O CO_2 CO ν(arC-H) ν(C=O) ν(a/kC-H)	3.57	494 666	495	CO_2 CO	**14.18**
P-A-M	4.98	151	145	H_2O	4.89	260 347	261 327	H_2O^{tr} CO_2 CO ν(C-H) ν(C=O)	3.36	490 672	490	CO_2, CO	**13.40**

P-A-B	5.47	167	155	H_2O	6.10	255	264 332	H_2O^{tr} CO_2 CO ν(C-H) ν(C=O)	3.95	487 674	491	CO_2 CO	**15.58**

**From Smiljanić et al. (2020). Legend: [a] – endothermic; [b] - exothermic; [tr] – traces; Δw – mass loss; total Δw – mass loss in region 50 - 1100˚C;*

The total mass loss (%) was the lowest for unmodified zeolite-rich tuffs and increased with the addition of surfactants from monolayer to bilayer composites. As far as surfactants are considered, a slightly higher mass loss was noticed when ARQ was used.

In the temperature region from 50 to 200 °C, mass loss was the highest, mainly due to dehydration and, in some SMNZs samples, also because of the loss to loosely bound surfactant (CO_2 in traces).

For SMNZs in the second region (200-400 °C), a mass loss is related to the combustion (exothermic peaks) of tightly bound surfactant molecules. This was confirmed by the occurrence of aliphatic C-H stretching vibration at FTIR spectra – ν(C-H), along with H_2O^{tr}, CO_2, and CO. When CPyCl was used for functionalization, very low-intensity peaks of aromatic C-H stretching vibration – ν(arC-H) were present above 3000 cm^{-1} Additionally, EGA shows for all SMNZs a vibration around 1740 cm^{-1}, due to the stretching of carbonyl group – ν(C=O); this peak along with small peaks at spectra of P-C-B (at 2802 cm^{-1} and 2709 cm^{-1} from C-H stretching in aldehydes/ketones – ν(a/k C-H)) most likely indicates the presence of aliphatic aldehydes produced in the oxidation process. These C-H and C=O stretching vibrations were absent in the 400-700 °C temperature range. Most likely, the temperatures were high enough to directly transform the remaining organic phase in CO_2 and CO (confirmed in EGA).

Above 700 °C, no reactions occur as it was confirmed by an almost flat mass loss line (Figs. S2 and S5) of all samples in this temperature range as well as no gas detection (accordingly, this temperature region is not given in Table 3). Small mass loss in this region can be calculated as the difference between total mass loss (from 50 °C to 1100 °C) and the sum of mass losses from 50 °C to 700 °C.

Results of the thermal analysis indicated that SMNZs start to degrade at temperatures around 200 °C, giving a better insight into their thermal stability. This could be of great

importance for the potential application of SMNZs in real systems for wastewater treatment. Another conclusion was that surfactant molecules are degraded in the range from 200-600 °C; this information has brought an idea that thermal treatment could be utilized for the removal of organic phase from zeolite after adsorption namely, the regeneration of zeolite. However, to understand if the thermal treatment is useful for this purpose and if recovered zeolite can be modified again, new experiments that will focus on the changes in zeolite structure after removal of organic phase, and efficiency of the secondary surfactant modification, are necessary and will be performed in the future.

4.2.2 ATR-FTIR

ATR–FTIR spectra of starting materials and prepared SMNZs composites were compared, and the main adsorption bands were assigned. (Figs. 5 and 6.)

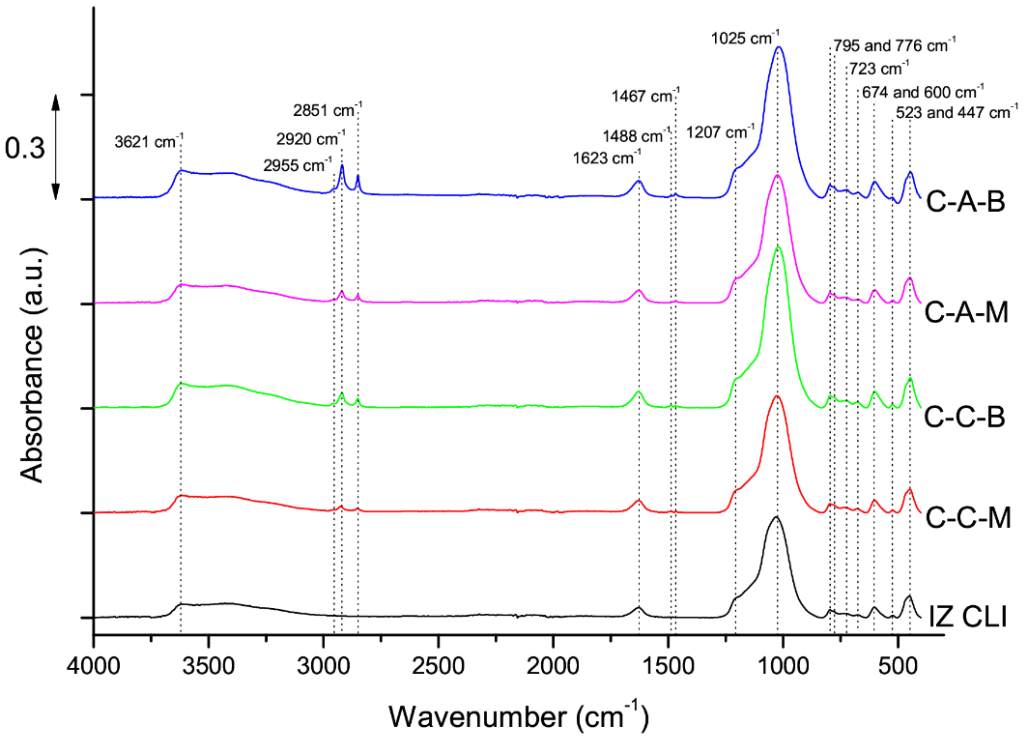

Fig. 5. *ATR–FTIR spectra of starting material IZ CLI and its composites (C-C-M, C-C-B, C-A-M and C-A-B). From (Smiljanić et al., 2020).*

In Fig.5, ATR-FTIR spectra of IZ CLI and its SMNZs were presented and, the following peaks were assigned:

- a broad peak around 3621 cm^{-1} from O-H stretching vibration in water molecules;
- the low-intensity peak at 2955 cm^{-1} from the CH_3 group of surfactant molecules;
- peaks at 2920 cm^{-1} and 2851 cm^{-1} belong to the asymmetric and symmetric C-H stretching vibrations of CH_2 groups in the alkyl chain of surfactant molecules;
- the peak at 1623 cm^{-1} originates from O-H bending vibration of water molecules;
- low-intensity peaks at 1488 cm^{-1} and 1467 cm^{-1} are from C-H bending vibration in surfactant molecules.

The following adsorption bands characteristic for vibration of primary and secondary building units of silicates (Cappelletti et al., 2017; Izzo et al., 2019; Mercurio et al., 2018):

- the shoulder at 1207 cm^{-1} and peak at 1025 cm^{-1} are from asymmetric stretching of T-O, where T represents Si or Al, and O is an oxygen atom;
- peaks at 795 cm^{-1} and 776 cm^{-1} are from asymmetric stretching of T-O-T;
- the peak at 723 cm^{-1} belongs to symmetric stretching of T-O-T;
- peaks at 674 cm^{-1}, 600 cm^{-1}, 523 cm^{-1}, and 447 cm^{-1} are characteristic for T-O-T bending vibrations.

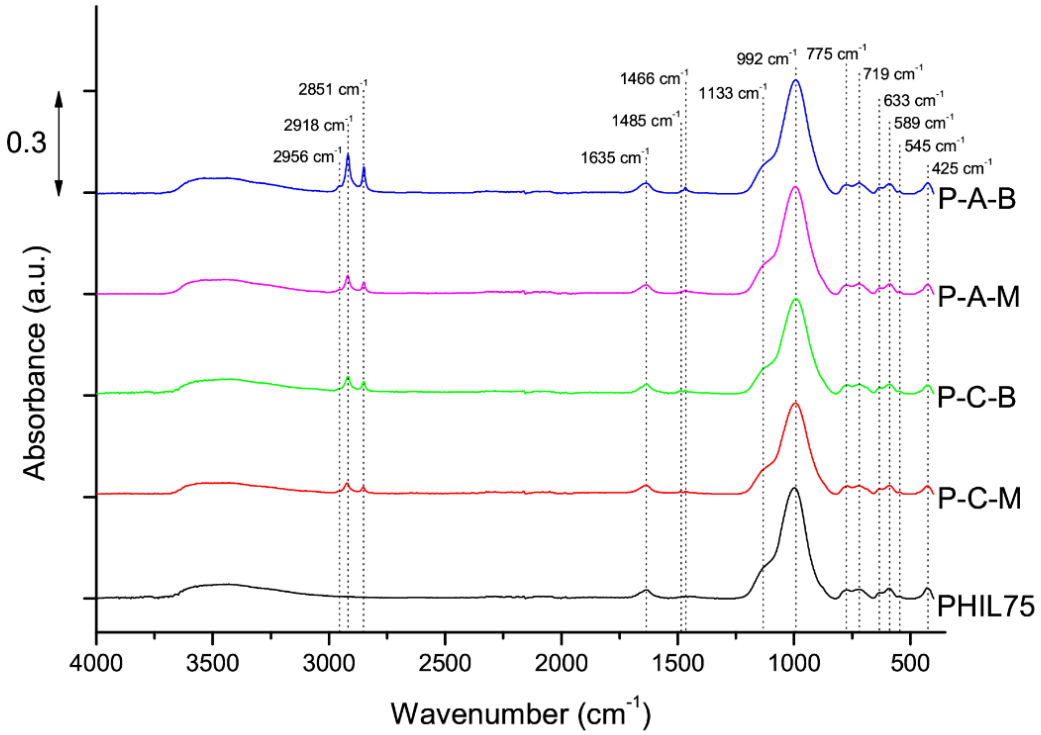

Fig. 6. *ATR–FTIR spectra of starting material PHIL75 and its composites (P-C-M, P-C-B, P-A-M and P-A-B). From (Smiljanić et al., 2020).*

Similar results were obtained when PHIL75 was used as a starting material, as well as for its SMNZs composites (Fig. 6).

- a broad peak at around 3500 cm^{-1} and a smaller one at 1635 cm^{-1} belong to O-H stretching and bending vibrations in water molecules, respectively;
- peaks at 2956 cm^{-1}, 2918 cm^{-1}, and 2851 cm^{-1} represent C-H stretching vibration of surfactant molecules;
- peaks at 1485 cm^{-1} and 1466 cm^{-1} are bending C-H vibration of surfactant molecules
- A shoulder at 992 cm^{-1} and a high-intensity peak at 1133 cm^{-1} are characteristic asymmetric stretching vibrations of T-O group;
- 775 cm^{-1} and 719 cm^{-1} represent asymmetric and symmetric T-O-T stretching vibrations;
- 633 cm^{-1}, 589 cm^{-1}, 545 cm^{-1} and 425 cm^{-1} are T-O-T bending vibrations.

For both zeolites, the intensities of peaks characteristic for the presence of surfactants (around 2920 cm^{-1} and 2850 cm^{-1}) increased with increasing their amounts at each zeolitic surface. The second observation was that peak intensities are higher for SMNZs modified with

ARQ than for composites with CPyCl. These results confirmed the presence of surfactant molecules in SMNZs and that functionalization did not cause any changes in the structure of starting materials.

4.2.3 Point of the zero charge

The pH at which the sorbent surface has an equal amount of positive and negative active sites (the surface has zero net charge) is called the point of zero charge (pH_{pzc}). The batch equilibration technique used for the determination of pH_{pzc} is based on the assumption that zeolite surface groups can dissociate or associate an additional proton from the solution depending on the properties of the powder and the pH of the solution (Čerović et al., 2007; Daković et al., 2010).

The change of the solution pH will cause the protonation or deprotonation of active surface sites, and adsorbent will, in a certain range of solution pH, act as a buffer, trying to reach the pH_{pzc} value. For example, if solution pH > pH_{pzc} (property of adsorbent), the hydroxyl group will start to dissociate. The surface will become negatively charged; simultaneously, the concentration of protons in the solution will increase, leading to a decrease in pH value. If pH < pH_{pzc}, hydroxyl groups will associate protons from solution, the surface will become positive, while pH will increase to reach pH_{pzc} (Daković et al., 2010).

The curve $pH_f = f(pH_i)$ will have a plateau that represents the pH range where the zeolitic surface will behave as a buffer (Figs. 7 and 8). To simplify the determination of pH_{pzc}, plots $\Delta pH = f(pH_i)$ were prepared (where $\Delta pH = pH_f - pH_i$, and point zero charge is actually the inflection point of the curve) and are given in Figs. S8 and S9. If pH_f is higher than pH_i, the ΔpH will be positive, indicating an increase in pH. Different ionic strengths of electrolyte KNO_3 were not influencing the $pH_f = f(pH_i)$ curves; in other words, the curves were overlapping and this is an indication that K^+ or NO_3^- ions were not specifically adsorbed on the adsorbents` surface. Determined pH_{pzc} values for all materials are listed in Table 4.

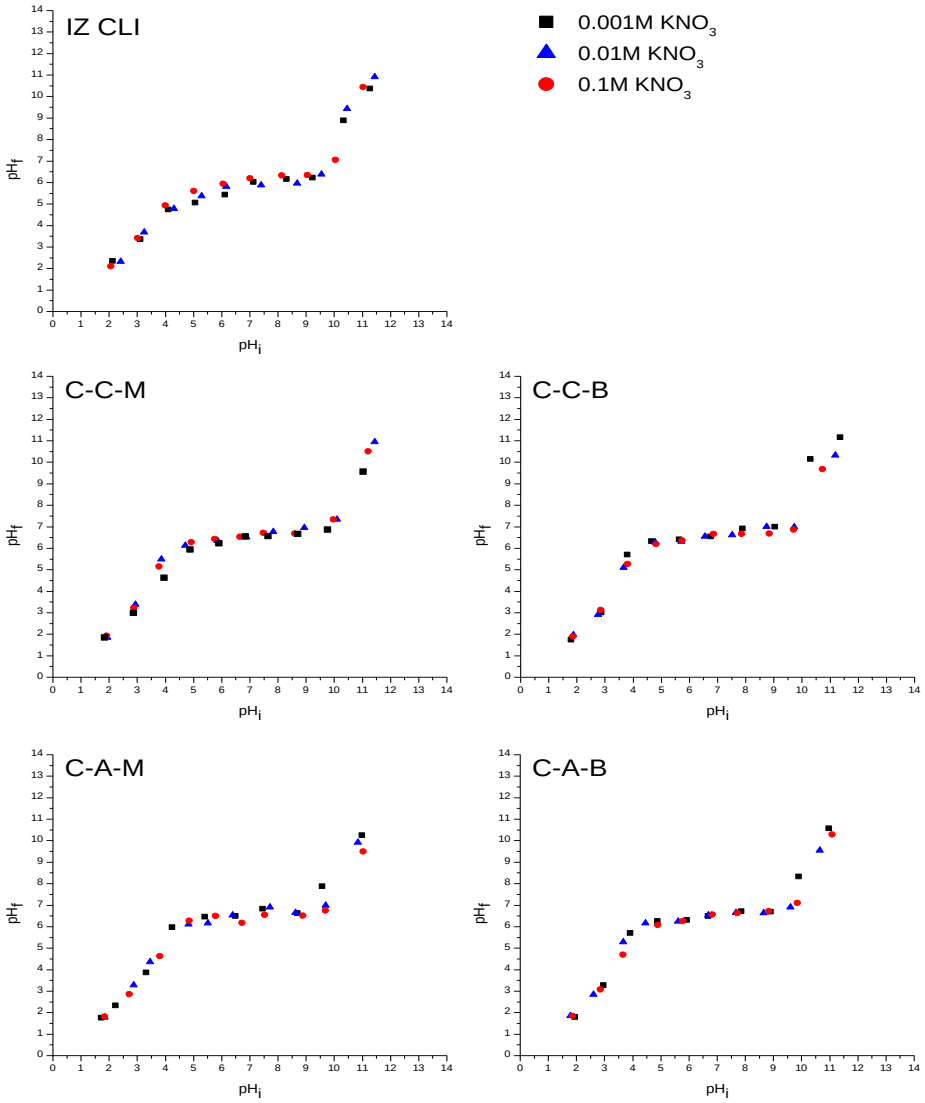

Fig. 7. *$pH_f = f(pH_i)$ plots for starting material IZ CLI and its composites (C-C-M, C-C-B, C-A-M, and C-A-B). Experiments were performed using three different concentrations of KNO_3 (0.001 M, 0.01 M, and 0.1 M).*

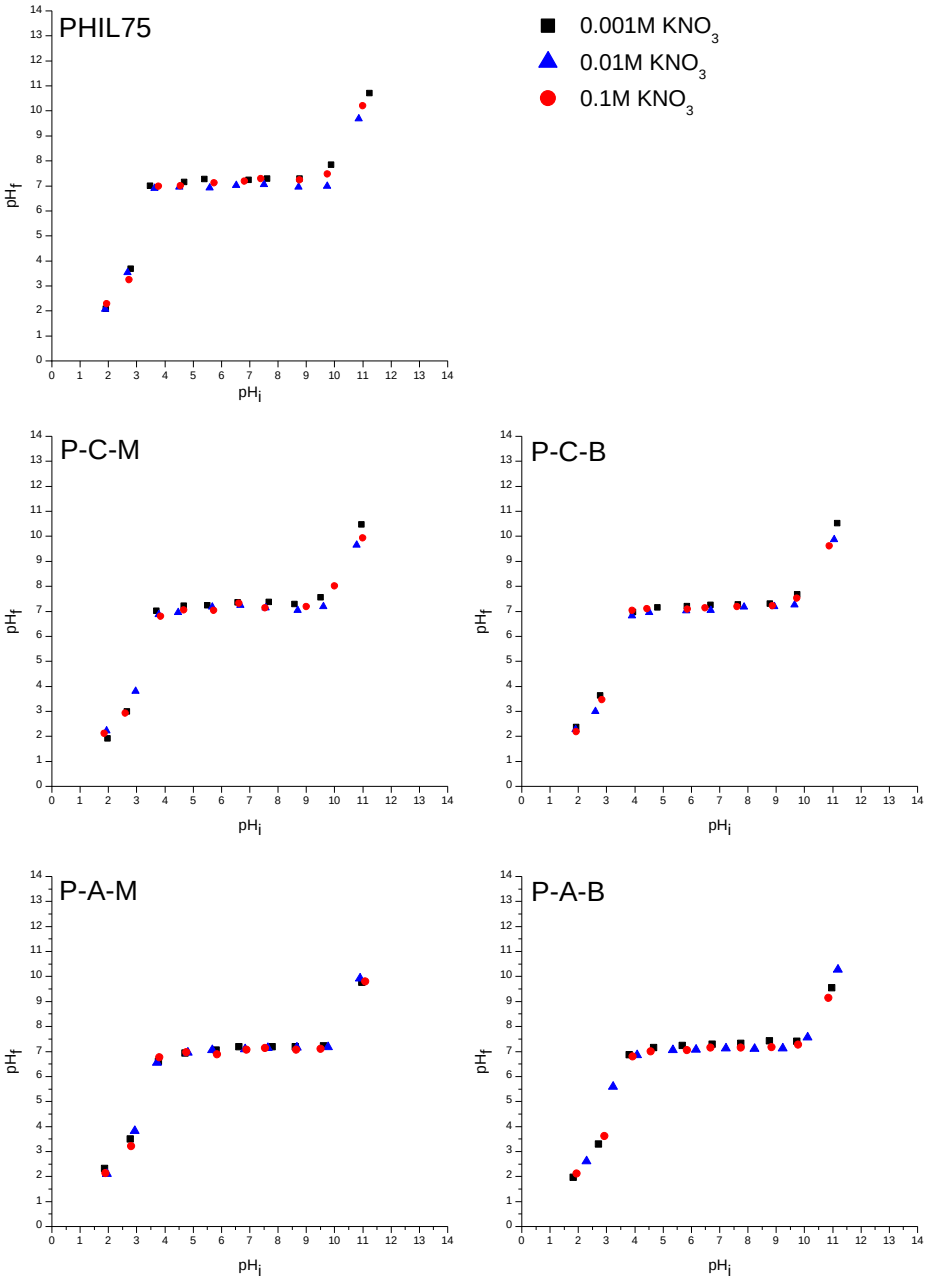

Fig. 8. *$pH_f = f(pH_i)$ plots for starting material PHIL75 and its composites (P-C-M, P-C-B, P-A-M, and P-A-B). Experiments were performed using three different concentrations of KNO_3 (0.001 M, 0.01 M, and 0.1 M)*

Table 4. *Mean pH_{pzc} for starting materials and all prepared composites*

Adsorbent	**pH_{pzc}**	**Adsorbent**	**pH_{pzc}**
IZ CLI	5.5±0.5	PHIL75	7.2±0.2
C-C-M	6.43±0.09	P-C-M	7.2±0.2
C-C-B	6.51±0.02	P-C-B	7.17±0.08
C-A-M	6.5±0.2	P-A-M	7.12±0.05
C-A-B	6.45±0.03	P-A-B	7.2±0.1

As can be seen from Table 4, in the case of clinoptilolite-rich tuff, the modification of surface has led to a slight increase of pH_{pzc} value, while for phillipsite-rich tuff, this value remained the same. Chutia et al. (2009) reported that modification of natural mordenite and clinoptilolite with HDTMA has led to an increase of pH_{pzc} from 4.2 to 6.4, and from 5.2 to 6.5, respectively (Chutia et al., 2009). In another case, when clinoptilolite was modified with HDTMA (30 mM), pH_{pzc} has not changed, remaining at around 6.9 (Dávila-Estrada et al., 2018). Composites containing different amounts of benzalkonium chloride adsorbed on the clinoptilolite have shown the same pH_{pzc} values of 6.8 (Marković et al., 2017b). In another study, clinoptilolite-rich tuff was modified with different amounts of octadecyldimethylbenzyl ammonium (ODTMA), and their pH_{pzc} values were 6.8±0.1 and 7.0±0.1, respectively. The authors concluded that these values are similar since, after modification, SMNZs have surface functional groups with similar acid and basic characteristics as the natural zeolitic tuff (Daković et al., 2010).

In the case when SMNZs ($pH_{pzc} \approx 6.5$, with plateau from 6 to 10) were tested for the removal of arsenates, and it was noticed that adsorption of arsenates decreased when pH was above 10 (after plateau ended), most probably because the adsorbent surface was more negative and thus causing repulsion of arsenate anions, indicating that charge of adsorbent won't suddenly switch from positive to negative (Chutia et al., 2009). Considering that for all composites in this study, measured pH_{pzc} values were around or above 6.5, and all adsorbents showed a plateau in the range of initial pHs from ~5 to ~10, we can consider that at all these pH_i, pH_f is almost equal to pH_{pzc}. From these results and because pH in WWTPs is from 6-8, further equilibrium runs will be performed at pH = 6.5. A value close to neutral pH but still

around or below pH_{pzc} for all composites provides the absence of net negative charge of the adsorbents.

4.2.4 Zeta potential measurement and surfactant stability

Zeta potential is an important characteristic of colloidal systems, and it is defined as the electric potential at the slipping plane, which separates a mobile fluid from the fluid that remains attached to the surface (Liu et al., 2018). Zeta potential measurement was performed to obtain information about the surface charge of zeolite-rich tuffs and prepared SMNZs and surfactant stability after adsorption on the zeolite surface. Surfactant stability is of great importance for the possible application of SMNZs for the removal of CoEC. Actually, desorption of surfactant molecules from the surface would not only largely affect drug adsorption (Haggerty and Bowman, 1994) but also can be an environmental threat since surfactants themselves are considered as CoEC. For this reason, prepared composites were extensively washed with distilled water since the low ionic strength of distilled water would cause desorption of surfactant molecules (Li et al., 1998b).

Zeta potential for IZ CLI and its composites (Fig. 9) showed that the initial negative surface of IZ CLI (–37.9 mV) turned slightly positive for C-C-M (7.17 mV), confirming the formation of a monolayer. On the other hand, the zeta potential for C-A-M remained negative (–14.2 mV). The explanation of this behavior could be the difference in the number of surfactant tails and consequently their different arrangement at the zeolitic surface. In the preparation process, surfactant concentration was above CMC (surfactant molecules in solution were organized in micelles), and according to the literature, when a monolayer is formed, the initial adsorption of surfactant will be in the form of a micelle, which will later rearrange in more homogenous monolayer. Based on these premises, the micelles of two-tailed ARQ (Fig. 2 B) could be randomly attached at the surface, but the increased hydrophobic interactions between the tails could prevent re-arrangement in monolayer, thus leaving part of the zeolitic surface negative and uncovered. On the other hand, CPyCl with one tail is probably more easily rearranged at the zeolitic surface.

Composites with surfactant in amounts of 200% of ECEC had positive zeta potential values (for C-C-B 37.7 mV and for C-A-B 36.1 mV), which confirmed the reverse of charge from

negative to positive, thus, the formation of bilayers at the zeolitic surfaces. In order to simulate extreme conditions, an extensive washing of samples with distilled water was carried out, leading to the following modifications of zeta potential values:

- C-C-M from 7.17 mV to –7.93 mV;
- C-C-B from 37.7 mV to –7.08 mV;
- C-A-M from –14.2 mV to –24.3 mV;
- C-A-B from 36.1 mV to 35.6 mV.

Actually, clinoptilolite composites with CPyCl shown that slight removal of surfactant occurred when monolayer was present at zeolitic surface (C-C-M), while more extensive washing of the surfactant happened when a bilayer was present at the surface (C-C-B). The zeta potential values of C-C-M and C-C-B after intensive washing were very similar (around –7 mV), confirming desorption of CPyCl from the bilayer, leaving a monolayer at the surface of C-C-B. In the C-A-M case, zeta potential became more negative, probably due to the removal of part of the surfactant from the micelle. However, for sample C-A-B, the zeta potential after intensive washing remained practically unchanged, confirming close packing of micelles (bilayer) of ARQ at the clinoptilolite surface and consequent higher stability.

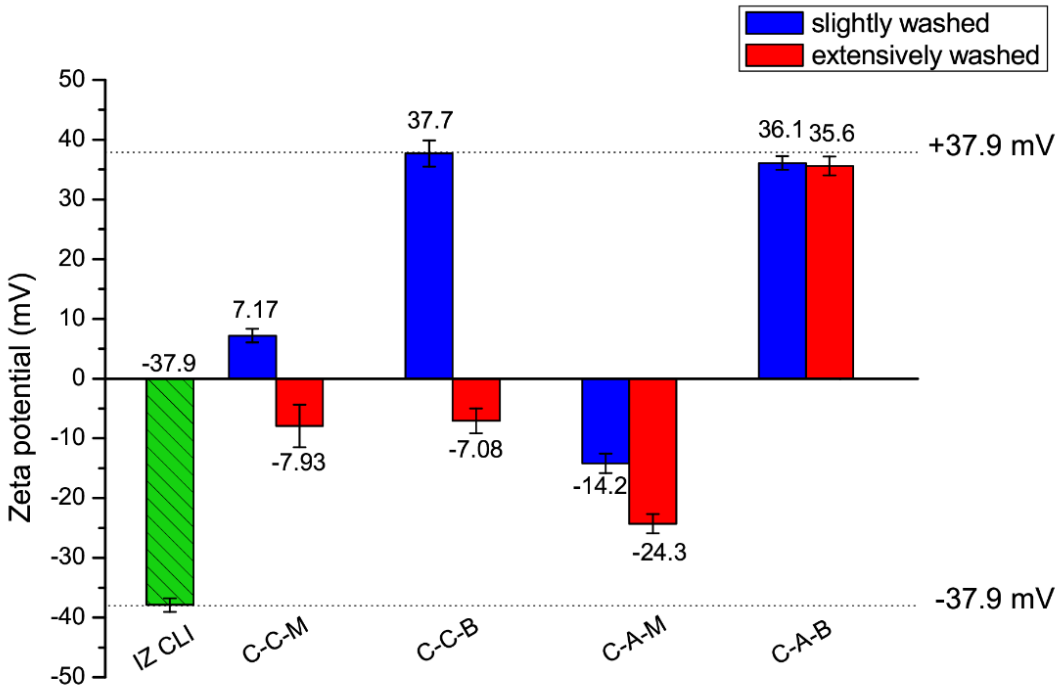

Fig.9. *Graphical representation of zeta potential for starting material IZ CLI (sparse green pattern) and composites (C-C-M, C-C-B, C-A-M, C-A-B) before (blue) and after (red) extensive washing. This figure was published in Smiljanić et al. (2020).*

Zeta potential measurements showed that the negative surface charge of PHIL75 (–36.8 mV) changed after modification with CPyCl (2.83 mV for P-C-M and 30.6 mV for P-C-B), as well after modification with ARQ (2.03 mV for P-A-M and 33.5 mV for P-A-B) (Fig. 10). When both surfactants were added in an amount equal to 100% of ECEC, the zeta potential was close to zero, indicating that the phillipsite surface was almost entirely neutral (hydrophobic). When the amount of surfactants was equal to 200% of ECEC, a bilayer of both surfactants was formed at the phillipsite surface, making the surface positive.

After intensive washing, zeta potential for phillipsite composites P-C-M, P-C-B, and P-A-M became negative, confirming desorption of surfactants from the phillipsite surface (Fig. 10). The zeta potential changed for:

- P-C-M from 2.83 mV to –7.44 mV;
- P-C-B from 30.6 mV to –4.53 mV;
- P-A-M from 2.03 mV to –23.1 mV;

- P-A-B from 33.5 mV to 33.5 mV;

These results suggest that in the P-C-M case, a part of the monolayer was removed from the zeolite surface, while P-C-B had a significant loss of surfactant becoming more similar to monolayer composite. After extensive washing of P-A-M, most of the surfactant was removed. Zeta potential of P-A-B remained positive, confirming higher stability of the composite and that desorption of surfactant did not occur. With the assumption that extensive washing represents conditions more extreme than those available in batch, only slightly washed composites were used for further drug adsorption isotherm experiments and kinetic runs. It is interesting to notice that when ARQ was used for modification, regardless of the starting material, monolayers were very unstable, while bilayers have shown great stability. The literature reported that the surfactant orientation on the zeolite surface depends on the number of surfactant molecules, where the greater amounts will favor ordering (Sullivan et al., 1998b, 1997). This could be the possible explanation for the greater stability of bilayers prepared with ARQ.

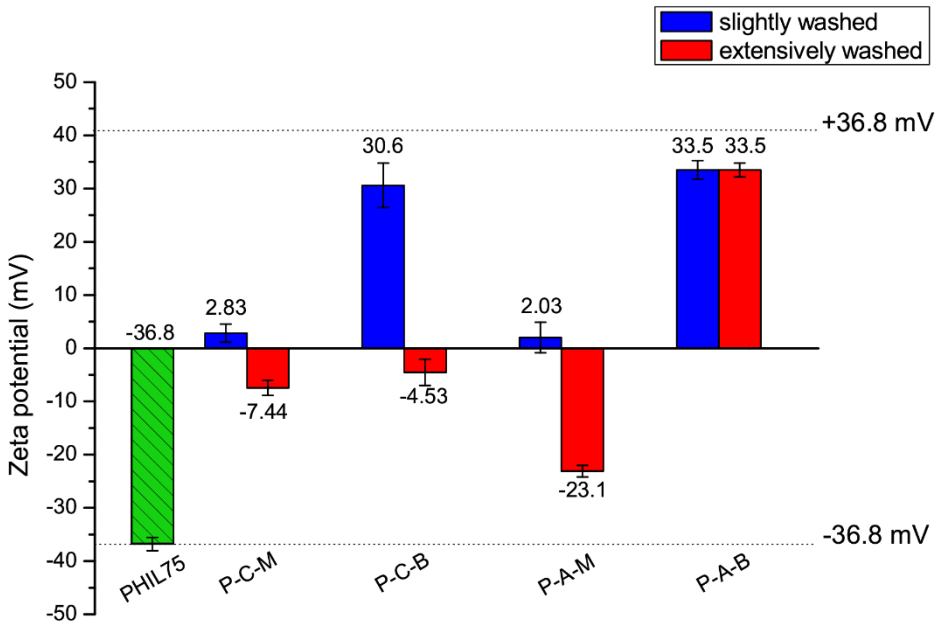

Fig. 10. *Graphical representation of zeta potential for starting material PHIL75 (sparse green pattern) and composites (P-C-M, P-C-B, P-A-M, P-A-B) before (blue) and after (red) extensive washing. This figure was published in Smiljanić et al. (2020).*

4.3 Adsorption of NSAIDs

4.3.1 Adsorption isotherms

The adsorption is usually well described by isotherms, which provide the adsorbate loading on the adsorbent as a function of equilibrium concentration (for liquid phase solutes) at a constant temperature. Adsorption isotherms for DCF, KET, IBU, and NAP on all SMNZs are shown in Figs. 11-14. Based on the equilibrium runs, the adsorption of the chosen four drugs decreased in the following order: X-C-B > X-A-B > X-C-M > X-A-M, where X is C and/or P standing for IZ CLI and PHIL75, respectively. In general, higher adsorption capacities were reported when clinoptilolite-rich tuff was used as the starting material, most likely due to the higher percentage of zeolite content in the tuff. Also, increasing the amount of each surfactant at the zeolite surfaces increased the adsorption of drugs; in other words – positively-charged bilayers gave the best results, confirming that ionic exchange significantly contributes to the drug adsorption.

The only exception from the rule is that P-C-M and P-A-B have reversed places in the case of IBU, but also, these two composites had similar values for DCF and NAP. This suggests that P-A-B (when phillipsite-rich tuff with lower Si/Al ratio was combined with two-tailed ARQ), despite the positive surface charge (confirmed by zeta potential measurement) and ability to adsorb drugs, does not achieve adsorptions as high as those obtained with zeolites modified with CPyCl, thus suggesting that the type of zeolite and surfactant arrangement on the surface have a crucial influence on drug adsorption (Daković et al., 2005, 2003; Krajišnik et al., 2013a; Marković et al., 2017b). Other important factors that will influence the adsorption are properties of adsorbates, such as water solubility and polarity (Zhu et al., 2000, 1998). DCF, KET, IBU, and NAP are low polar, hydrophobic molecules and, based on pKa, exist in the anionic form at investigated pH.

Equilibrium runs of these NSAIDs by all composites showed non-linear isotherms (Figs. 11-14), indicating that hydrophobic partitioning into the organic phase happens simultaneously with the ionic exchange (Daković et al., 2005, 2003; Krajišnik et al., 2013a; Marković et al., 2017a). If the hydrophobic partitioning was the only mechanism, the isotherms would be linear. In monolayer cases, anionic drug molecules can be adsorbed thanks to electrostatic interactions with cationic surfactant heads attached directly to zeolite surface and

hydrophobic interactions between the alkyl surfactants chains and hydrophobic part of the drug. In the case of the bilayer, besides these interactions, ion exchange of counter Cl^- in surfactant molecule and anionic form of drugs occurred (Fig. 15).

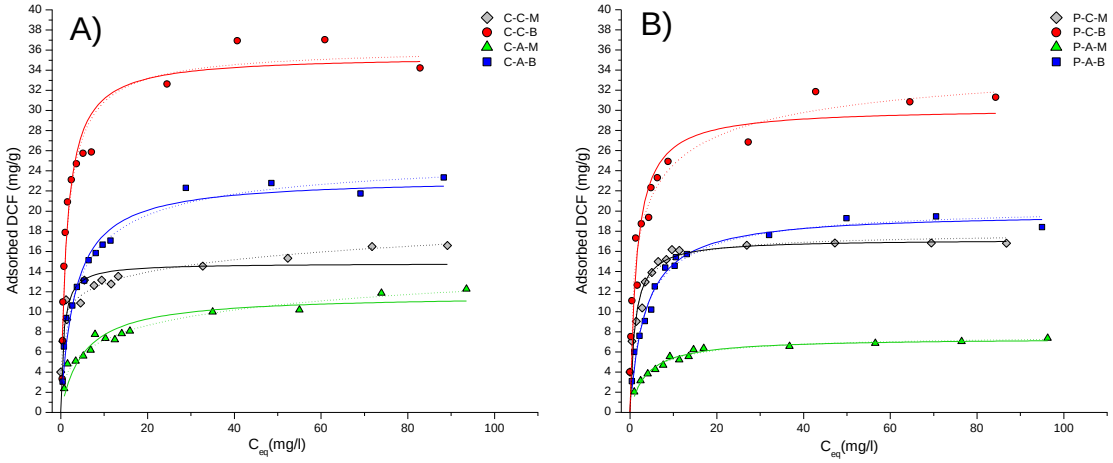

Fig. 11. *Equilibrium isotherms of DCF adsorption on: A) composites of IZ CLI; B) composites of PHIL75. Solid line represents Langmuir isotherm model, and dotted line is Sips isotherm model. The scale of y-axes goes from 0 to 40 mg/g (Smiljanić et al., 2020).*

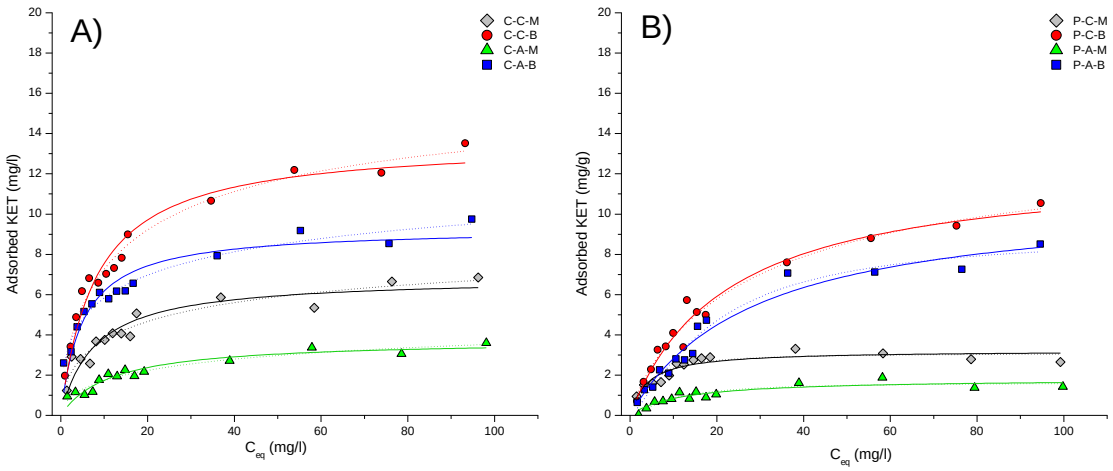

Fig. 12. *Equilibrium isotherms of KET adsorption on: A) composites of IZ CLI; B) composites of PHIL75. Solid line represents Langmuir isotherm model, and dotted line is Sips isotherm model. The scale of y-axes goes from 0 to 20 mg/g (Smiljanić et al., 2020).*

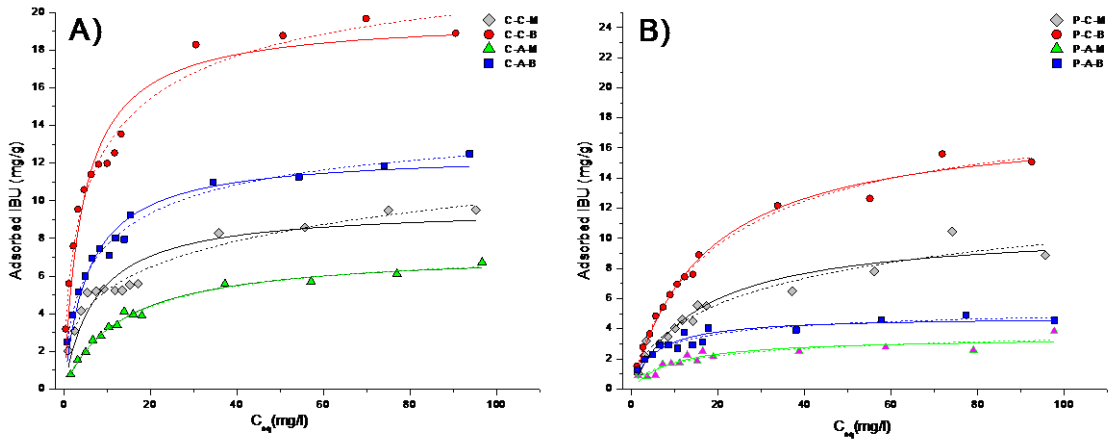

Fig. 13. *Equilibrium isotherms of IBU adsorption on: A) composites of IZ CLI; B) composites of PHIL75. Solid line represents Langmuir isotherm model, and dotted line is Sips isotherm model. The scale of y-axes goes from 0 to 20 mg/g (Smiljanić et al., 2021).*

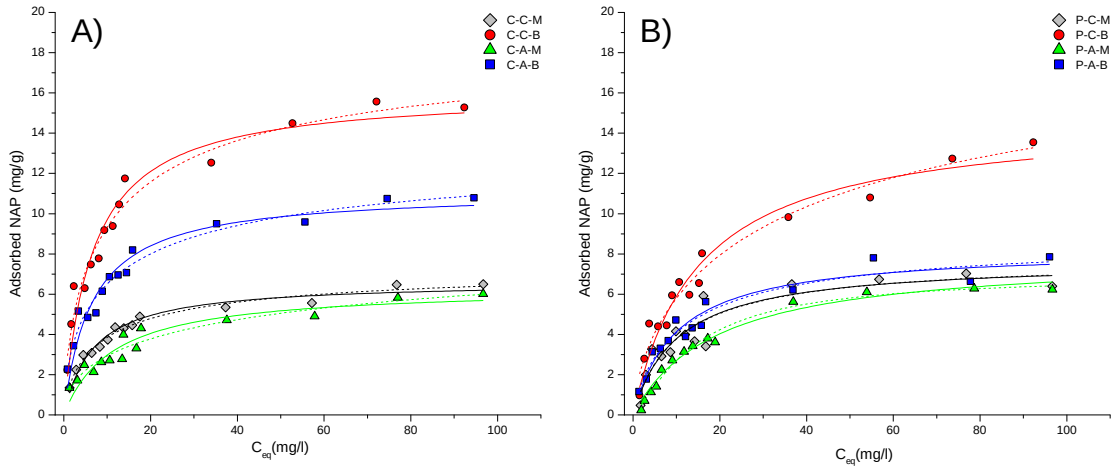

Fig. 14. *Equilibrium isotherms of NAP adsorption on: A) composites of IZ CLI; B) composites of PHIL75. Solid line represents Langmuir isotherm model, and dotted line is Sips isotherm model. The scale of y-axes goes from 0 to 20 mg/g (Smiljanić et al., 2021).*

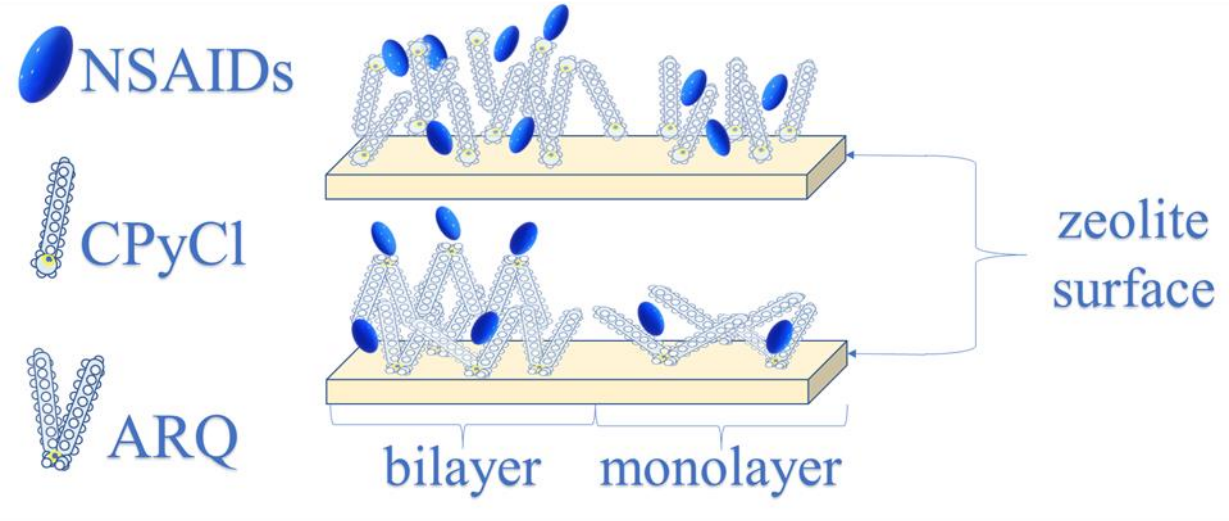

Fig. 15. *Graphical representation of drug adsorption onto monolayer/bilayer composites prepared with different surfactants (Smiljanić et al., 2020).*

Two mathematical models were used to better understand the adsorption mechanism of drugs on the prepared composites: Langmuir isotherm (two-parameter model) and Sips isotherm (three-parameter model).

Langmuir isotherm (Eq. 2) assumes adsorption on a definite number of sites with equal affinity for the adsorbate. Adsorbate molecules can adsorb only in one layer, and the isotherm has a plateau. Considering that an ion exchange process should not give multilayer adsorbate adsorption, the Langmuir isotherm model could be an appropriate model for our system. Still, possible difficulties this model could have because of the hydrophobic partitioning as an additional adsorption mechanism.

$$Q_e = \frac{Q_{max} K_l C_e}{1 + K_l C_e} \qquad \text{(Eq. 2).}$$

where Q_{max} (mg/g) is the highest concentration of adsorbed molecules, K_l (L/mg) is Langmuir constant, Q_e (mg/g) and C_e (mg/L) are the amounts of loaded drugs and solution concentration at the equilibrium (Foo and Hameed, 2010).

Sips isotherm (Eq. 3) combines Langmuir and Freundlich models while considering the heterogeneity of adsorbents. At low adsorbate concentrations, this model reduces to the Freundlich isotherm, while at high concentrations, it behaves like the Langmuir model (Foo and Hameed, 2010; Hamdaoui and Naffrechoux, 2007; Tosun, 2012). When n = 1, the Sips equation reduces to the Langmuir equation, implying a homogeneous adsorption process. In some cases, n can be higher, indicating cooperative adsorption (Keren et al., 2015). In theory, this model could take into account hydrophobic partitioning and give information about material heterogeneity.

$$Q_e = \frac{Q_{max}(K_S C_e)^n}{1+(K_S C_e)^n} \quad \text{(Eq. 3).}$$

where Q_{max} (mg/g) is the highest concentration of adsorbed molecules, K_S (L/mg) is Sips constant, n is Sips model exponent, Q_e (mg/g) and C_e (mg/L) are the amounts of loaded drugs and solution concentration at the equilibrium (Foo and Hameed, 2010).

The selected mathematical models were evaluated considering the determination of correlation coefficients (R^2), and statistical method for non-linear regression (Costa et al., 2003; Spiess and Neumeyer, 2010) such as Akaike Information Criterion (AIC) (Eq. 4) and Akaike weight parameter (AIC*w* – indicates the probability that the model is the best among the whole set of considered models (Glatting et al., 2007)). A mathematical model with lower values of AIC (higher AIC*w*) is considered as a better approximation of experimental data. According to literature, these methods take into account the number of parameters of the mathematical model (p), the number of experimental points (n), and N - the number of residuals ($x_i, \ldots, x_n$) from the non-linear least-squares fit:

$$AIC = 2p - (-N * (\ln 2\pi + 1 - \ln N + \ln \textstyle\sum_{i=1}^{n} x_i^2)) \quad \text{(Eq. 4)}$$

The relative isotherm parameters of adsorption isotherms (K, n, Q_{max}, R^2, AIC, and $AICw$) were calculated and presented in Table 5 (a and b).

Table 5 a). *Mathematical models for the adsorption isotherms: parameters and goodness - of - fit*

Drug	Sample	Model	Parameters			Goodness - of – fit		
			K (L/mg)	n	Q_{max} (mg/g)	R^2	AIC	AIC*w*
DCF	C-C-M	Langmuir	1.5±0.5		14.8±0.7	0.767	21.16	0.001
		Sips	0.04±0.01	0.2±0.1	37±7	0.939	4.61	0.999
	C-C-B	**Langmuir**	0.7±0.1		35±2	0.952	30.32	0.858
		Sips	0.7±0.2	0.9±0.2	36±2	0.949	33.92	0.142
	C-A-M	Langmuir	0.19±0.04		11.7±0.7	0.884	4.59	0.003
		Sips	0.03±0.04	0.4±0.2	20±7	0.960	-7.27	0.997
	C-A-B	Langmuir	0.31±0.05		23.3±0.8	0.957	13.73	0.071
		Sips	0.23±0.05	0.72±0.09	26±2	0.975	8.58	0.929
	P-C-M	**Langmuir**	0.9±0.3		17.2±0.7	0.877	16.67	0.814
		Sips	0.9±0.3	0.8±0.3	18±2	0.876	19.62	0.186
	P-C-B	Langmuir	0.7±0.2		30±2	0.905	34.54	0.045
		Sips	0.4±0.2	0.5±0.2	37±5	0.950	28.44	0.955
	P-A-M	**Langmuir**	0.27±0.03		7.4±0.2	0.967	-28.74	0.596
		Sips	0.25±0.04	0.8±0.1	7.8±0.4	0.972	-27.96	0.404
	P-A-B	**Langmuir**	0.29±0.03		19.9±0.5	0.976	0.35	0.717
		Sips	0.27±0.04	0.87±0.09	20.6±0.9	0.977	2.22	0.282
KET	C-C-M	Langmuir	0.13±0.03		6.9±0.5	0.881	-10.35	0.357
		Sips	0.04±0.06	0.6±0.2	10±4	0.911	-11.52	0.643
	C-C-B	Langmuir	0.12±0.02		13.6±0.6	0.957	-3.88	0.052
		Sips	0.06±0.03	0.7±0.1	17±3	0.977	-9.69	0.948
	C-A-M	Langmuir	0.09±0.02		3.7±0.3	0.902	-30.54	0.414
		Sips	0.02±0.04	0.6±0.2	9±3	0.924	-31.24	0.586
	C-A-B	Langmuir	0.20±0.04		9.3±0.5	0.898	-5.02	0.002
		Sips	0.04±0.05	0.5±0.1	15±4	0.967	-18.00	0.998
	P-C-M	**Langmuir**	0.25±0.06		3.2±0.2	0.839	-29.29	0.826
		Sips	0.25±0.07	1.2±0.3	3.2±0.3	0.836	-26.17	0.174
	P-C-B	**Langmuir**	0.045±0.006		12.5±0.7	0.971	-12.38	0.838
		Sips	0.03±0.02	0.9±0.2	14.1±3	0.969	-9.10	0.162
	P-A-M	**Langmuir**	0.08±0.03		1.8±0.2	0.830	-38.33	0.788
		Sips	0.11±0.06	1.4±0.5	1.6±0.4	0.833	-35.71	0.212

	P-A-B	**Langmuir**	0.035±0.006		10.9±0.8	0.960	-12.32	0.722
		Sips	0.05±0.02	1.3±0.3	9±1	0.963	-10.40	0.278

*Smiljanić et al. (2020)

Table 5 b). *Mathematical models for the adsorption isotherms: parameters and goodness - of - fit*

Drug	**Sample**	**Model**	**Parameters**			**Goodness - of – fit**		
			K (L/mg)	n	Q_{max} (mg/g)	R^2	AIC	AIC*w*
IBU	C-C-M	Langmuir	0.14±0.03		9.6±0.6	0.874	0.24	0.003
		Sips	0.004±0.003	0.4±0.2	24±19	0.954	-11.11	0.997
	C-C-B	Langmuir	0.23±0.04		19.7±0.8	0.942	12.01	0.004
		Sips	0.12±0.05	0.61±0.09	25±3	0.978	1.07	0.996
	C-A-M	**Langmuir**	0.076±0.006		7.3±0.2	0.987	-38.19	0.852
		Sips	0.07±0.02	0.9±0.1	7.6±0.5	0.986	-34.69	0.148
	C-A-B	Langmuir	0.17±0.02		12.5±0.5	0.959	-7.56	0.003
		Sips	0.10±0.03	0.64±0.08	15±2	0.986	-19.13	0.997
	P-C-M	**Langmuir**	0.07±0.02		10.7±0.8	0.921	-2.14	0.539
		Sips	0.02±0.03	0.6±0.2	17±9	0.934	-1.82	0.461
	P-C-B	**Langmuir**	0.060±0.005		17.9±0.6	0.986	-12.03	0.760
		Sips	0.4±0.2	0.5±0.2	37±5	0.950	-9.73	0.240
	P-A-M	**Langmuir**	0.11±0.03		3.4±0.3	0.821	-23.11	0.819
		Sips	0.06±0.08	0.7±0.3	4±2	0.818	-20.09	0.181
	P-A-B	**Langmuir**	0.19±0.03		4.8±0.3	0.880	-21.67	0.621
		Sips	0.12±0.07	0.7±0.2	5.7±0.9	0.895	-20.68	0.379
NAP	C-C-M	Langmuir	0.15±0.02		6.6±0.2	0.966	-29.61	0.193
		Sips	0.10±0.03	0.73±0.09	7.6±0.6	0.978	-32.47	0.807
	C-C-B	Langmuir	0.15±0.03		16.1±0.7	0.946	4.64	0.203
		Sips	0.09±0.04	0.7±0.2	19±3	0.964	1.91	0.797
	C-A-M	Langmuir	0.09±0.02		6.3±0.5	0.899	-14.79	0.313
		Sips	0.02±0.03	0.5±0.2	11±6	0.926	-16.35	0.687
	C-A-B	Langmuir	0.15±0.03		11.1±0.5	0.940	-5.95	0.057
		Sips	0.08±0.04	0.6±0.2	14±2	0.967	-11.55	0.943
	P-C-M	**Langmuir**	0.10±0.03		7.7±0.6	0.865	-2.63	0.882
		Sips	0.09±0.04	0.97±0.09	8±2	0.852	1.39	1.118

P-C-B	Langmuir	0.07±0.01		14.8±0.8	0.954	-0.42	0.374
	Sips	0.02±0.03	0.7±0.2	21±7	0.965	-1.45	0.626
P-A-M	Langmuir	0.052±0.006		7.5±0.4	0.979	-26.93	0.187
	Sips	0.070±0.008	1.3±0.2	6.9±0.3	0.986	-29.86	0.813
P-A-B	**Langmuir**	0.10±0.02		8.3±0.5	0.934	-11.94	0.839
	Sips	0.08±0.04	0.8±0.2	9±2	0.932	-8.63	0.161

**Smiljanić et al. (2021)*

For DCF and KET, values of AIC were favorable (lower) for both models the same number of times (most of the times R^2 was in good agreement with AIC), while for IBU and NAP Langmuir model was slightly prevailing. However, the connection between models and monolayer/bilayer surfactant formation or different starting material was not observed.

As far as the starting material is considered, almost all the isotherms obtained using IZ CLI (14/16) had a better fit with the Sips model, while for PHIL75 Langmuir model worked best (13/16). Between the isotherms obtained with all the adsorbates (DCF, KET, IBU, and NAP), under the same conditions and using the same adsorbents, the two models are almost equally represented (17 and 15 for Sips and Langmuir, respectively).

In some cases, the Sips isotherm model predicts Q_{max} values higher than the experimental ones, also with high standard errors. According to theoretical knowledge, the Sips model at low concentrations (such as in this work: 2-100 mg/L) behaves like the Freundlich model; thus, it cannot predict a realistic Q_{max} value. On the other hand, Q_{max} obtained from the Langmuir model was in agreement with the experimental data. Assuming that the ion exchange process should not give multilayer adsorbate adsorption, the Langmuir isotherm could be a good model for our system, with slight imperfections in the goodness-of-fit most likely due to the hydrophobic partitioning as an additional adsorption mechanism.

According to the Langmuir model, sample C-C-B had the highest adsorption capacities for all used adsorbates – 35 mg/g, 19 mg/g, 16.1 mg/g, and 13.5 mg/g for DCF, IBU, NAP, and KET, respectively. The lowest adsorption capacities were reported for DCF, IBU, and KET when P-A-M was used (7.4 mg/g, 3.4 mg/g, and 1.8 mg/g, respectively), while for NAP, the C-A-M sample had the lowest results (6.3 mg/g).

In Table 6, for each composite, the relative order of the maximum adsorption capacities (Q_{max}) obtained from the Langmuir model (previously reported in Table 5) for all the investigated drugs is reported.

Table 6. *Selectivity sequences of drugs based on Q_{max} from Langmuir model.*

Adsorbent	Drug order
C-C-M	DCF>IBU>NAP≈KET
C-C-B	DCF>IBU>NAP>KET
C-A-M	DCF>IBU>NAP>KET
C-A-B	DCF>IBU>NAP>KET
P-C-M	DCF>IBU>NAP>KET
P-C-B	DCF>IBU>NAP>KET
P-A-M	DCF≈NAP>IBU>KET
P-A-B	DCF>KET>NAP>IBU

**Smiljanić et al. (2021)*

From Table 6 it is obvious that, for almost all composites, the specific order between drugs exists (DCF>IBU>NAP>KET) and can be explained with the physicochemical properties of drugs reported in Table 2.

As previously mentioned, pKa values of drugs are lower than the pH (6.5) used in the experiments, indicating that these drugs exist in solution in anionic forms. Thus, nonlinear isotherms confirmed that partitioning together with ion exchange of anionic form of drugs occurred.

Besides pKa, other drugs' properties may have an influence on their adsorption. (Zhu et al., 2000, 1998). Different drug uptake by SMNZs may be due to differences in their chemical structures. DCF, NAP, and KET molecules have two aromatic rings, while IBU has one (Fig. 3). In DCF rings are the phenylacetic and chlorine functionalized, linked with the secondary amino group. The repulsions between the acetate group and the Cl atoms cause the aromatic rings to twist with respect to each other (the twist angle is about 69°). The secondary amino group forms a bifurcated intramolecular hydrogen bond with the carbonyl oxygen and the chlorine atoms. KET has the phenyl ring without substituents, and the secondary amino group is replaced by a carbonyl group. Consequently, repulsions between phenyl rings are weaker

(lower angle of twist), and intramolecular hydrogen bonds are weaker, which leads to the higher mobility of phenyl rings in KET compared to DCF (Kozlowska et al., 2017). Lower flexibility of DCF molecule could contribute to higher hydrophobic partitioning into the organic phase. Both IBU and NAP have a hydrophilic (polar) carboxylate group; IBU also has hydrophobic phenyl and isobutyl groups, while NAP has an additional polar group – the methoxy group and hydrophobic naphthalene ring (Chang et al., 2010). Each mentioned group, according to their polarity, will contribute to the total hydrophobicity of the drug molecule which part they are. So as a direct consequence of the chemical structure, the hydrophobicity of the drugs (Table 2) should be discussed.

Hydrophobicity is represented by $logK_{ow}$, where K_{ow} is the partition coefficient - the ratio of the concentration of a solute between water and octanol. The values of $logK_{ow}$ for DCF, IBU, NAP, and KET are 4.52, 3.97, 3.18, and 3.17, respectively (Turk Sekulic et al., 2019). This suggests the following order of hydrophobicity: DCF>IBU>NAP>KET. Also, this confirms that, in most cases, the order of drugs shown in Table 6 is following the hydrophobicity order, whereas the most hydrophobic (DCF) is adsorbed in the highest quantities. These results are in agreement with the results obtained for organoclays (clays modified with long-chain surfactants) when the more hydrophobic molecules were better adsorbed (Groisman et al., 2004).

Since experiments in different studies were done under different experimental conditions, it is not easy to make a comparison, especially when removal efficiencies are used as a parameter to describe adsorbent. For this reason, the adsorption capacity expressed in mg of adsorbate per g of adsorbent (mg/g) is preferred.

Adsorption of NSAIDs on similar adsorbents – zeolites (clinoptilolite and phillipsite) (considering only bilayer forms) has shown that the phillipsite-rich tuff modified with CPyCl had DCF uptake 46.90 mg/g (Marković et al., 2016), while phillipsite- and clinoptilolite-rich tuffs modified with CPyCl could adsorb around 21 mg/g and 18 mg/g of IBU, respectively (Izzo et al., 2019; Mercurio et al., 2018). Clinoptilolite-rich tuffs modified with CPyCl (Krajišnik et al., 2011) and with HDTMA-Br (Sun et al., 2017) were adsorbing 134.93 mmol/kg (42.37 mg/g) and 145 mmol/kg (46.11 mg/g) of DCF, respectively. The reported values were slightly higher than the values reported in Table 5, and it is hard to compare because, in these studies, zeolite-rich tuffs having a different mineralogical composition were used, experiments were done with the higher initial drug concentrations, etc. Data on adsorption of drugs on

zeolites functionalized with ARQ were not found. The literature is also lacking on the data on adsorption of KET and NAP onto SMNZs.

Other adsorbents were also tested for the removal of NSAIDs from water. For example, low-cost activated carbon prepared from olive-waste cakes was used as an adsorbent for DCF, NAP, IBU, and KET; the maximum adsorption capacities (Langmuir model) were 56.2 mg/g, 39.5 mg/g, 12.6 mg/g, and 24.7 mg/g (Baccar et al., 2012). $NiFe_2O_4$/activated carbon composite was tested for the removal of IBU and KET, and experimental data fitted according to the Langmuir isotherm suggested that the adsorption capacities of material were 97.53 mg/g and 87.91 mg/g for IBU and KET, respectively. In the same study, a small review on IBU and KET adsorption capacities by different types of activated carbons was given, and ranged from 12.7 to 378.1 mg/g for IBU and from 24.7 to 400 mg/g for KET (Fröhlich et al., 2019 and references therein). Activated carbon prepared from effluent treatment plant sludge of the beverage industry had a capacity for IBU and KET uptake of 105 mg/g and 57 mg/g (based on Sips isotherm) (Streit et al., 2021).

Tomul et al. (2020) tested biochars for the removal of NAP, and compared the obtained results with NAP adsorption capacities of other adsorbents (Tomul et al., 2020, Supplementary material). The following NAP adsorption capacities were reported: biochars (4.28-324 mg/g), activated carbons (17.6-290 mg/g), metalorganic frameworks (9.16-132 mg/g), clays (0.869-37.0 mg/g), and polymeric resins (2.85-4.51 mg/g) (Tomul et al., 2020). The aminated β-cyclodextrin magnetic nanoparticles could adsorb also NAP in the amount of 1.656 mg/g (Ghosh et al., 2013; Rathi et al., 2020). The adsorption of DCF and IBU was tested using porous graphene with uptakes of 91.59 mg/g and 47.85 mg/g, respectively, and graphene oxide had capacities of 2.43 mg/g and 10.01 mg/g of DCF and IBU, respectively (Khalil et al., 2020). Singh et al. (2012) studied the adsorption of IBU by using a synthesized magnetic carbon-iron nanocomposite. The closest to experimental conditions used in this thesis was test number 10 (Table 3 from Singh et al., 2012), which had removal of 20.56% (30.84 mg/g). In this work, equilibrium runs for all four drugs gave composites adsorption capacities between 1.8 and 35 mg/g (Langmuir isotherm model, Table 4), indicating that our composites could be effective for the removal of investigated drugs. However, some of them were much effective than our composites.

4.3.1.1 Adsorption of NSAIDs by selected SMNZ in Grindstone creek water

Previous results have shown, the best adsorbent of removal of investigated NSAIDs was C-C-B. Additional equilibrium runs were performed by using this composite and Grindstone creek water as a medium instead of buffer solution. The obtained isotherms are compared with isotherms obtained for the same composite in the buffer, and results are presented in Fig. 16. Results showed that "real water" caused a decrease in the adsorption of DCF and IBU, while adsorption of NAP and KET was quite similar. These are only preliminary experiments, and the chemical content of the creek water was not determined; thus, it is very difficult to predict what was influencing the decrease of adsorption of some drugs. Hydrophobic partitioning of drugs could be affected by the presence of other organic compounds in the creek water that could also partition between surfactant tails; other organic/inorganic anions could further compete for the ion exchange sites at adsorbent surface. The differences in adsorption of some drugs in buffer solution and creek water are especially visible at the higher initial concentrations of the drugs. A possible explanation for this behavior could be that at higher drug concentrations, DCF and IBU molecules, although dominant species, compete for the same adsorption sites with compounds from creek water. For the creek water system, neither Langmuir nor Sips model worked especially well (Table S2). Despite reduced adsorption of DCF and IBU in the creek water medium, these adsorbents are still effective in removal of investigated NSAIDs. However, additional experiments are necessary to understand better the influence of other molecules/anions on the adsorption of NSAIDs, and as the next step in this research, the influence of the two inorganic anions on adsorption of investigated drugs was tested (Section 4.3.2.2).

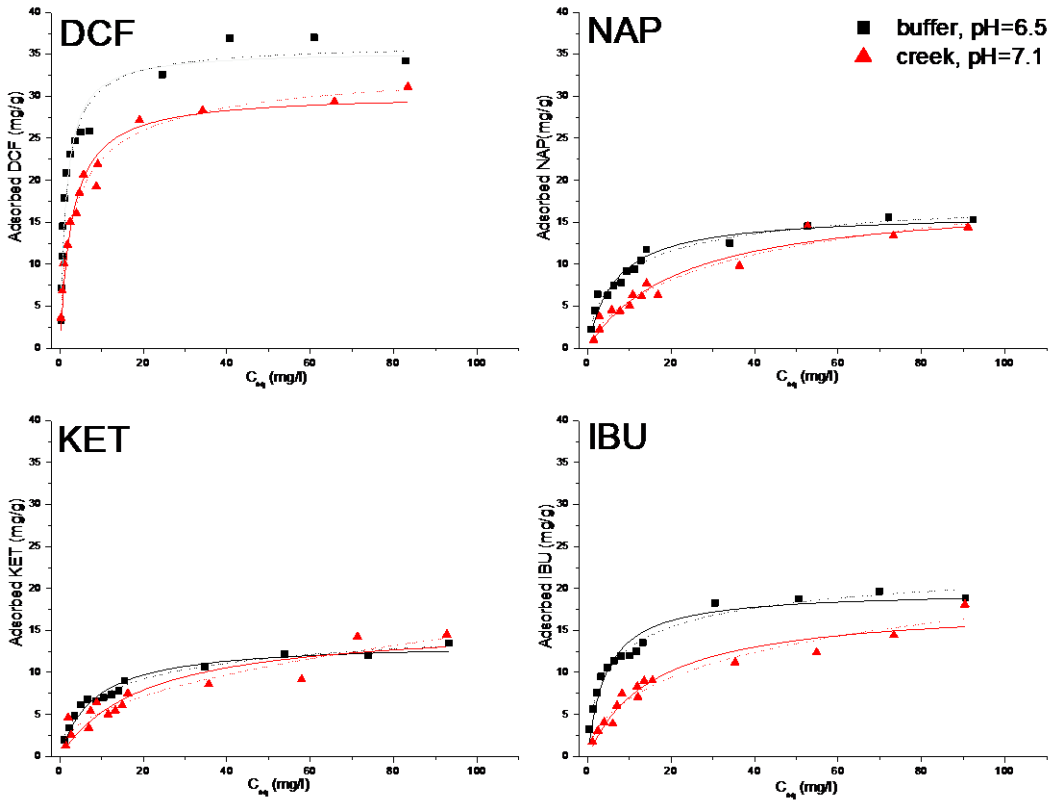

Fig. 16. *Equilibrium isotherms of C-C-B and drugs (DCF, IBU, NAP, and KET) in the buffer (red triangles) and creek water (black squares). Solid line represents Langmuir isotherm model, and dotted line is Sips isotherm model.*

4.3.2 Kinetic runs

4.3.2.1 Kinetic runs conducted in distilled water

Kinetic runs (Figs. 17 and 18) for all drugs were performed with their initial concentration of 20 mg/L. Depending on the adsorbent-adsorbate combination, the time to reach equilibrium was around 20-30 min. Kinetic runs confirmed the adsorption order previously reported in Section 4.3.1: X-C-B > X-A-B > X-C-M > X-A-M, where X is C and/or P representing IZ CLI and PHIL75, respectively. The exception from this rule was noticed in KET adsorption when X-A-B and X-C-B had switched positions in the above-given order.

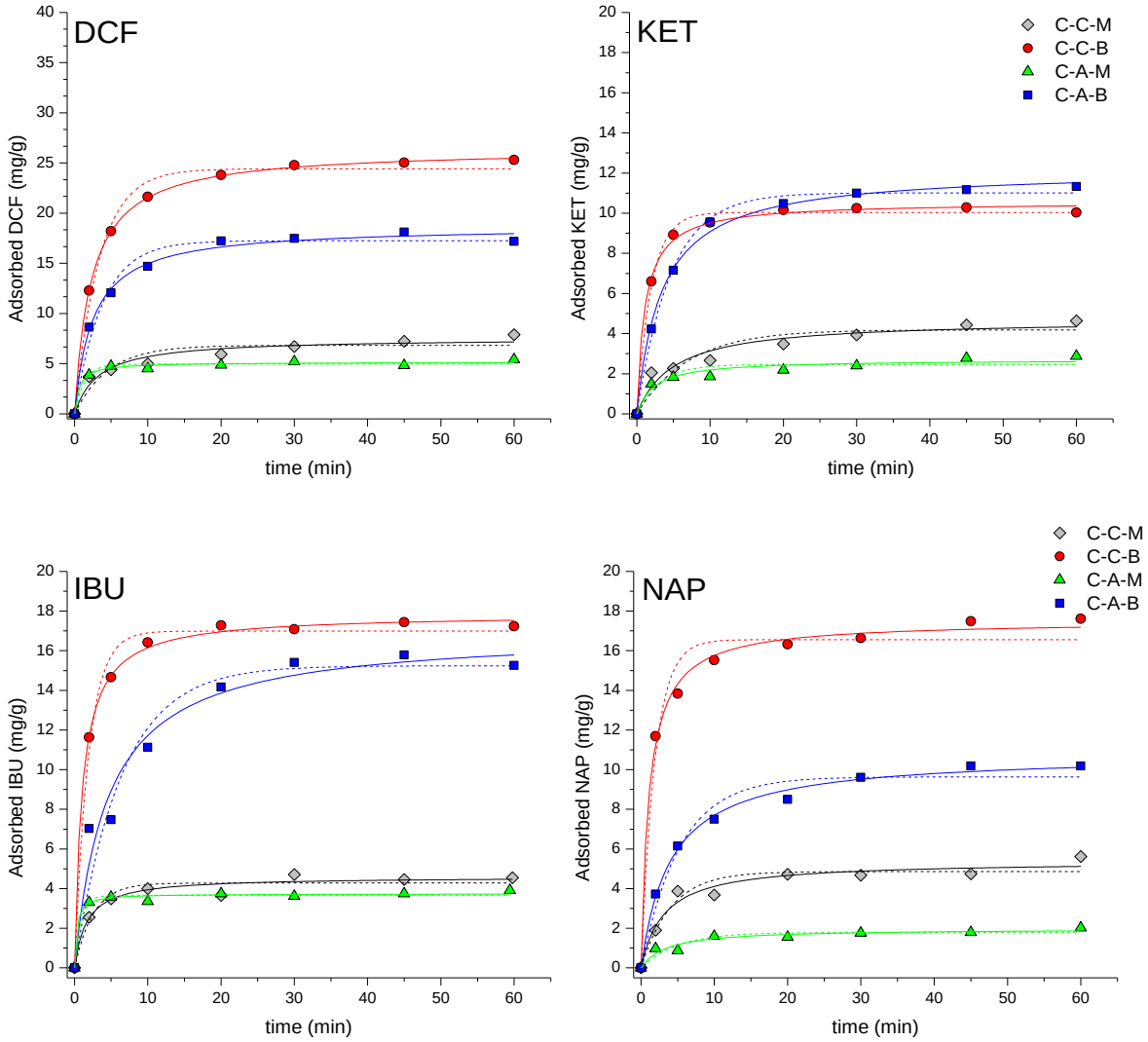

Fig. 17. *Kinetic runs for composites of IZ CLI: DCF (upper left; y-axes scale is from 0-40 mg/g), KET, IBU, and NAP (upper right, bottom left and bottom right, respectively; y-axes scale is from 0-20 mg/g). Two mathematical models were represented with dotted line (pseudo-first order) and solid line (pseudo-second order). Published in Smiljanić et al. (2020, 2021).*

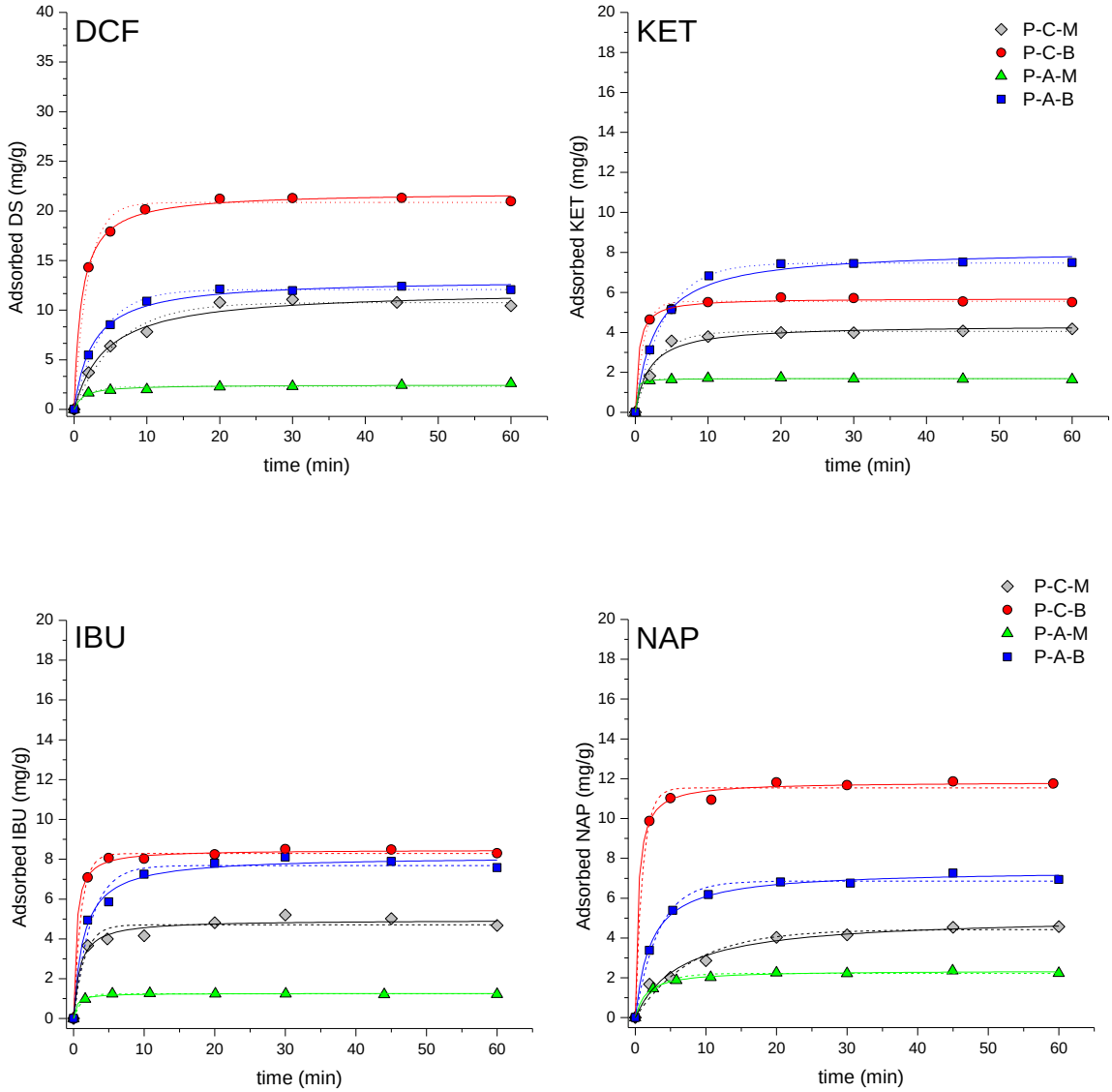

Fig. 18. *Kinetic runs for composites of PHIL75: DCF (upper left; y-axes scale is from 0-40 mg/g), KET, IBU, and NAP (upper right, bottom left and bottom right, respectively; y-axes scale is from 0-20 mg/g). Two mathematical models were represented with dotted line (pseudo-first order) and solid line (pseudo-second order). Published in Smiljanić et al. (2020, 2021).*

The adsorption process as a function of time is described by the kinetic equation of the specific order. A model that fits experimental data well can be used to describe the adsorption mechanism and reaction rate-limiting step. According to literature, the adsorption of the drug by SMNZs generally follows the pseudo-first order (PFO) (Eq. 5) and pseudo-second order (PSO) (Eq. 6) kinetics (Bowman, 2003; de Gennaro et al., 2015; Ho, 2006, 2004; Serri et al., 2016). Both models assume that the interaction between solute/adsorbate and the adsorbent surface is the rate-limiting step in the adsorption process. PSO model assumes that there is a

collision between two independent unoccupied sites on the adsorbent (in the equation for PSO, for this reason, exists squared term) (Hubbe et al., 2019). Pseudo-first order and pseudo-second order kinetic models are expressed as:

$$Q_t = Q_m(1 - e^{-K_1 t}) \quad \text{(Eq. 5)}$$

$$Q_t = \frac{K_2 Q_m^2 t}{1 + K_2 Q_m t} \quad \text{(Eq. 6)}$$

where Q_t is the amount of drug-loaded by SMNZ (mg/g) as a function of time *t* (min), Q_m is the drug concentration at equilibrium, K_1 and K_2 are the pseudo-first and the pseudo-second order constants, respectively. In the same way as in the case of isotherm models, to estimate the goodness - of - fit correlation coefficient (R^2), AIC and AIC*w* were used (Table 7 a and b).

Based on the AIC (AIC*w),* 26 out of 32 kinetic runs indicate the validity of the pseudo-second order model for drug adsorption by SMNZs. All clinoptilolite-based composites favored PSO, whereas, for few phillipsite composites, PFO worked slightly better (P-C-M, P-A-M, and P-A-B). In almost all cases, both used models had similar and satisfyingly high R^2 (which is in good agreement with the AIC*w* parameter).

Taking into account the nature of SMNZs and simultaneous ionic exchange and hydrophobic partitioning as two mechanisms of sorption, it is hard to determine the rate-limiting step for these systems. The initial concentration, pH value and temperature are conditions that have an influence on the parameters K_1 and K_2. Since the experiments were conducted at room temperature, using single initial concentration without controlling pH value, these parameters will not be discussed. On the other hand, Q_m values are slightly higher for the PSO comparing to PFO as the consequence of mathematical equations.

Hubbe et al. (2019), in the review article, reported some interesting issues connected to PSO (Hubbe et al., 2019). They explained that PSO does not correspond to any specific physical situation, and it happens to be able to fit typical adsorption data as an approximation. Actually, a good fit can be a consequence of the mathematic approach: PFO has an asymptote for longer experimental times ($t \rightarrow \infty$), whereas PSO does not have this limitation (Hubbe et al., 2019; Plazinski et al., 2009). For this reason, if there are no enough early-time data points (and equilibrium points prevail), PSO could be favored from the goodness-of-fit aspect (Plazinski et al., 2009). Another important factor is the initial adsorbate concentration. If this

concentration is high enough, and bulk concentration does not change significantly during the experiment, PFO should give a good fit. On the other hand, when the change in bulk concentration is significant, the PSO equation should be better (Azizian, 2004).

The two chosen models are considered simple kinetic models that do not describe the actual rates and mechanisms of sorption systems when surfaces are inhomogeneous and simultaneous transport and chemical phenomena occur. Therefore, a good correlation between these models and experimental data is a useful tool for prediction and comparison, but it will not likely predict the true reaction rate or mechanism (Coleman et al., 2006).

Table 7 a). *Mathematical models of kinetic runs: parameters and goodness - of - fit*

Drug	**Sample**	**Model**	**Parameters**			**Goodness - of – fit**			***RE (%)**
			K_1 (min^{-1})	K_2 (g mg^{-1} min^{-1})	Q_{max} (mg/g)	R^2	AIC	AIC*w*	
DCF	C-C-M	PFO	0.22±0.07		6.8±0.5	0.874	7.88	0.038	20.11
		PSO		0.04 ±0.02	7.6±0.5	0.944	1.33	0.964	
	C-C-B	PFO	0.29±0.03		24.4±0.5	0.987	10.11	0.001	64.76
		PSO		0.0167 ±0.0004	26.43±0.09	0.999	-22.69	0.999	
	C-A-M	PFO	0.8±0.2		5.0±0.2	0.972	-9.91	0.193	13.90
		PSO		0.30±0.09	5.2±0.2	0.980	-12.77	0.807	
	C-A-B	PFO	0.27±0.04		17.3±0.5	0.977	8.79	0.006	44.33
		PSO		0.021 ±0.003	18.7±0.4	0.994	-1.33	0.994	
	P-C-M	**PFO**	0.17±0.02		10.8±0.3	0.982	-0.12	0.987	26.78
		PSO		0.019 ±0.004	12.0±0.5	0.979	8.85	0.013	
	P-C-B	PFO	0.52±0.06		20.9±0.4	0.989	5.40	0.001	52.88
		PSO		0.044 ±0.004	21.9±0.3	0.998	-7.78	0.999	
	P-A-M	PFO	0.5±0.2		2.3±0.1	0.934	-14.93	0.020	6.65
		PSO		0.34 ±0.09	2.48±0.08	0.975	-22.68	0.980	
	P-A-B	**PFO**	0.26±0.02		12.1±0.2	0.995	-8.85	0.809	30.69
		PSO		0.030 ±0.004	13.1 ±0.3	0.993	-5.96	0.191	
KET	C-C-M	PFO	0.14±0.05		4.2±0.4	0.870	0.16	0.066	11.70
		PSO		0.04±0.02	4.7±0.4	0.933	-5.12	0.933	
	C-C-B	PFO	0.51±0.04		10.0±0.2	0.994	-11.01	0.097	25.34
		PSO		0.086±0.009	10.6±0.2	0.997	-15.45	0.903	
	C-A-M	PFO	0.3±0.2		2.5±0.2	0.853	-7.08	0.054	7.23

		PSO		0.16±0.06	2.7±0.2	0.928	-12.81	0.946	
	C-A-B	PFO	0.21±0.02		11.0±0.2	0.995	-10.97	0.336	28.57
		PSO		0.024±0.003	12.2±0.2	0.996	-12.34	0.664	
	P-C-M	**PFO**	0.34±0.04		4.06±0.08	0.989	-20.27	0.982	10.53
		PSO		0.12±0.03	4.4±0.2	0.971	-12.22	0.018	
	P-C-B	PFO	0.9±0.1		5.55±0.07	0.993	-18.96	0.045	13.88
		PSO		0.38±0.06	5.71±0.06	0.997	-25.07	0.955	
	P-A-M	**PFO**	1.4±0.2		1.68±0.02	0.997	-44.37	0.525	4.15
		PSO		4.5±0.7	1.70±0.02	0.997	-44.17	0.475	
	P-A-B	**PFO**	0.25±0.01		7.47±0.06	0.998	-25.36	0.999	18.96
		PSO		0.044±0.007	8.2±0.2	0.990	-10.70	0.001	

*Smiljanić et al., 2020

Table 7 b). *Mathematical models of kinetic runs: parameters and goodness - of - fit*

Drug	**Sample**	**Model**	**Parameters**			**Goodness - of - fit**			***RE (%)**
			K_1 (min $^{-1}$)	K_2 (g mg $^{-1}$ min $^{-1}$)	Q_{max} (mg/g)	R^2	AIC	AIC*w*	
IBU	C-C-M	PFO	0.40±0.09		4.3±0.2	0.945	-6.38	0.116	10.68
		PSO		0.13±0.04	4.6±0.2	0.967	-10.44	0.884	
	C-C-B	PFO	0.52±0.05		17.0±0.3	0.990	1.43	0.001	43.09
		PSO		0.053±0.004	17.8±0.2	0.998	-14.14	0.999	
	C-A-M	PFO	1.2±0.3		3.66±0.08	0.982	-18.45	0.208	9.21
		PSO		0.9±0.4	3.74±0.08	0.987	-21.12	0.792	
	C-A-B	PFO	0.16±0.03		15.2±0.8	0.943	14.31	0.132	35.78
		PSO		0.013±0.004	17.0±0.9	0.964	10.55	0.868	
	P-C-M	PFO	0.7±0.2		4.7±0.2	0.944	-5.08	0.053	11.69
		PSO		0.24±0.08	5.0±0.2	0.973	-10.83	0.947	
	P-C-B	PFO	0.96±0.08		8.29±0.08	0.996	-18.04	0.088	20.70
		PSO		0.31±0.05	8.48±0.07	0.998	-22.71	0.912	
	P-A-M	**PFO**	0.94±0.05		1.240±0.008	0.998	-54.37	0.999	3.08
		PSO		1.9±0.5	1.27±0.03	0.990	-40.73	0.001	
	P-A-B	PFO	0.41±0.07		7.7±0.3	0.968	-18.04	0.088	18.89
		PSO		0.09±0.02	8.1±0.2	0.988	-22.71	0.912	

NAP	C-C-M	PFO	0.25±0.06		4.9±0.3	0.931	-1.94	0.151	13.36
		PSO		0.06±0.02	5.4±0.2	0.995	-5.40	0.849	
	C-C-B	PFO	0.53±0.09		16.6±0.5	0.970	9.85	0.001	45.19
		PSO		0.7±0.2	19±3	0.995	-5.06	0.999	
	C-A-M	PFO	0.20±0.06		1.8±0.2	0.880	-13.77	0.169	5.36
		PSO		0.15±0.06	2.0±0.2	0.919	-16.96	0.831	
	C-A-B	PFO	0.19±0.03		9.6±0.4	0.968	2.53	0.001	25.94
		PSO		0.023±0.003	10.8±0.2	0.995	-11.78	0.999	
	P-C-M	PFO	0.13±0.03		4.4±0.2	0.960	-8.17	0.089	10.35
		PSO		0.031±0.007	5.1±0.3	0.978	-12.83	0.911	
	P-C-B	PFO	1.0±0.2		11.5±0.2	0.992	-6.61	0.017	29.56
		PSO		0.21±0.04	11.8±0.2	0.997	-14.69	0.983	
	P-A-M	PFO	0.38±0.05		2.22±0.05	0.982	-26.39	0.004	5.34
		PSO		0.27±0.03	2.37±0.04	0.995	-37.18	0.996	
	P-A-B	PFO	0.30±0.03		6.9±0.2	0.989	-12.07	0.033	17.38
		PSO		0.062±0.006	7.4±0.2	0.995	-18.86	0.967	

*Smiljanić et al., 2021

For the relative comparison of the composites' effectiveness in the removal of drugs, removal efficiencies (RE) were calculated (Eq. 7) and given in Table 7.

$$\text{RE}\ (\%) = \frac{100\ (C_0 - C_f)}{C_0} \qquad \text{(Eq. 7)}$$

where C_0 and C_f are the initial and final drug concentrations (the last measured point), respectively. Here should be emphasized that in Eq. 7, there is no influence of the mass of the adsorbent. So when compared with other RE reported in the literature, experimental conditions are of great importance. Under the experimental conditions used in this study (C_0 = 20 mg/L, solution volume 1 L, and mass of adsorbent 0.5 g), RE was in the range 3.08-64.76 % (Table 6). The highest drug removal rate was recorded for DCF (6.65-64.75% depending on composite), while results for IBU, KET, and NAP are lower and more similar. Considering surfactant coverage, bilayer composites had higher RE values.

4.3.2.2 Interference of sulfates and bicarbonates on kinetics: the case of ibuprofen and naproxen

Kinetic runs carried out for IBU and NAP adsorption by SMNZs in the presence of sulfates and bicarbonates were compared with kinetics performed in distilled water (Section 4.3.2.1.) and presented in Figs. 19-22. Composites containing bilayer of surfactants (Figs. 19 and 20, respectively) have shown a decrease in IBU and NAP adsorption. Since in bilayers the ion exchange exists as an adsorption mechanism, other inorganic anions probably compete with anionic form of both drugs for the same adsorption sites reducing, as a consequence, the adsorption of IBU or NAP (Fig. 23). Similar behavior was evidenced for chromate removal by SMNZs (clinoptilolite modified with 200 mmol/kg HDTMA-Br) in the presence of sulfates and nitrates, where it was shown that sulfates and nitrates competed with chromates for the same active sites on the adsorbent (Li et al., 1998a). Another case was reported in the study when the adsorption of perchlorates on the SMNZs (clinoptilolite-rich rock modified with 219 mmol/kg of HDTMA-Br) was interfered with by nitrates (Zhang et al., 2007).

Kinetics were modeled by PFO and PSO, and parameters were reported in Table S3. For simplicity reasons, on Figs. 19-22, the only model with a better fit – PSO was plotted. From Fig. 19, it can be seen that IBU adsorption on bilayer composites decreased in the presence of inorganic anions (according to Tables 6 b), and S3: RE changed from 43.09% to 28.02%, from 35.78% to 16.14%, and from 18.89% to 11.13%, for C-C-B, C-A-B, and P-A-B, respectively, as aforementioned, due to the adsorption of such anions on the same active sites where drug molecules are usually adsorbed. However, the same decrease in adsorption was not observed for the P-C-B composite (20.70% ≈ 21.51%). A possible explanation for this is the specific combination of IBU-phillipsite-bilayered CPyCl, where the particular arrangement of the P-C-B composites` components will promote adsorption of IBU instead of other anions. The same adsorbents in combination with another drug (NAP) have shown a decrease when inorganic anions are present – from 45.19 to 32.03 %, 25.94 to 16.32 %, 29.56 to 20.91 %, and 17.38 to 9.4 %, for C-C-B, C-A-B, P-C-B, and P-A-B, respectively (Fig. 20).

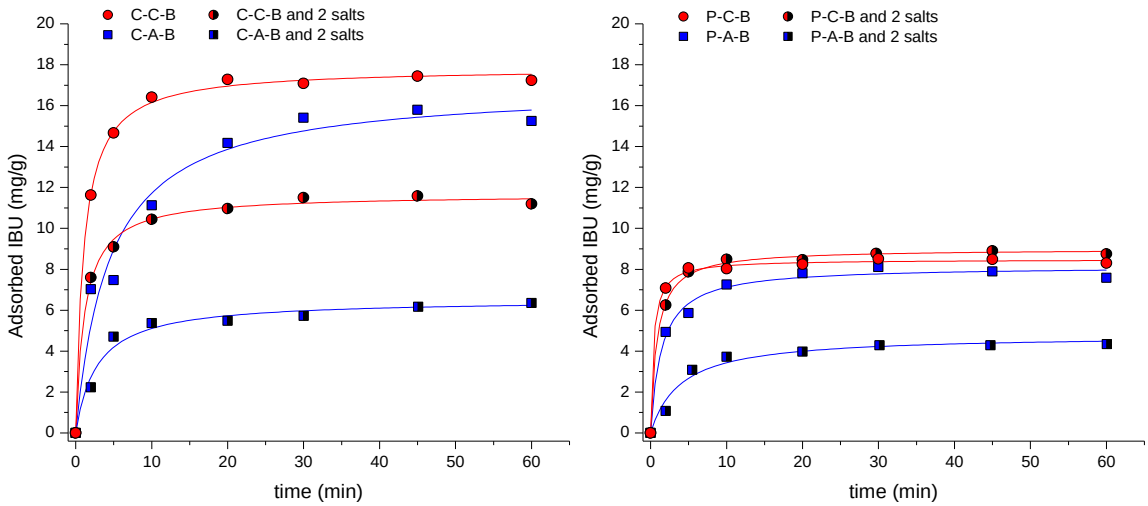

Fig. 19. *Kinetic runs for IBU: bilayer composites C-C-B and C-A-B (on the left) and bilayer composites P-C-B and P-A-B (on the right). Systems without salts added are represented with full-colored symbols, while kinetics in a mixture of two salts are represented using half-black symbols. The pseudo-second order is represented with a solid line. (Smiljanić et al., 2021).*

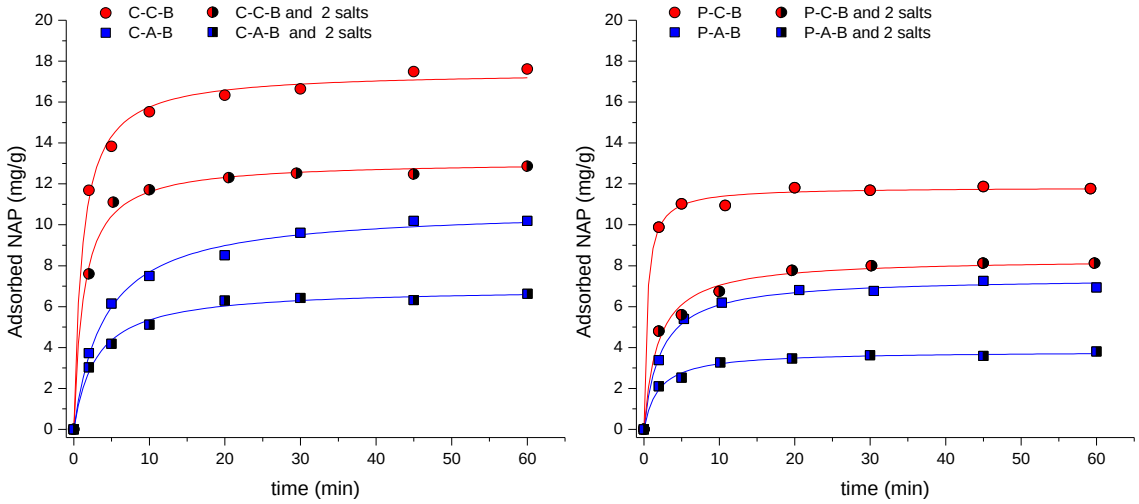

Fig. 20. *Kinetic runs for NAP: bilayer composites C-C-B and C-A-B (on the left) and bilayer composites P-C-B and P-A-B (on the right). Systems without salts added are represented with full-colored symbols, while kinetics in a mixture of two salts are represented using half-black symbols. The pseudo-second order is represented with a solid line. (Smiljanić et al., 2021).*

The adsorption of drugs by monolayer composites was only slightly affected by the presence of sulfates and bicarbonates (Figs. 21 and 22) since drugs are mainly hydrophobically

partitioned between the hydrophobic tails of surfactant molecules, and comparing to bilayers, there is no many active sites for which inorganic anions and drugs could compete. In cases of composites prepared with CPyCl, C-C-M and P-C-M, the addition of two salts did not significantly change the adsorption of IBU (RE changed from 10.68 to 11.30%, and from 11.69 to 11.61% for C-C-M and P-C-M, respectively) (Fig. 21). Monolayers with ARQ evidenced a small decrease in IBU adsorption for the C-A-M composite (9.21 to 6.70 %) and a small increase for P-A-M (from 3.08 to 5.69%). In the case of NAP (Fig. 22), monolayer composite C-C-M showed a small decrease in adsorption (from 13.36 to 10.30%), a slight increase for C-A-M and P-C-M composites (5.36 to 6.72 %, and 10.35 to 13.22%, respectively), while for P-A-M, adsorption of NAP has not changed significantly (5.34 % ≈ 5.81%).

It is not easy to predict what is the exact reason for this behavior. A comparison between IBU and NAP adsorption by all monolayer composites in the presence of anions provides insufficient data necessary to identify any pattern in behavior, pointing that each drug-adsorbent-salt system has some specific interactions.

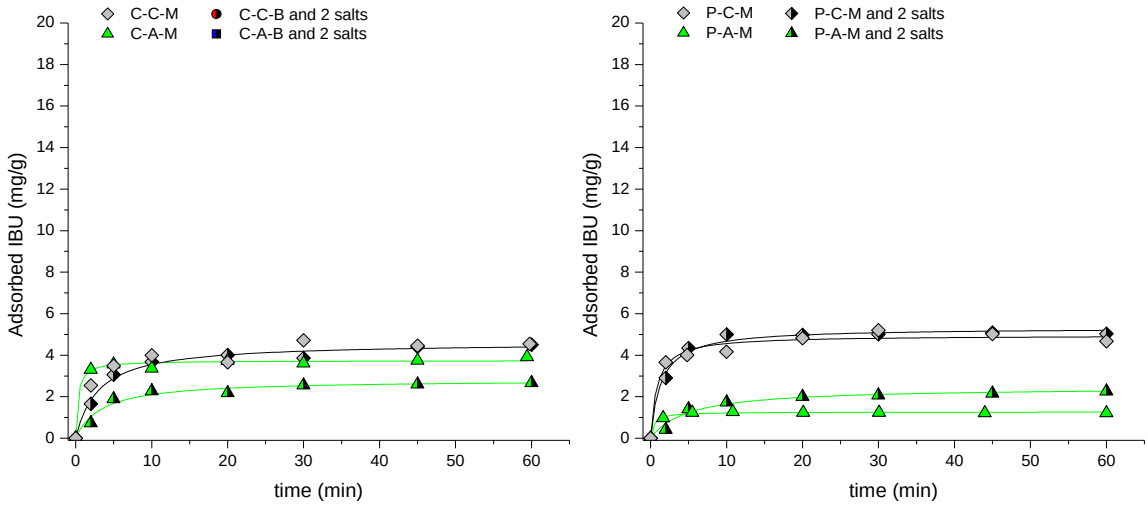

Fig. 21. *Kinetic runs for IBU: monolayer composites C-C-M and C-A-M (on the left) and monolayer composites P-C-M and P-A-M (on the right). Systems without salts added are represented with full-colored symbols, while kinetics in a mixture of two salts are represented using half-black symbols. The pseudo-second order is represented with a solid line. (Smiljanić et al., 2021).*

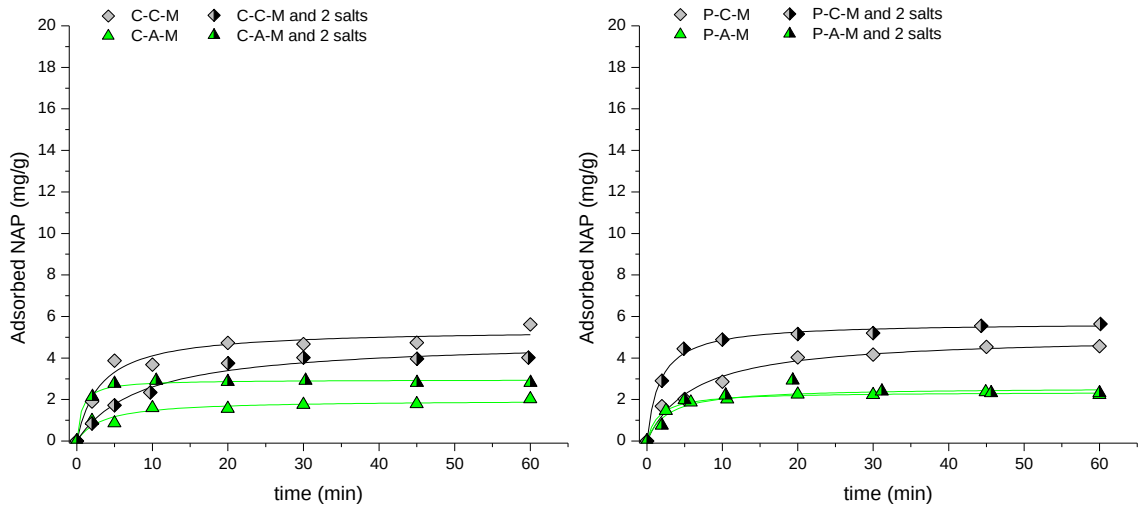

Fig. 22. *Kinetic runs for NAP: monolayer composites C-C-M and C-A-M (on the left) and monolayer composites P-C-M and P-A-M (on the right). Systems without salts added are represented with full-colored symbols, while kinetics in a mixture of two salts are represented using half-black symbols. The pseudo-second order is represented with a solid line. (Smiljanić et al., 2021)*

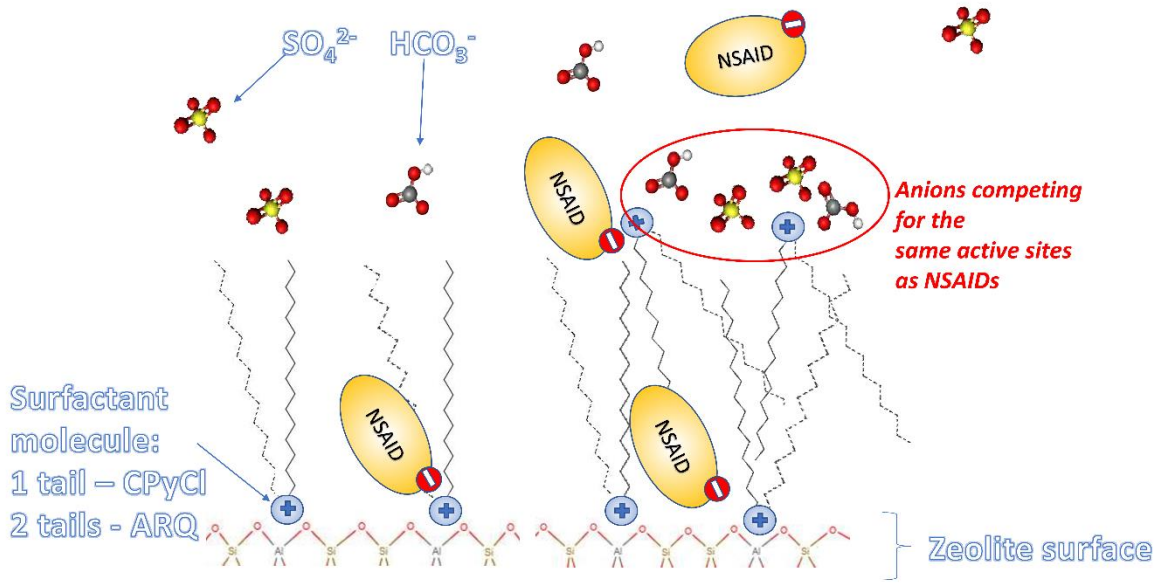

Fig. 23*. Scheme of the competitive adsorption of inorganic anions with NSAID in the case of monolayer formation (on the left) and bilayer formation (on the right). (Smiljanić et al., 2021)*

4.3.2.3 Adsorption of drugs by activated charcoal

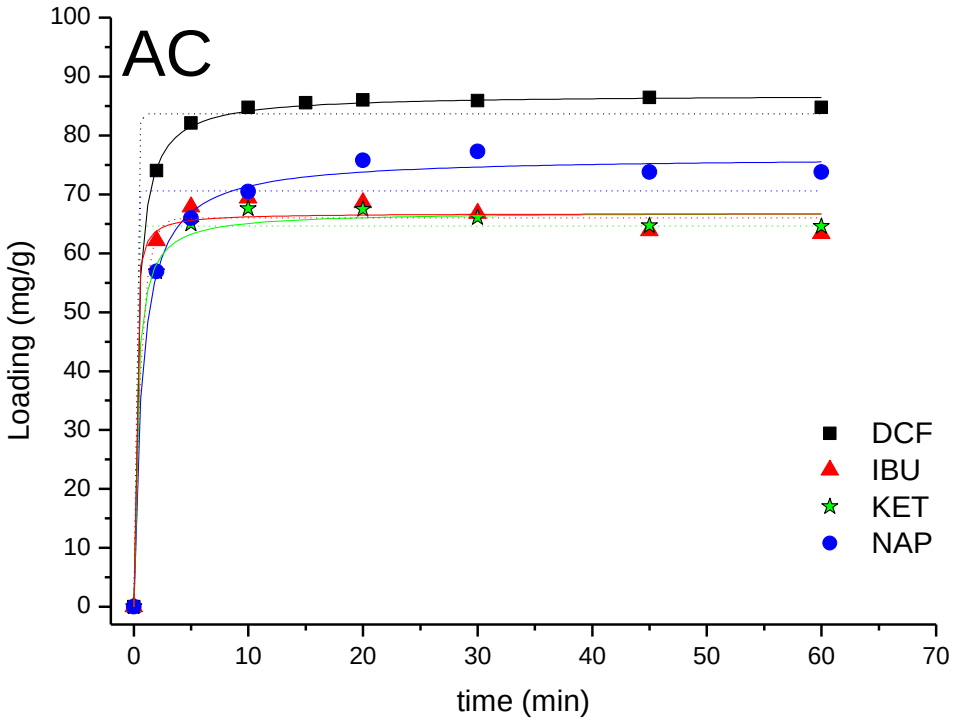

Fig. 24. *Kinetics run for activated charcoal (AC) and NSAIDs (DCF, KET, IBU, and NAP). Dotted line (pseudo-first order model); solid line (pseudo-second order model).*

Kinetics experiments were performed for the adsorption of all four drugs by activated charcoal. PFO and PSO kinetic models were used to fit the experimental data, and obtained values are given in Table S4. The removal efficiencies when activated charcoal was used as adsorbent were 84.73%, 81.89%, 81.21%, and 87.34% for DCF, IBU, KET, and NAP, respectively (Table S4). The initial concentration of drugs was 20 mg/L, solution volume 1 L, and the mass of adsorbent was 0.25 g. Since the masses of adsorbents during the kinetic runs were different, to compare results obtained for AC with results obtained for the best performing SMNZ – C-C-B, the last measured point from kinetic curves at Figs. 17, 18, and 24 (calculated in mg of drugs per g of adsorbent) were considered instead of RE. Their ratios evidenced the better performances of AC, which adsorbed 3.35, 3.68, 6.43, and 4.19 times more DCF, IBU, KET, and NAP, respectively, thus confirming the much higher adsorption capacities of activated charcoals/carbons as reported in the literature and previously summarized in section 4.3.1.

Another important aspect for the possible application of adsorbents is their price. In many papers, it is stressed that natural zeolites are abundant and low-cost minerals and that can even be single-use sorbent (Inglezakis and Zorpas, 2012; Onyango et al., 2011; Torabian et al., 2010). However, surfactant, as another component necessary for the production of SMNZs, should be taken into consideration. On the laboratory scale, for the preparation of 100 g of C-C-B, it was necessary to use 100 g of clinoptilolite-rich tuff (for simplicity of calculation, the price of NZs was not considered, but the information about the price range is given in section 1.2.1.2) and 6.444 g of CPyCl (commercial price is around 500 €/kg, Sigma Aldrich). So, the production cost of SMNZ is 0.033 €/g of C-C-B. The cost of AC used for this experiment was around 0.025 €/g, and the removal performance was at least three times better. The price of ARQ is much lower, so the cost for the preparation of C-A-B is around 0.01 €/g. Since this study shows that natural zeolites modified with surfactant could be successfully used for the removal of different drugs, further experiments should be focused on the improvement of drug adsorption capacities on modification processes by using cheaper and/or lower amounts of surfactants. As previously mentioned, the advantage of SMNZs is that they preserve their ability to sorb cations, enabling them to remove not only drug molecules but also other pollutants. Also, maybe some new applications, like separation of anionic species/drugs, will be considered for which SMNZs could have great potential. And lastly, the final decision about the efficiency-cost ratio should be made for the specific system when all parameters are taken into consideration.

4.3.2.4 Characterization after adsorption of NSAIDs

4.3.2.4.1 Zeta potential

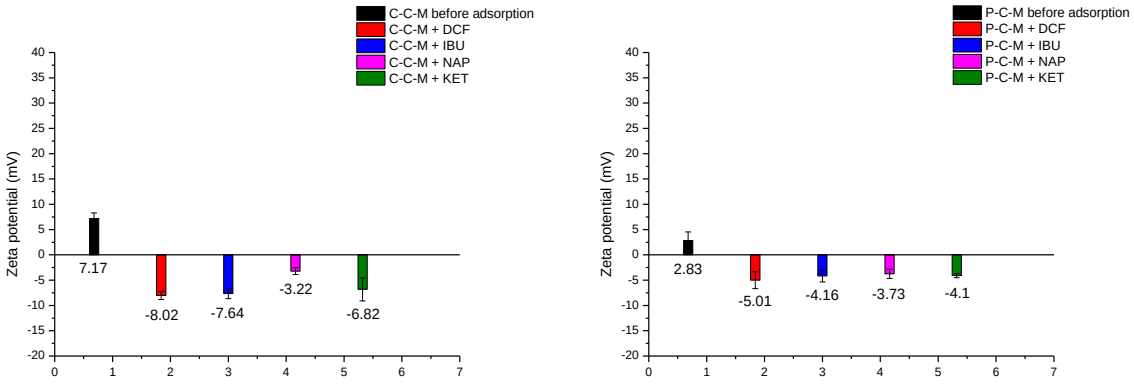

Fig. 25. *Graphical representation of zeta potential for C-C-M (on the left) and P-C-M (on the right) before and after adsorption of NSAIDs (DCF – red, IBU – blue, NAP – magenta, KET – olive green).*

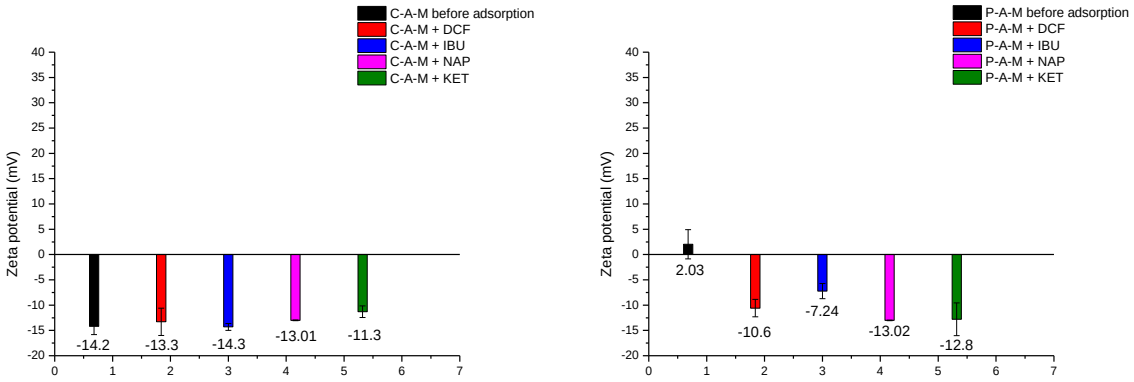

Fig. 26. *Graphical representation of zeta potential for C-A-M (on the left) and P-A-M (on the right) before and after adsorption of NSAIDs (DCF – red, IBU – blue, NAP – magenta, KET – olive green).*

Both composites with monolayers prepared with CPyCl have changed zeta potential from slightly positive to slightly negative (Fig. 25). Most likely, after drug adsorption, some parts of drug molecules were oriented in a way that increased the negative charge of the particles. For all drugs, similar behavior was noticed. The same behavior was also recorded for ARQ monolayers, with the sole difference that C-A-M had negative zeta potential even before adsorption (Fig. 26). This could imply that there no adsorption occurred. However, the removal

efficiencies for the C-A-M were higher than for P-A-M. Considering zeta potential and REs from Table 7, no connection was noticed.

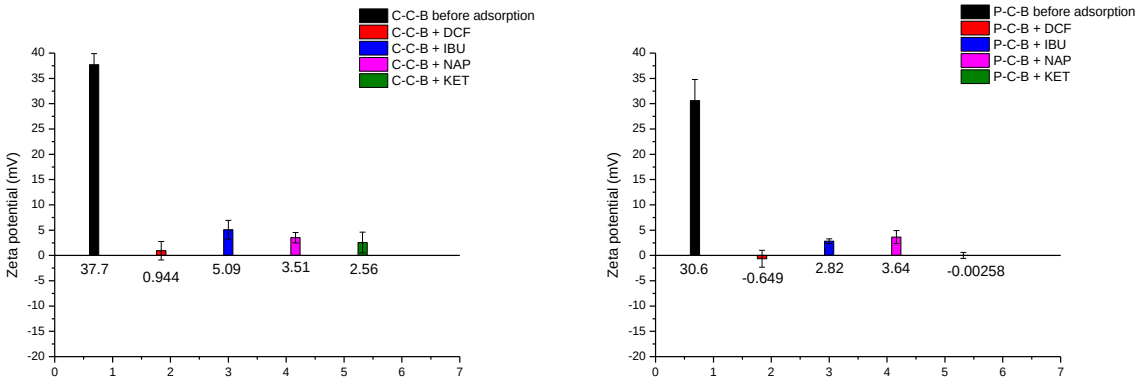

Fig.27. *Graphical representation of zeta potential for C-C-B (on the left) and P-C-B (on the right) before and after adsorption of NSAIDs (DCF – red, IBU – blue, NAP – magenta, KET – olive green).*

Composites with bilayer prepared with CPyCl, have changed their zeta potential from positive (before adsorption) to slightly positive, to almost neutral potential (Fig. 27). This could imply that drug molecules uniformly covered the surface of bilayer composites, compensating the surface charge. Again no connection between zeta potential values and the RE was observed. This could mean that C-C-B/P-C-B have a certain number of active sites on the bilayer surface onto which anionic part of drug molecules could be ion-exchanged, and all four drugs will exchange in similar amounts, while hydrophobic partitioning will make the total RE of drugs differ between each other.

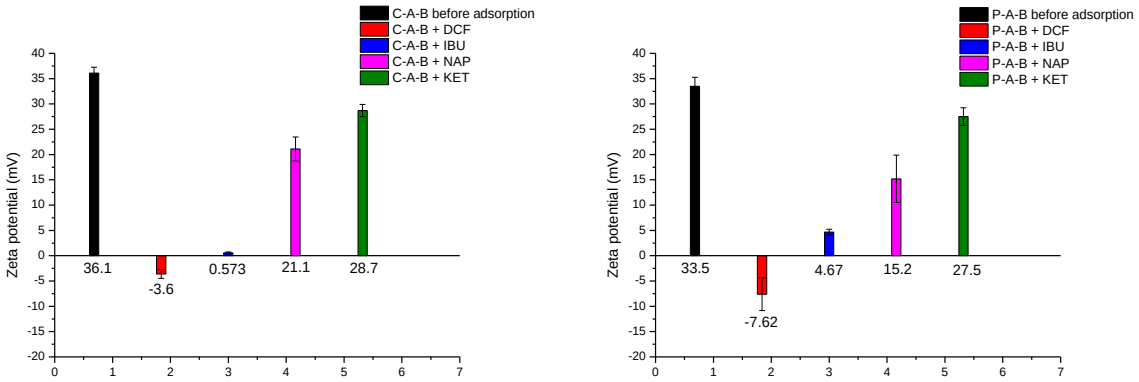

Fig.28. *Graphical representation of zeta potential for C-A-B (on the left) and P-A-B (on the right) before and after adsorption of NSAIDs (DCF – red, IBU – blue, NAP – magenta, KET – olive green).*

For composite with bilayers prepared using ARQ, different behavior between drugs was noticed (Fig. 28). Adsorption of DCF changed zeta potential to negative, compared to C-C-B and P-C-B when adsorption of DCF changed surface charge to neutral (Fig. 27). However, this should not be considered as an indication of the higher DCF uptake, since in previously reported in Table 6 that C-C-B and P-C-B had higher uptakes comparing to C-A-B and P-A-B, respectively. IBU defines an almost neutral surface (similar to the case of composite with CPyCl bilayers), while adsorption of NAP and KET does not modify the positive surface charge of the composite containing ARQ bilayer. Unfortunately, at the moment, the exact reason for such a behavior is unknown. Still, it confirms the presence of the drugs in SMNZs and points that drug adsorption may be dependant on surfactant type and its organization at the zeolite surface, as well as on the specific interactions with drugs.

4.3.2.4.2 ATR-FTIR

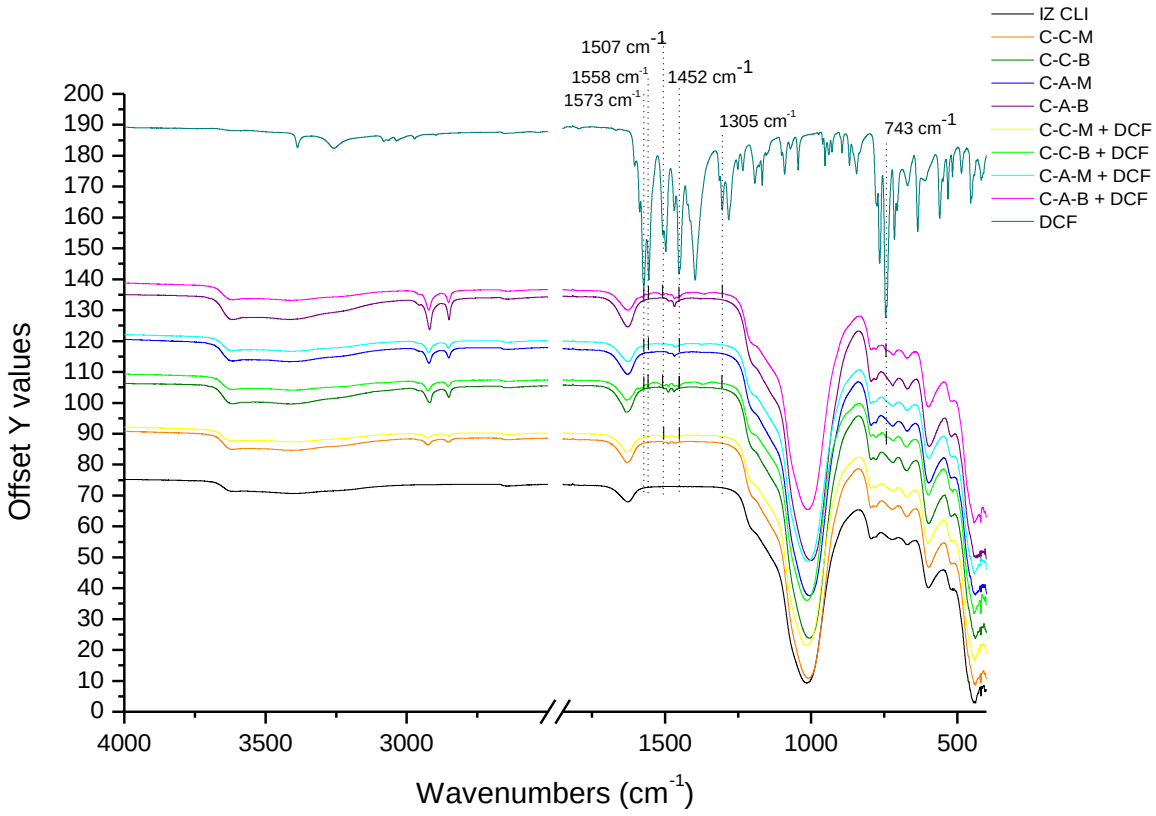

Fig. 29. *ATR–FTIR spectra of DCF, starting material IZ CLI and its composites (C-C-M, C-C-B, C-A-M and C-A-B) before and after adsorption of DCF.*

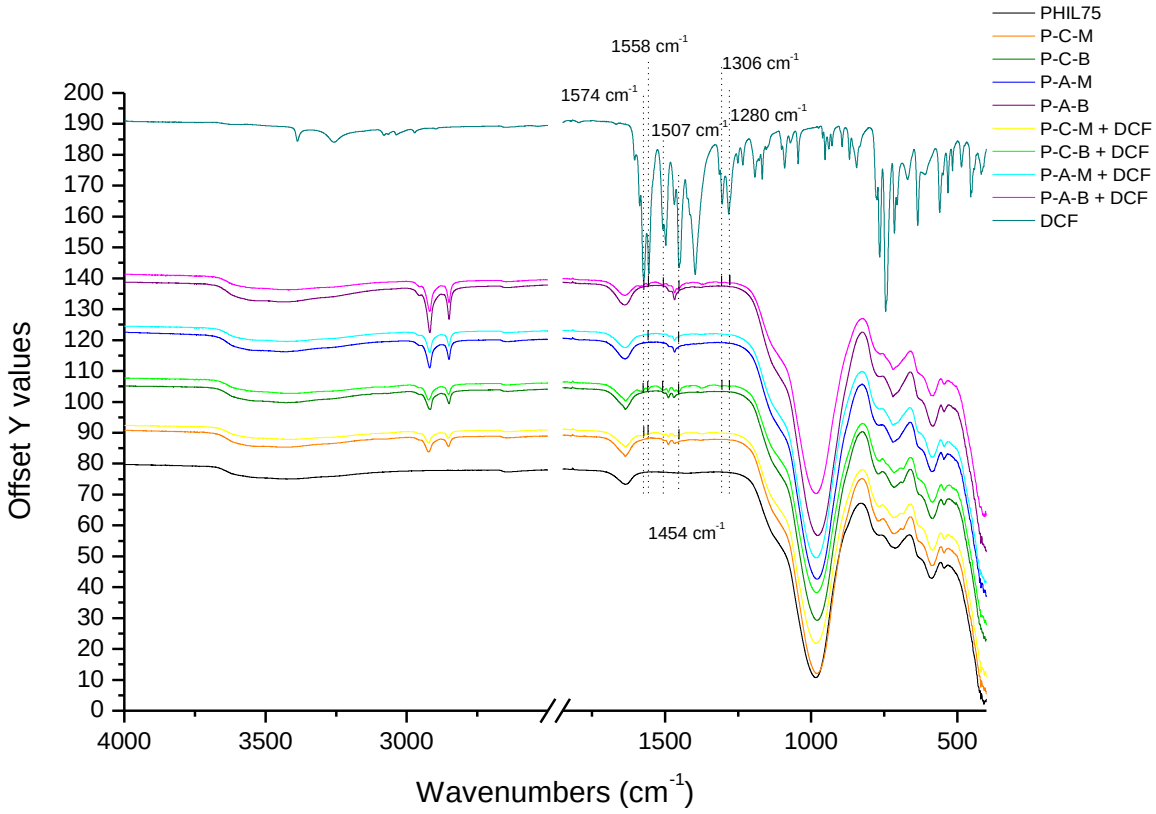

Fig. 30. *ATR–FTIR spectra of DCF, starting material PHIL75 and its composites (P-C-M, P-C-B, P-A-M, and P-A-B) before and after adsorption of DCF.*

Comparison of spectra of pure DCF and composites before and after adsorption of this drug have shown the presence of low-intensity peaks belonging to DCF in spectra of composites, confirming the presence of drug at the surface of adsorbent.

Thus, peaks at 1573 cm^{-1}, 1558 cm^{-1}, 1507 cm^{-1}, and 1452 cm^{-1}, 1305 cm^{-1}, and 742 cm^{-1} appearing in IZ CLI composites after DCF adsorption belong to the DCF, confirming the adsorption of this drug (Fig. 29). Intensities of these peaks increased in composites with bilayer formation C-C-B + DCF and C-A-B + DCF, confirming the results of kinetic runs and the highest adsorption of DCF in bilayer composites. On the contrary, monolayer composites have shown only two or three of the mentioned peaks confirming lower adsorption of this drug by these SMNZs.

Similarly, peaks at 1574 cm^{-1}, 1558 cm^{-1}, 1507 cm^{-1}, and 1454 cm^{-1}, 1306 cm^{-1} have appeared in PHIL75 composites after adsorption of DCF (Fig. 30). Bilayers after adsorption were showing all these peaks while monolayers were showing only peaks at 1574 cm^{-1}, 1558 cm^{-1}, and 1454 cm^{-1}.

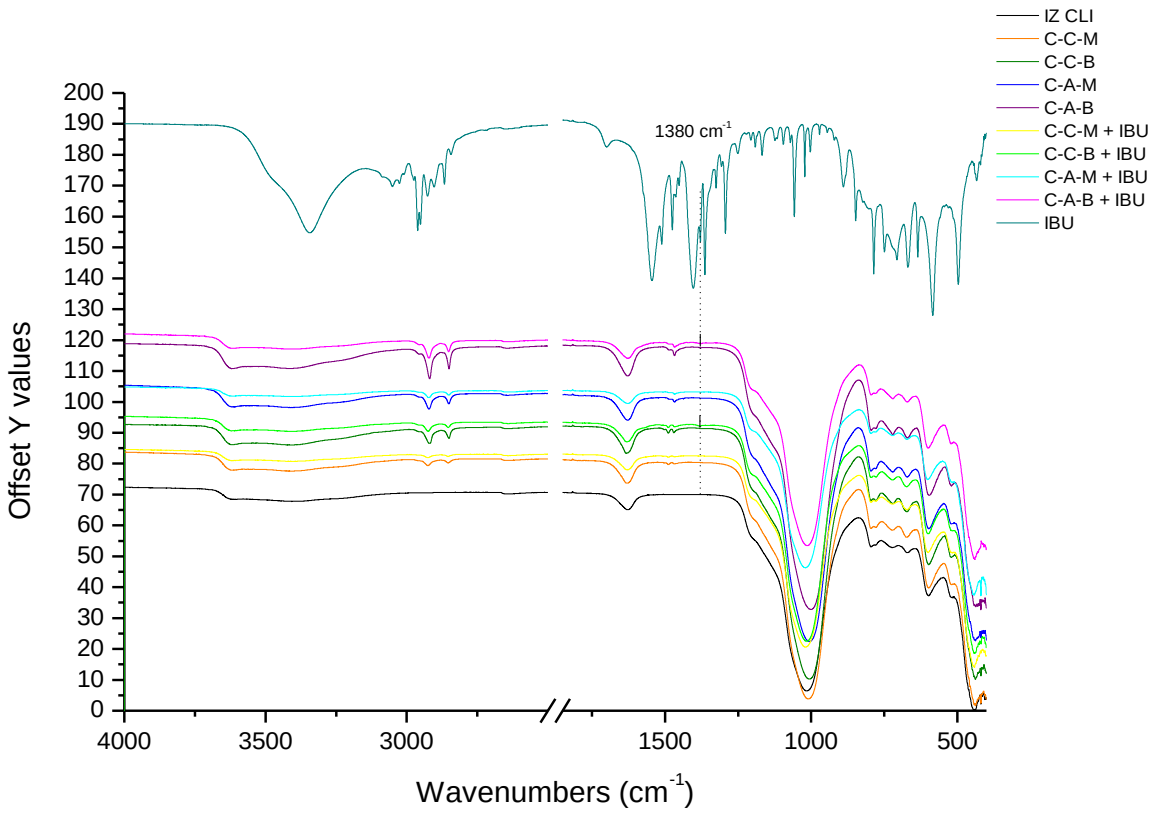

Fig. 31. *ATR–FTIR spectra of IBU, starting material IZ CLI and its composites (C-C-M, C-C-B, C-A-M and C-A-B) before and after adsorption of IBU.*

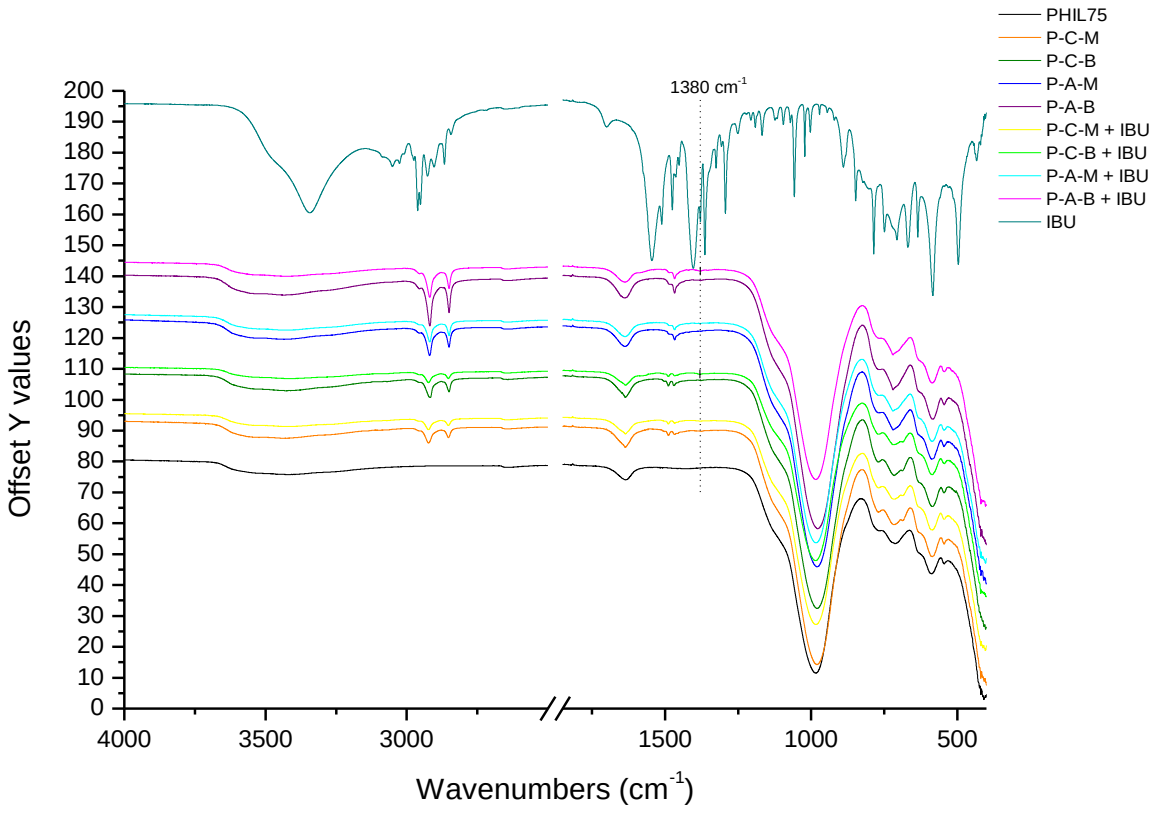

Fig. 32. *ATR–FTIR spectra of IBU, starting material PHIL75 and its composites (P-C-M, P-C-B, P-A-M and P-A-B) before and after adsorption of IBU.*

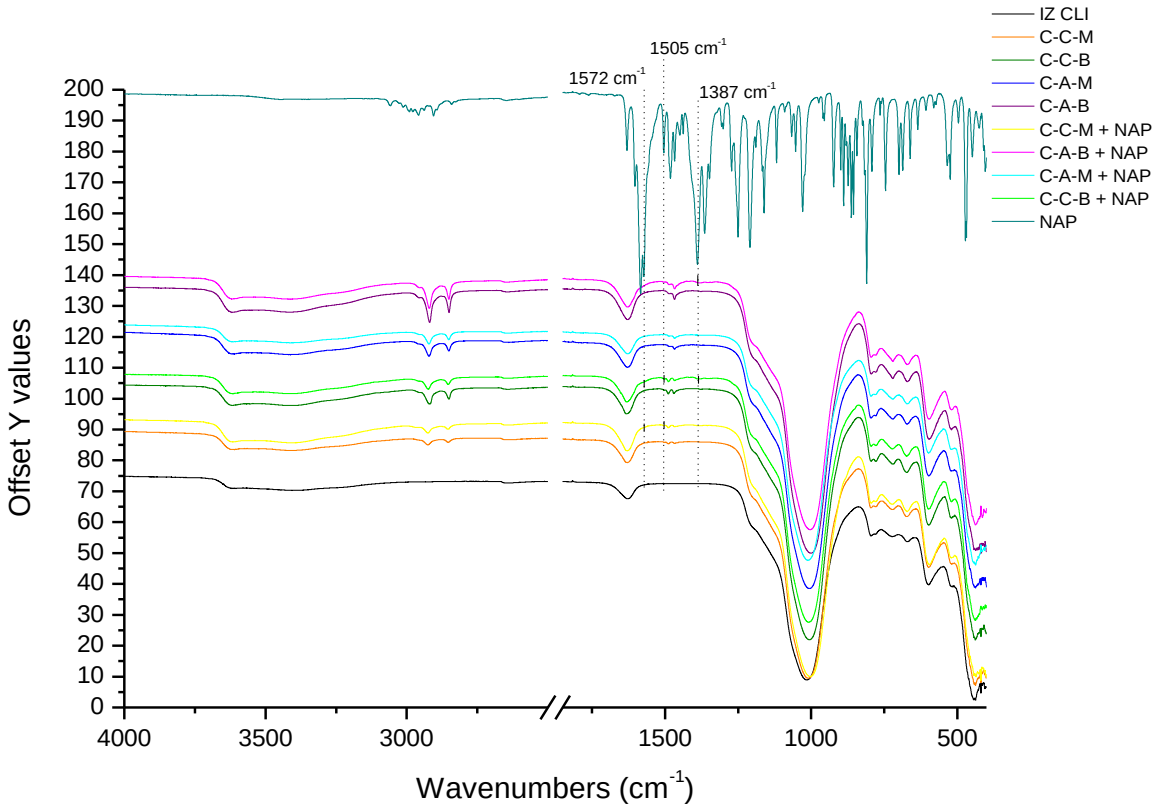

Fig. 33. *ATR–FTIR spectra of NAP, starting material IZ CLI and its composites (C-C-M, C-C-B, C-A-M and C-A-B) before and after adsorption of NAP.*

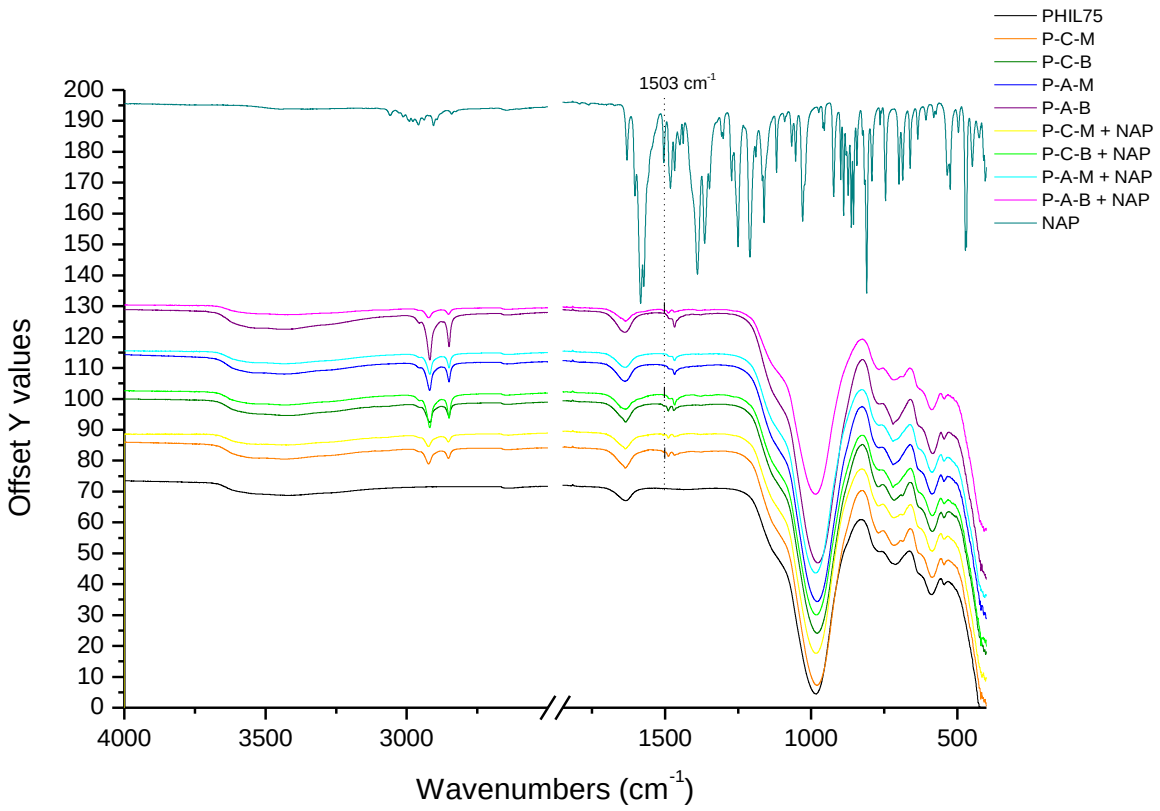

Fig. 34. *ATR–FTIR spectra of NAP, starting material PHIL75 and its composites (P-C-M, P-C-B, P-A-M, and P-A-B) before and after adsorption of NAP.*

In Figs. 31 and 32, FTIR spectra before and after IBU adsorption on IZ CLI and PHIL75 composites are presented. Only the peak at 1380 cm^{-1}, which belongs to IBU, was present in bilayer composites (C-C-B and C-A-B after adsorption). When NAP was adsorbed (Figs. 33 and 34), similar behavior was noticed. In the case of clinoptilolite-based composites, peaks belonging to NAP (1572 cm^{-1}, 1505 cm^{-1}, and 1387 cm^{-1}) have appeared in both bilayers and C-C-M, whereas in phillipsite-based composites, only one peak characteristic for pure NAP was present after adsorption (1503 cm^{-1}). When KET was adsorbed (Figs. 34 and 35), the only peak at 1283 cm^{-1}, originating from KET, was present in bilayer composites. Most likely, the amount of sorbed IBU, NAP, and KET is too low, and other peaks originating from these drugs were not visible.

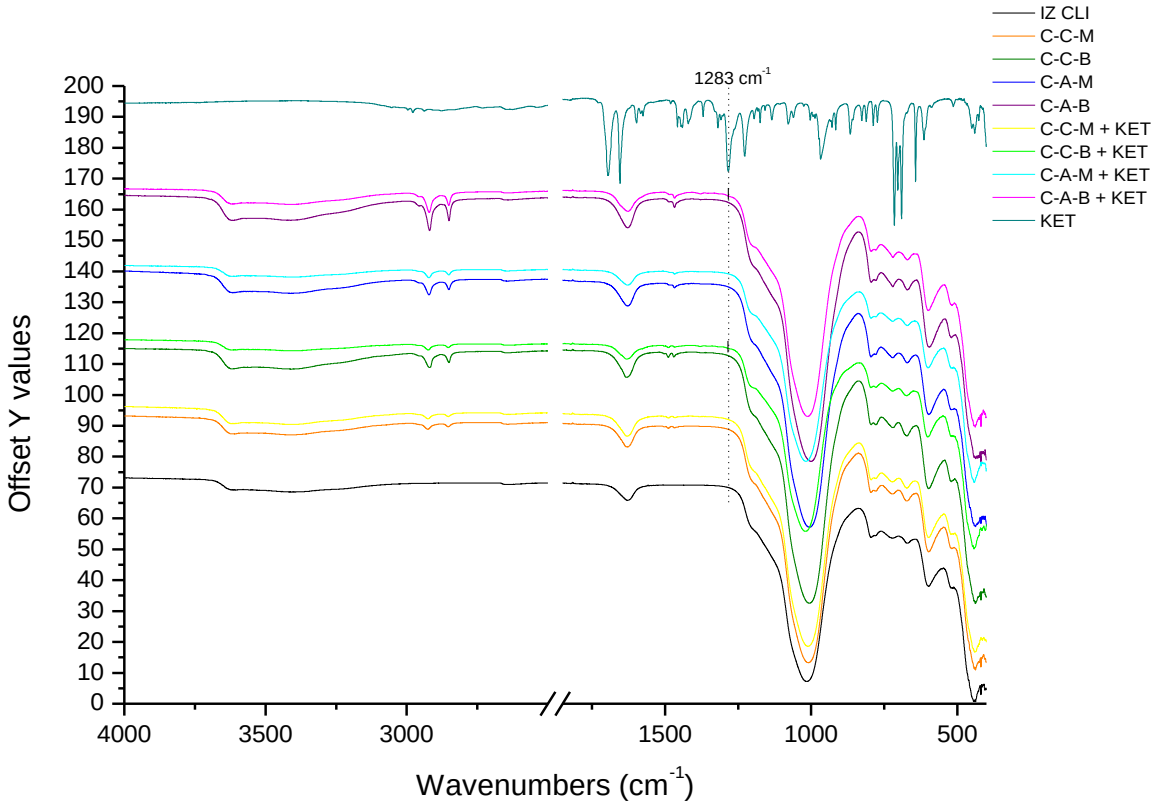

Fig. 35. *ATR–FTIR spectra of KET, starting material IZ CLI and its composites (C-C-M, C-C-B, C-A-M, and C-A-B) before and after adsorption of KET.*

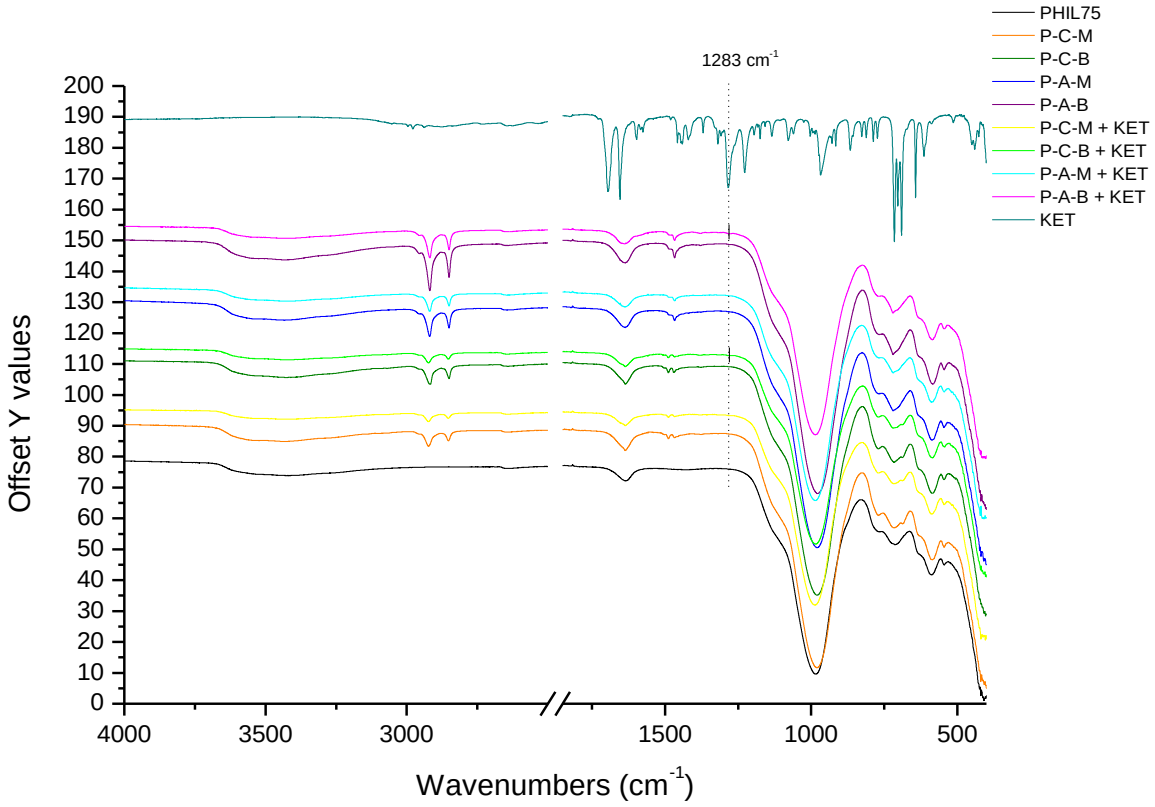

Fig. 36. *ATR–FTIR spectra of KET, starting material PHIL75 and its composites (P-C-M, P-C-B, P-A-M, and P-A-B) before and after adsorption of KET.*

5 Conclusions

Two zeolite-rich tuffs were modified with two cationic surfactants in amounts necessary to obtain monolayers and bilayers, characterized, and tested for the removal of NSAIDs – DCF, KET, NAP, and IBU for water treatment purposes.

The STA with EGA and ATR-FTIR analysis were used to get information about the thermal stability of composites, to confirm the presence of the surfactant molecules at zeolitic surfaces, and that functionalization did not damage the internal structure of zeolites. This aspect is relevant whenever applications requiring a simultaneous removal of heavy metal cations and anionic molecules are considered.

Zeta potential measurements showed the change of the surface charge from negative (starting materials) to neutral (monolayer of surfactants at zeolitic surfaces) and to the positive charge (bilayer of surfactants at zeolitic surfaces), confirming the success of the modification process. Another very important, although negative, result is that extensive washing with distilled water removed surfactant molecules from the zeolite surface, both in monolayer and especially in bilayer forms. The only exception occurred when bilayer composites were prepared using ARQ (C-A-B and P-A-B). Also, it is interesting to notice that the presence of two tails in ARQ was preventing the formation of a complete monolayer on clinoptilolite (C-A-M), while both P-A-M (although formed completely) and C-A-M have shown very low stability of this surfactant. Since surfactants are CoEC and their stability on zeolite surface is of great importance, these results are suggesting that with a proper selection of components for modifications of zeolites, SMNZs can be safe for environmental application.

Determination of pH_{pzc} (buffering capacity in the pH range from ~5 to ~10, and pH_{pzc} values around 6.5 and 7.2, for IZ CLI and PHIL75 composites, respectively) contributed to a better understanding of the surface properties of the adsorbents and helped in choosing the optimal experimental conditions.

Adsorption isotherms showed that the bilayer composites had higher adsorption capacities indicating that besides hydrophobic partitioning of hydrophobic part of drugs on surfactant tails (characteristic for composites with monolayer), ion exchange of anionic part of the drugs with counter anions from bilayers was the additional adsorption mechanism. Zeolitic content and properties of the tuff, the type and amount of surfactants, and the drug properties (such as hydrophobicity and pKa value) determined the adsorption capacities of the eight investigated

composites, in the range 1–35 mg/g. The highest adsorption by composites was observed in the DCF case due to its highest hydrophobicity DCF, also the adsorption of the other three drugs, in most cases, followed their hydrophobicity order. Considering that much lower levels (ng/L) of emerging contaminants usually occur in water systems, these composites could serve as effective, low-cost adsorbents in the water treatment processes.

Kinetic runs have confirmed that adsorption of NSAIDs by SMNZs is a fast process, mainly occurring as physisorption. An additional set of kinetics runs, using only IBU and NAP, was performed in the presence of sulfates and bicarbonates and showed small changes in drug removal for monolayer composites while, when composites with bilayers are considered, the inorganic anions were competing with drug molecules for the same active sites resulting in lower drug adsorption. Kinetic runs performed using activated charcoal as the most utilized adsorbent have confirmed literature data about the high efficiency of this adsorbent. Compared to composites prepared in this work, activated charcoal had at least three times better results.

However, SMNZs are low-cost, safe, and available adsorbents for the potential removal of drugs simultaneously with inorganic cations. Further experiments on SMNZs for this application should focus on the precise definition of components (specific surfactants) that will improve the adsorption capacity of particular drugs. Adsorption of drugs under dynamic conditions (column runs) will also be studied and will provide more information for the optimization of the process leading to the potential practical application.

6 Supplementary material

6.1 Figures

- ***Section 4.2.1***

IZ CLI

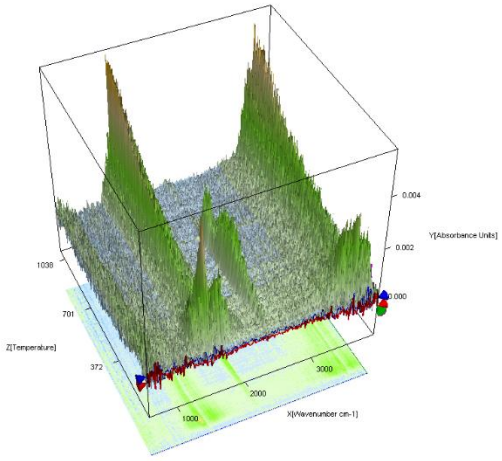

PHIL75

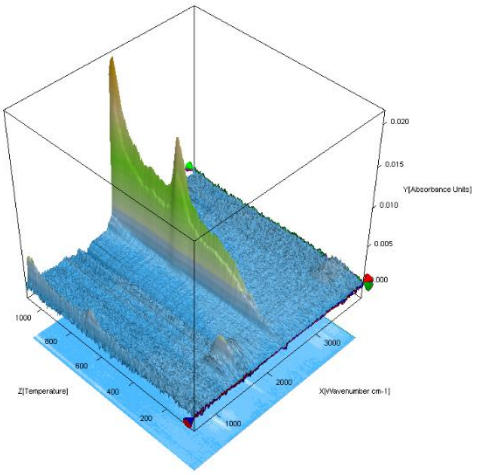

C-C-M

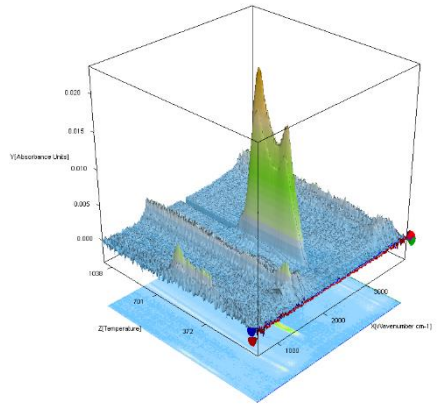

P-C-M

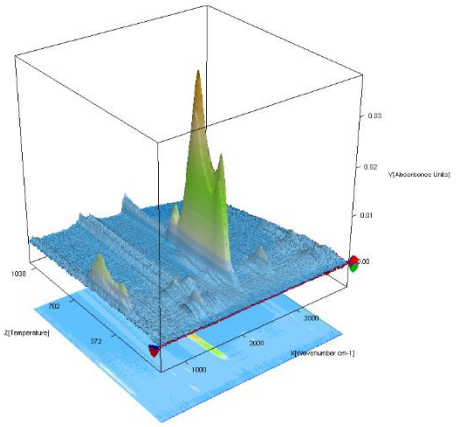

C-C-B

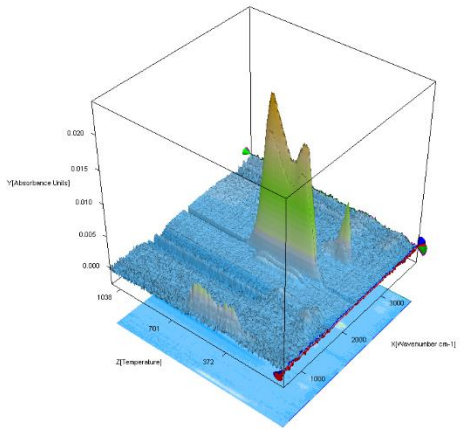

P-C-B

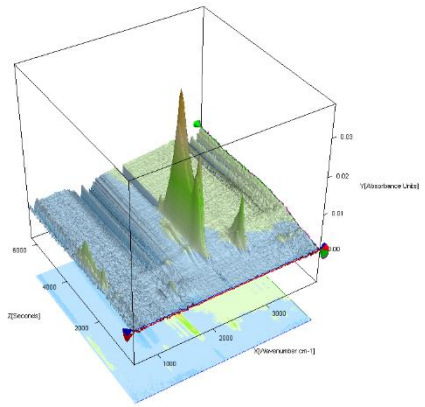

C-A-M

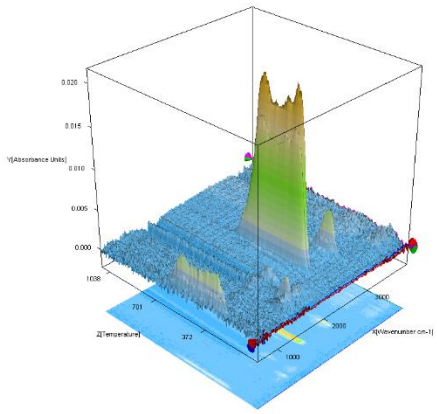

P-A-M

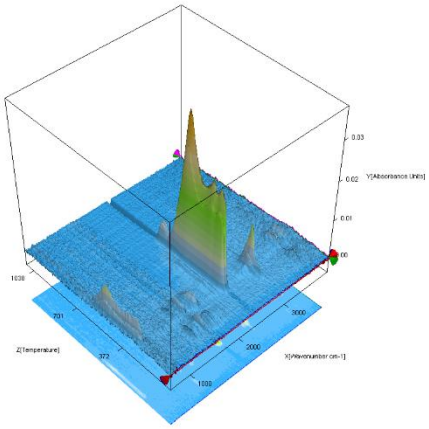

C-A-B

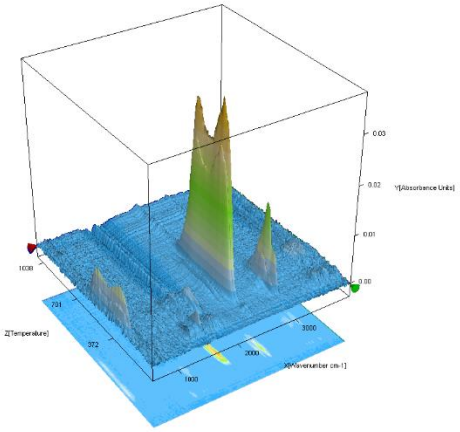

P-A-B

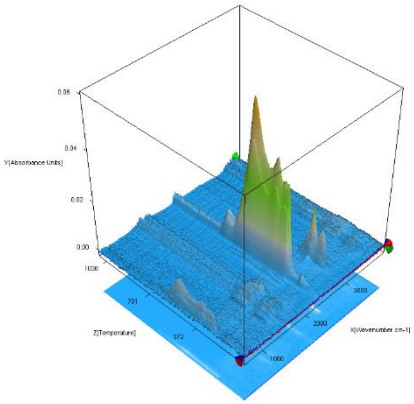

Fig. S1*. EGA plots for IZ CLI and PHIL75 (as starting materials) and their composites with surfactants.*

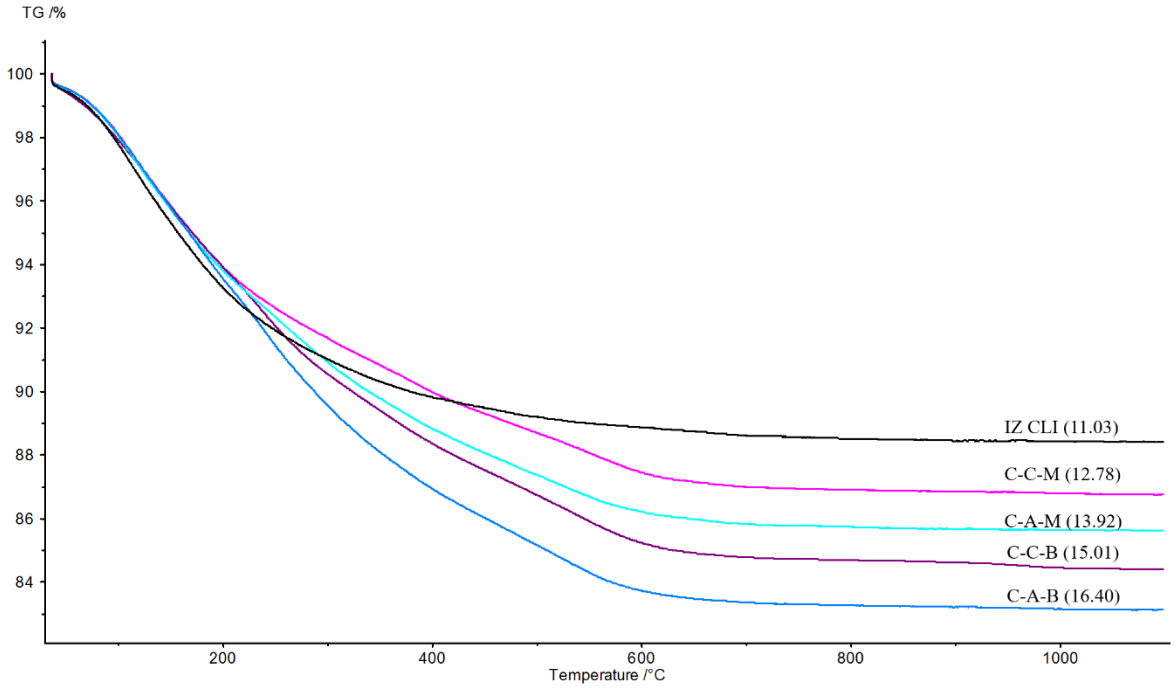

Fig. S2. *Thermogravimetric curves for IZ CLI and its composites. The mass loss (%) is given in the brackets.*

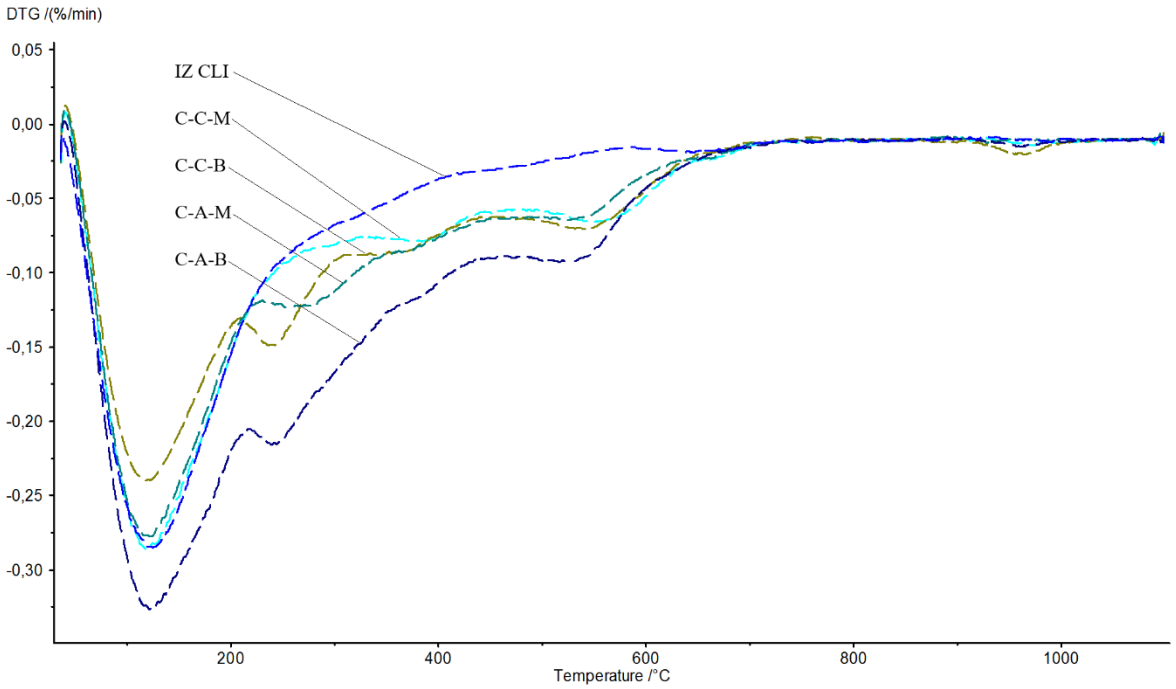

Fig. S3*. Differential curves for IZ CLI and its composites.*

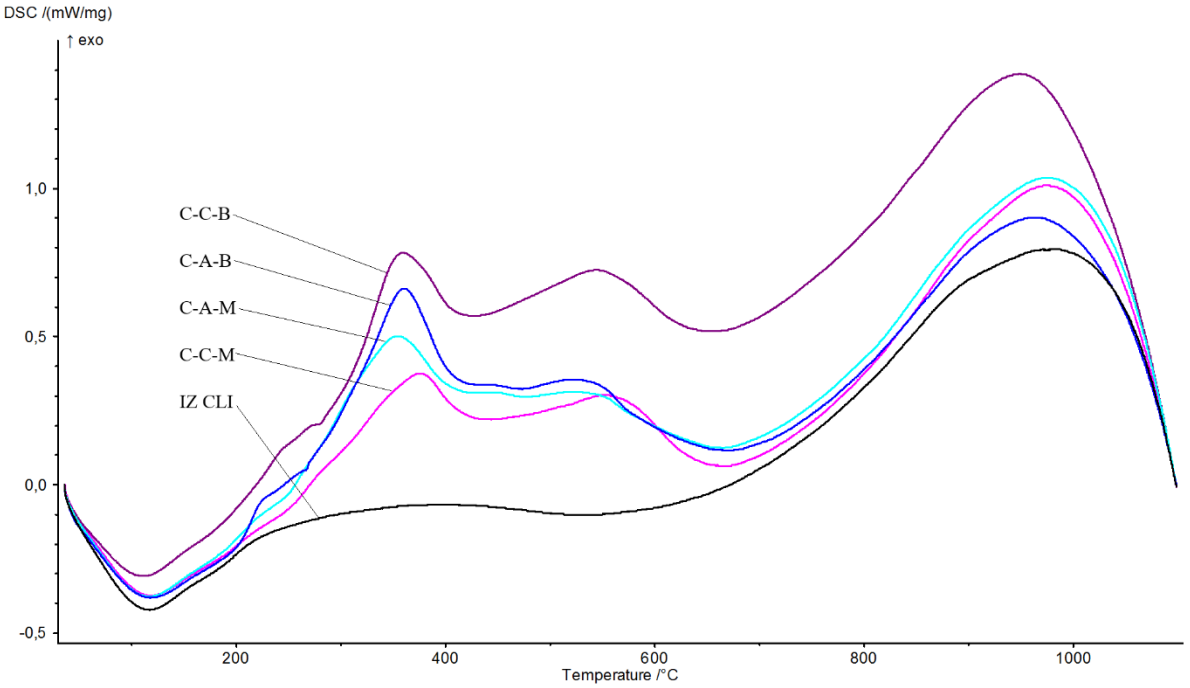

***Fig. S4**. DSC curves for PHIL75 and its composites.*

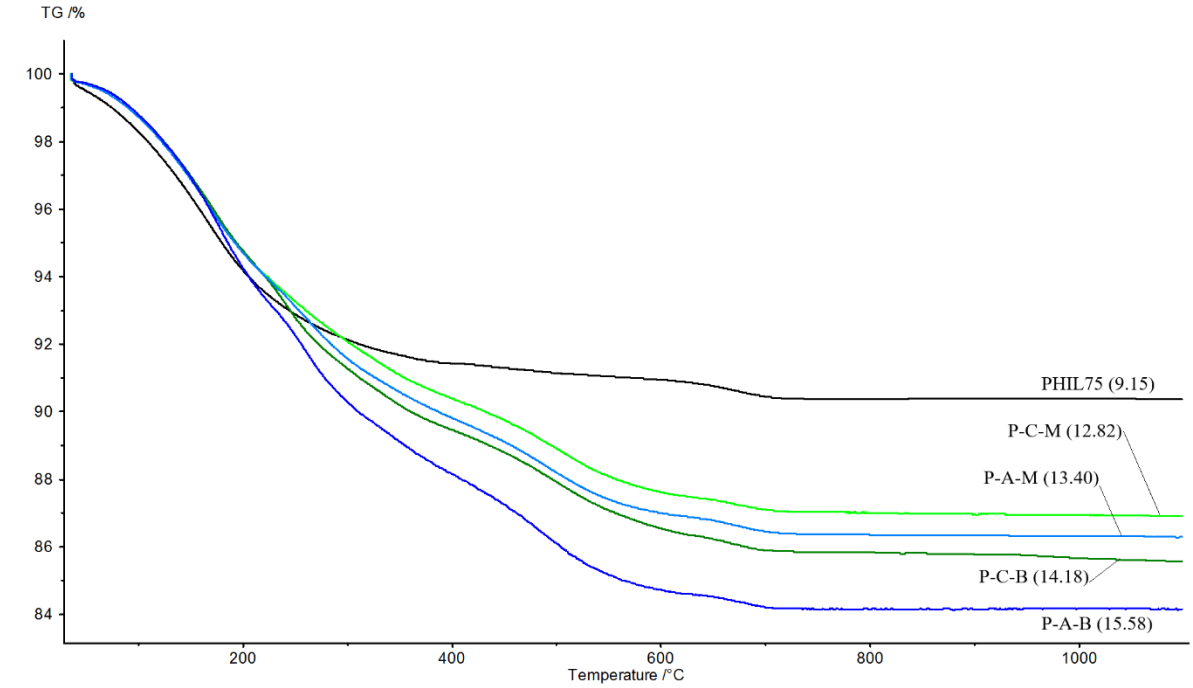

***Fig. S5**. Thermogravimetric curves for PHIL75 and its composites. The mass loss (%) is given in the brackets.*

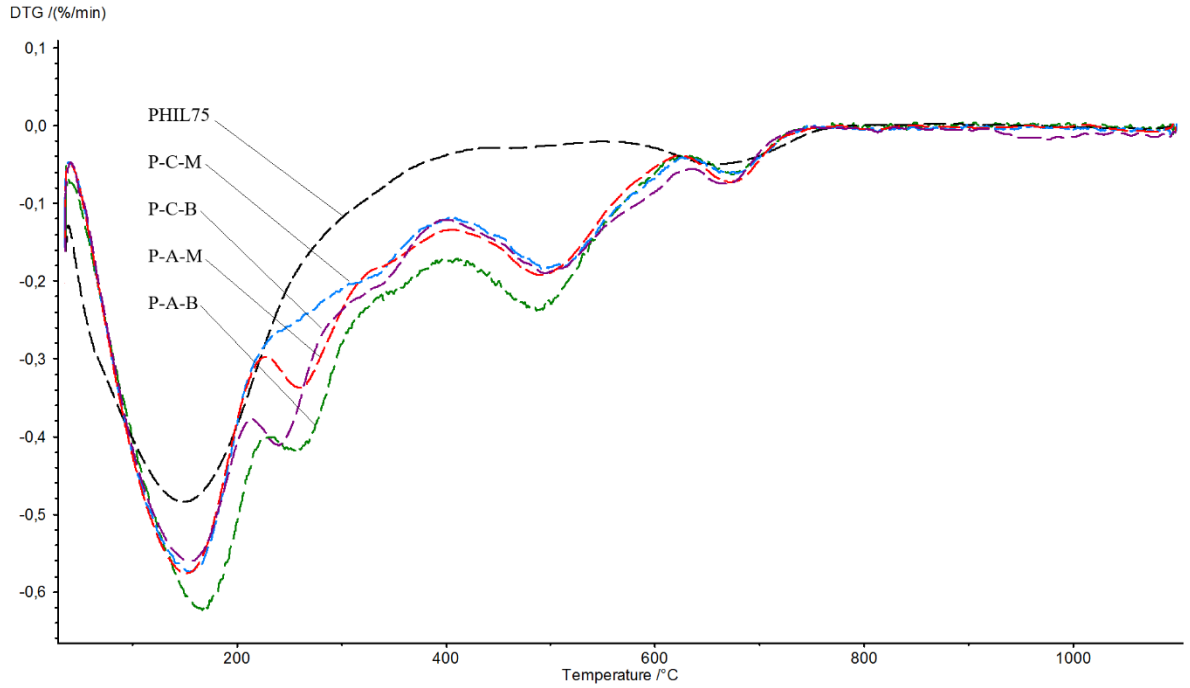

Fig. S6*. Differential curves for PHIL75 and its composites.*

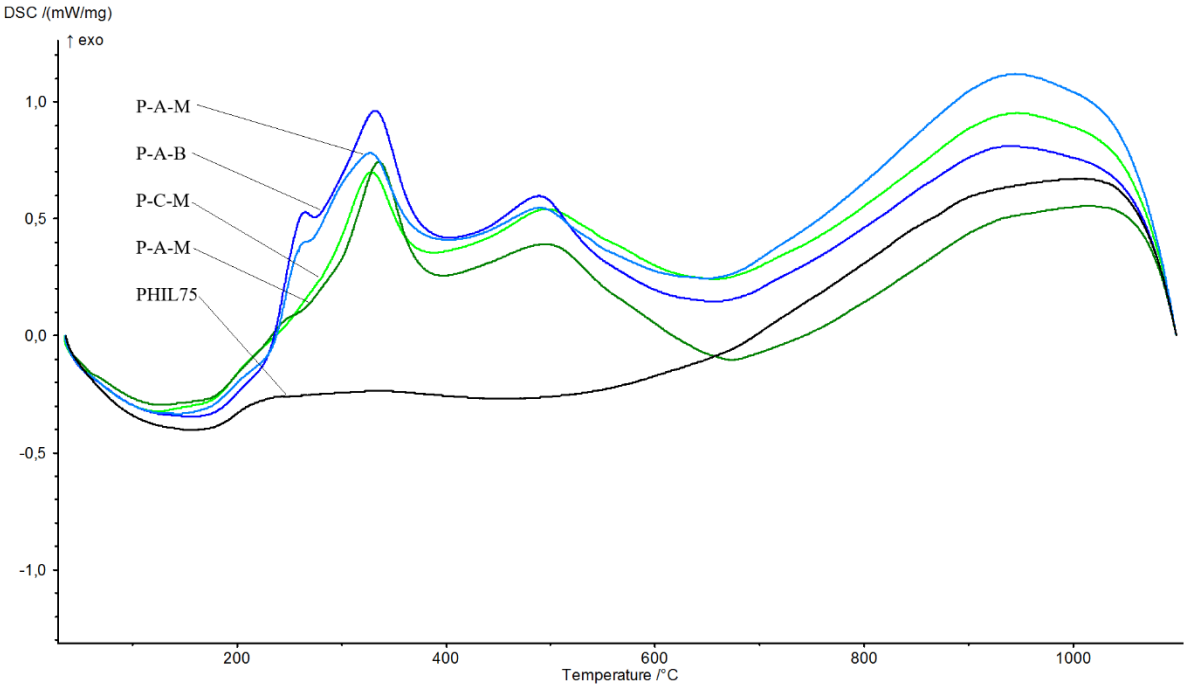

Fig. S7*. DSC curves for PHIL75 and its composites.*

❖ ***Section 4.2.3***

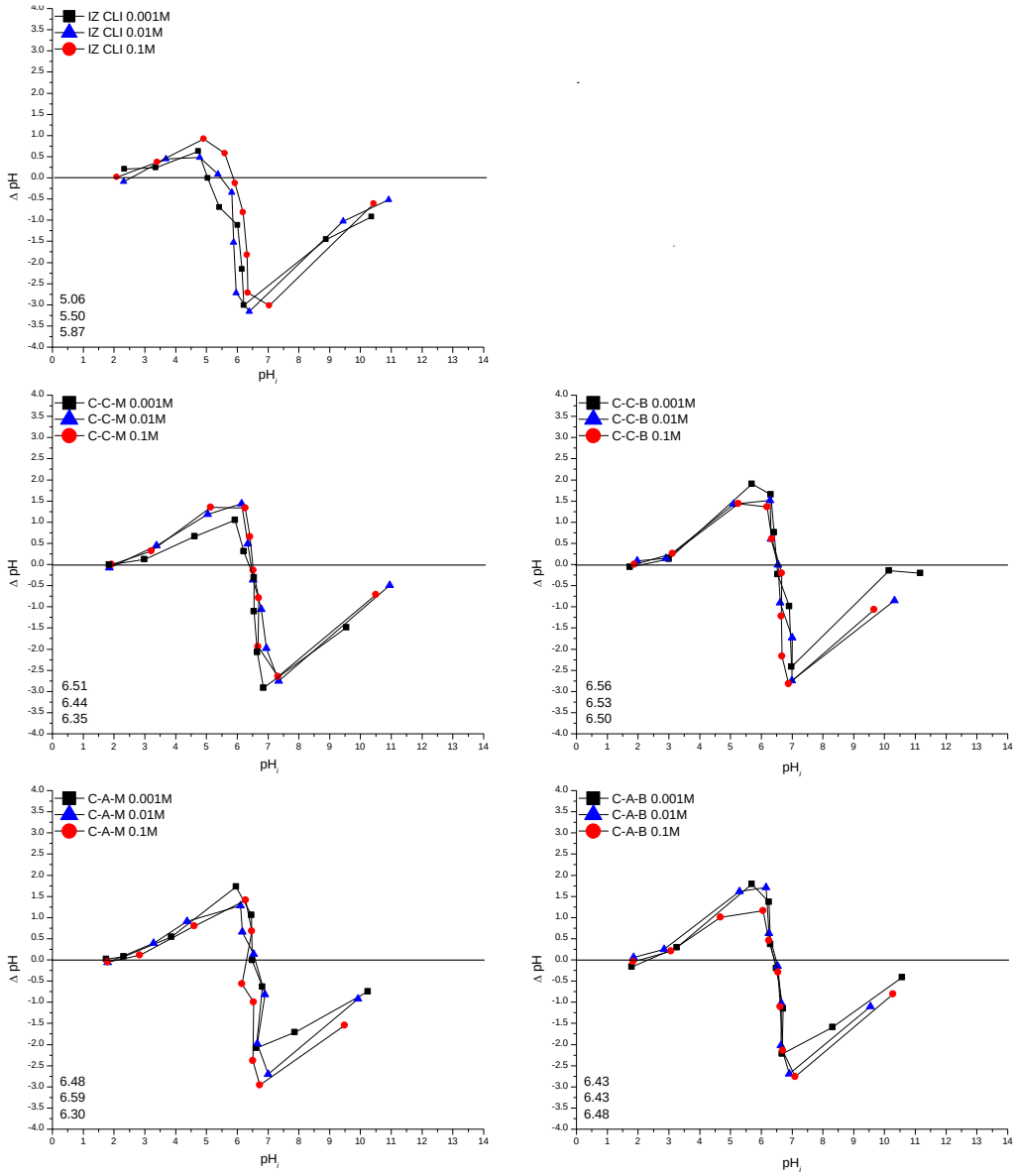

Fig. S8. *$\Delta pH = f(pH_i)$ plots for IZ CLI and its composites, where $\Delta pH = pH_f - pH_i$, and point zero charge is actually the inflection point of the curve.*

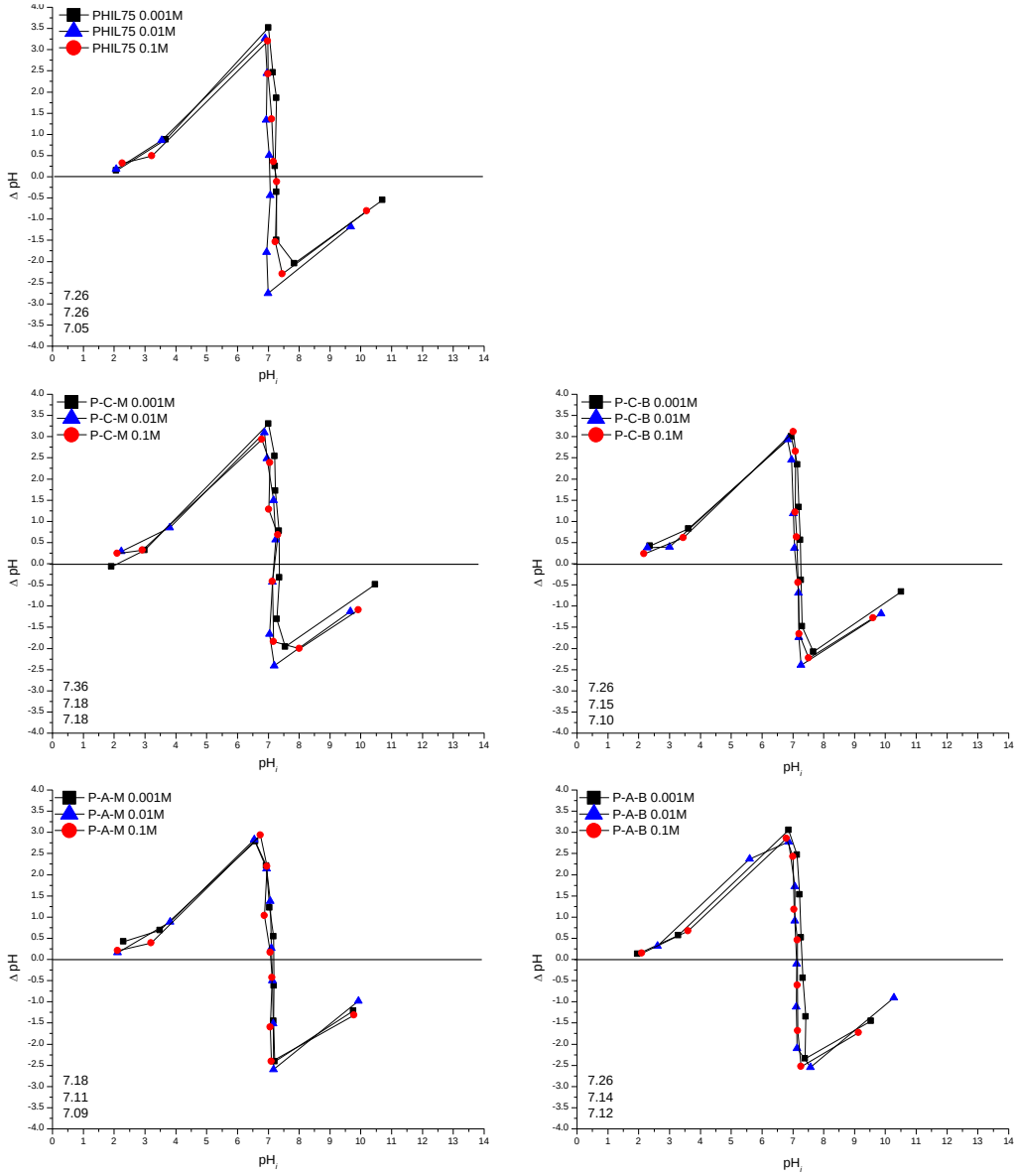

Fig. S9. *$\Delta pH = f(pH_i)$ plots for PHIL75 and its composites, where $\Delta pH = pH_f - pH_i$, and point zero charge is actually the inflection point of the curve.*

6.2 Tables

❖ **Section 1.2.3.1**

Table S1. Some properties of clinoptilolite and phillipsite

Natural zeolite	**Si/Al**	**Major cations**	**Channel geometry, (rings), nm, dim**	**Kinetic pore diameter nm**	**Max.H_2O capacity kg/kg**	**Total pore volume %**
Clinoptilolite	4.0-5.2	Na, Ca, K	(8) 0.26x0.47, (10) 0.30x0.76, (8) 0.33x0.46, 2D	0.35	0.14	34
Phillipsite	1.3-3.4	K, Na, Ca	(8) 0.38x0.38, (8) 0.30x0.43, (8) 0.32x0.33, 3D	0.26	0.22	30

Data from (Ackley et al., 2003)

❖ **Section 4.3.1.1**

Table S2 Mathematical models for the adsorption isotherms performed using C-C-B in Grindstone creek water as the medium: parameters and goodness - of - fit

Drug	**Model**	**Parameters**			**Goodness - of – fit**		
		K (l/mg)	n	Q_{max} (mg/g)	R^2	AIC	AICw
DCF	Langmuir	0.36±0.05		30±2	0.960	21.43	0.011
	Sips	0.24±0.06	0.68±0.08	35±2	0.983	12.48	0.989
KET	Langmuir	0.05±0.02		16±2	0.825	20.01	0.189
	Sips	(0.008±8) 10^{-9}	0.4±0.2	(8±300) 10^{4}	0.883	11.09	0.811
IBU	Langmuir	0.06±0.02		18±2	0.933	11.18	0.551
	Sips	0.01±0.03	0.6±0.2	34±25	0.943	11.58	0.449
NAP	Langmuir	0.045±0.008		18±2	0.944	7.31	0.757
	Sips	0.02±0.03	0.8±0.2	24±9	0.946	9.59	0.243

❖ ***Section 4.3.2.2***

Table S3. Mathematical models of kinetic runs performed in the presence of two inorganic salts: parameters and goodness - of - fit

Drug	Sample	Model	Parameters			Goodness - of - fit			RE (%)
			K_1 (min^{-1})	K_2 (g mg^{-1} min^{-1})	Q_{max} (mg/g)	R^2	AIC	AIC*w*	
IBU	C-C-M	PFO	0.25±0.03		4.2±0.2	0.979	-14.07	0.194	11.30
		PSO		0.07±0.02	4.6±0.2	0.985	-16.92	0.806	
	C-C-B	PFO	0.0.50±0.08		11.0±0.3	0.975	1.97	0.001	28.02
		PSO		0.074±0.008	11.7±0.2	0.996	-12.57	0.999	
	C-A-M	PFO	0.23±004		2.5±0.1	0.963	-16.97	0.616	6.69
		PSO		0.10±0.03	2.8±0.2	0.958	-16.03	0.384	
	C-A-B	PFO	0.27±0.04		5.9±0.2	0.979	-8.22	0.620	16.14
		PSO		0.06±0.02	6.5±0.3	0.976	-7.24	0.380	
	P-C-M	PFO	0.42±0.02		5.03±0.03	0.999	-36.94	0.999	11.61
		PSO		0.14±0.03	5.3±0.2	0.988	-16.05	0.001	
	P-C-B	PFO	0.61±0.05		8.6±0.1	0.995	-14.50	0.028	21.51
		PSO		0.13±0.02	9.00±0.08	0.998	-21.62	0.972	
	P-A-M	**PFO**	0.94±0.05		1.240±0.008	0.998	-54.37	0.999	5.69
		PSO		1.9±0.5	1.27±0.03	0.990	-40.73	0.001	
	P-A-B	PFO	0.20±0.02		4.3±0.1	0.986	-16.63	0.962	11.13
		PSO		0.05±0.01	4.8±0.3	0.970	-10.16	0.038	
NAP	C-C-M	PFO	0.104±0.009		4.1±0.1	0.992	-20.95	0.971	10.30
		PSO		0.024±0.006	4.9±0.3	0.980	-13.91	0.029	
	C-C-B	PFO	0.46±0.03		12.4±0.2	0.995	-8.56	0.423	32.03
		PSO		0.060±0.007	13.1±0.2	0.995	-9.18	0.577	
	C-A-M	PFO	0.66±0.03		2.87±0.02	0.998	-40.70	0.999	6.72
		PSO		0.5±0.2	2.96±0.06	0.987	-25.27	0.001	
	C-A-B	PFO	0.23±0.04		6.3±0.2	0.971	-5.30	0.005	16.32
		PSO		0.050±0.006	6.9±0.2	0.992	-15.94	0.995	
	P-C-M	PFO	0.38±0.04		5.3±0.2	0.987	-14.35	0.047	13.22
		PSO		0.10±0.01	5.7±0.1	0.993	-20.36	0.953	
	P-C-B	PFO	0.34±0.07		7.8±0.3	0.949	2.29	0.004	20.91
		PSO		0.06±0.01	8.3±0.2	0.987	-8.83	0.996	
	P-A-M	PFO	0.27±0.04		2.36±0.07	0.981	-14.35	0.047	5.81
		PSO		0.14±0.05	2.6±0.1	0.949	-20.36	0.953	
	P-A-B	PFO	0.33±0.06		3.6±0.2	0.962	-12.50	0.006	9.40
		PSO		0.14±0.02	3.82±0.09	0.989	-22.76	0.994	

❖ ***Section 4.3.2.3***

Table S4. Mathematical models of kinetic runs with activated charcoal as adsorbent: parameters and goodness - of - fit

Drug	**Model**	**Parameters**			**Goodness - of – fit**			**RE (%)**
		K_1 (min^{-1})	K_2 ($g\ mg^{-1}\ min^{-1}$)	Q_{max} (mg/g)	R^2	AIC	AICw	
DCF	PFO	7±40000		84±2	0.981	34.08	0.001	95.71
	PSO		0.035±0.003	86.9±0.4	0.999	4.52	0.999	
KET	PFO	$12±10^8$		65±2	0.979	30.38	0.005	81.89
	PSO		0.05±0.02	67±1	0.979	19.88	0.995	
IBU	PFO	1.5±0.5		66±1	0.989	23.81	0.677	81.21
	PSO		0.2±0.2	67±2	0.987	25.29	0.323	
NAP	PFO	$13±10^9$		71±3	0.935	41.04	0.001	87.34
	PSO		0.019±0.003	76±1	0.946	18.35	0.999	

References

Abezgauz, L., Kuperkar, K., Hassan, P.A., Ramon, O., Bahadur, P., Danino, D., 2010. Effect of Hofmeister anions on micellization and micellar growth of the surfactant cetylpyridinium chloride. J. Colloid Interface Sci. 342, 83–92. https://doi.org/10.1016/j.jcis.2009.08.045

Ackley, M.W., Rege, S.U., Saxena, H., 2003. Application of natural zeolites in the purification and separation of gases. Microporous Mesoporous Mater. 61, 25–42. https://doi.org/10.1016/S1387-1811(03)00353-6

AkzoNobel SDS, 2009. ARQUAD 2HT-75 1–11.

Andronikashvili, T., Pagava, K., Kurashvili, T., Eprikashvili, L., 2009. Possibility of Application of Natural Zeolites for Medicinal Purposes. Bull. Georg. Natl. Acad. Sci. 3, 158–167.

Apreutesei, R.E., Catrinescu, C., Teodosiu, C., 2008. Surfactant-modified natural zeolites for environmental applications in water purification. Environ. Eng. Manag. J. 7, 149–161. https://doi.org/10.30638/eemj.2008.025

Avdeef, A., Berger, C.M., Brownell, C., 2000. pH Methods. Pharm. Res. 17, 85–89.

Azizian, S., 2004. Kinetic models of sorption: A theoretical analysis. J. Colloid Interface Sci. 276, 47–52. https://doi.org/10.1016/j.jcis.2004.03.048

Baccar, R., Sarrà, M., Bouzid, J., Feki, M., Blánquez, P., 2012. Removal of pharmaceutical compounds by activated carbon prepared from agricultural by-product. Chem. Eng. J. 211–212, 310–317. https://doi.org/10.1016/j.cej.2012.09.099

Barrer, R.M., Papadopoulos, R., Rees, L.V.C., 1967. Exchange of sodium in clinoptilolite by organic cations. J. Inorg. Nucl. Chem. 29, 2047–2063. https://doi.org/10.1016/0022-1902(67)80466-4

Bhatnagar, A., Sillanpää, M., 2017. Removal of natural organic matter (NOM) and its constituents from water by adsorption – A review. Chemosphere 166, 497–510. https://doi.org/10.1016/j.chemosphere.2016.09.098

Bhattarai, A., Shah, S.K., Yadav, A.K., 2013. Effect of Solvent Composition on the Critical Micelle Concentration of Cetylpyridinium Chloride in Ethanol-Water Mixed Solvent Media. Nepal J. Sci. Technol. 13, 89–93. https://doi.org/10.3126/njst.v13i1.7446

Bolong, N., Ismail, A.F., Salim, M.R., Matsuura, T., 2009. A review of the effects of emerging contaminants in wastewater and options for their removal. Desalination 239, 229–246. https://doi.org/10.1016/j.desal.2008.03.020

Bonnefille, B., Gomez, E., Courant, F., Escande, A., Fenet, H., 2018. Diclofenac in the marine environment: A review of its occurrence and effects. Mar. Pollut. Bull. 131, 496–506. https://doi.org/10.1016/j.marpolbul.2018.04.053

Bowman, R.S., 2003. Applications of surfactant-modified zeolites to environmental remediation. Microporous Mesoporous Mater. 61, 43–56. https://doi.org/10.1016/S1387-1811(03)00354-8

Bowman, R.S., Haggerty, G.M., Huddleston, R.G., Neel, D., Flynn, M.M., 1995. Sorption of Nonpolar Organic Compounds, Inorganic Cations, and Inorganic Oxyanions by Surfactant-Modified Zeolites 54–64. https://doi.org/10.1021/bk-1995-0594.ch005

Burian, M., Geisslinger, G., 2005. COX-dependent mechanisms involved in the antinociceptive action of NSAIDs at central and peripheral sites. Pharmacol. Ther. 107, 139–154. https://doi.org/10.1016/j.pharmthera.2005.02.004

Cappelletti, P., Colella, A., Langella, A., Mercurio, M., Catalanotti, L., Monetti, V., de Gennaro, B., 2017. Use of surface modified natural zeolite (SMNZ) in pharmaceutical preparations Part 1. Mineralogical and technological characterization of some industrial zeolite-rich rocks. Microporous Mesoporous Mater. 250, 232–244. https://doi.org/10.1016/j.micromeso.2015.05.048

CDH SDS, 2008. CAS No 103-47-9 Material Safety Data Sheet SDS / MSDS 1–6.

Čerović, L.S., Milonjić, S.K., Todorović, M.B., Trtanj, M.I., Pogozhev, Y.S., Blagoveschenskii, Y., Levashov, E.A., 2007. Point of zero charge of different carbides. Colloids Surfaces A Physicochem. Eng. Asp. 297, 1–6. https://doi.org/10.1016/j.colsurfa.2006.10.012

Cerri, G., Langella, A., Pansini, M., Cappelletti, P., 2002. Methods of determining cation exchange capacities for clinoptilolite-rich rocks of the Logudoro region in northern Sardinia, Italy. Clays Clay Miner. 50, 127–135.

Chutia, P., Kato, S., Kojima, T., Satokawa, S., 2009. Adsorption of As(V) on surfactant-modified natural zeolites. J. Hazard. Mater. 162, 204–211. https://doi.org/10.1016/j.jhazmat.2008.05.024

Çinar, Ö., 2005. New tool for evaluation of performance of wastewater treatment plant: Artificial neural network. Process Biochem. 40, 2980–2984. https://doi.org/10.1016/j.procbio.2005.01.012

Cleuvers, M., 2004. Mixture toxicity of the anti-inflammatory drugs diclofenac, ibuprofen, naproxen, and acetylsalicylic acid. Ecotoxicol. Environ. Saf. 59, 309–315. https://doi.org/10.1016/S0147-6513(03)00141-6

Coelho, A.D., Sans, C., Esplugas, S., Dezotti, M., 2010. Ozonation of NSAID: A Biodegradability and Toxicity Study. Ozone Sci. Eng. 32, 91–98. https://doi.org/10.1080/01919510903508162

Colella, C., 2011. A critical reconsideration of biomedical and veterinary applications of natural zeolites. Clay Miner. 46, 295–309. https://doi.org/10.1180/claymin.2011.046.2.295

Coleman, N.J., Brassington, D.S., Raza, A., Mendham, A.P., 2006. Sorption of Co2+ and Sr2+ by waste-derived 11 Å tobermorite. Waste Manag. 26, 260–267. https://doi.org/10.1016/j.wasman.2005.01.019

Comber, S.D.W., Rule, K.L., Conrad, A.U., Höss, S., Webb, S.F., Marshall, S., 2008. Bioaccumulation and toxicity of a cationic surfactant (DODMAC) in sediment dwelling freshwater invertebrates. Environ. Pollut. 153, 184–191. https://doi.org/10.1016/j.envpol.2007.07.032

Costa, F.O., Sousa, J.J.S., Pais, A.A.C.C., Formosinho, S.J., 2003. Comparison of dissolution profiles of ibuprofen pellets. J. Control. Release 89, 199–212.

https://doi.org/10.1016/S0168-3659(03)00033-6

Cruciani, G., 2006. Zeolites upon heating: Factors governing their thermal stability and structural changes. J. Phys. Chem. Solids 67, 1973–1994. https://doi.org/10.1016/j.jpcs.2006.05.057

Daković, A., Kragović, M., Rottinghaus, G.E., Sekulić, Ž., Milićević, S., Milonjić, S.K., Zarić, S., 2010. Influence of natural zeolitic tuff and organozeolites surface charge on sorption of ionizable fumonisin B1. Colloids Surfaces B Biointerfaces 76, 272–278. https://doi.org/10.1016/j.colsurfb.2009.11.003

Daković, A., Matijašević, S., Rottinghaus, G.E., Dondur, V., Pietrass, T., Clewett, C.F.M., 2007a. Adsorption of zearalenone by organomodified natural zeolitic tuff. J. Colloid Interface Sci. 311, 8–13. https://doi.org/10.1016/j.jcis.2007.02.033

Daković, A., Tomašević-Čanović, M., Dondur, V., Rottinghaus, G.E., Medaković, V., Zarić, S., 2005. Adsorption of mycotoxins by organozeolites. Colloids Surfaces B Biointerfaces 46, 20–25. https://doi.org/10.1016/j.colsurfb.2005.08.013

Daković, A., Tomašević-Čanović, M., Rottinghaus, G., Dondur, V., Mašić, Z., 2003. Adsorption of ochratoxin A on octadecyldimethyl benzyl ammonium exchanged-clinoptilolite-heulandite tuff. Colloids Surfaces B Biointerfaces 30, 157–165. https://doi.org/10.1016/S0927-7765(03)00067-5

Daković, A., Tomašević-Čanović, M., Rottinghaus, G.E., Matijašević, S., Sekulić, Ž., 2007b. Fumonisin B1 adsorption to octadecyldimethylbenzyl ammonium-modified clinoptilolite-rich zeolitic tuff. Microporous Mesoporous Mater. 105, 285–290. https://doi.org/10.1016/j.micromeso.2007.03.037

Dávila-Estrada, M., Ramírez-García, J.J., Solache-Ríos, M.J., Gallegos-Pérez, J.L., 2018. Kinetic and Equilibrium Sorption Studies of Ceftriaxone and Paracetamol by Surfactant-Modified Zeolite. Water. Air. Soil Pollut. 229. https://doi.org/10.1007/s11270-018-3783-4

de Gennaro, B., 2018. Surface modification of zeolites for environmental applications, in: Modified Clay and Zeolite Nanocomposite Materials: Environmental and Pharmaceutical Applications. Elsevier Inc., pp. 57–85. https://doi.org/10.1016/B978-0-12-814617-0.00009-8

de Gennaro, B., Aprea, P., Colella, C., Buondonno, A., 2007a. Comparative ion-exchange characterization of zeolitic and clayey materials for pedotechnical applications-Part 2: Interaction with nutrient cations. J. Porous Mater. 16, 667–673. https://doi.org/10.1007/s10934-008-9247-2

de Gennaro, B., Aprea, P., Liguori, B., Galzerano, B., Peluso, A., Caputo, D., 2020. Zeolite-rich composite materials for environmental remediation: Arsenic removal from water. Appl. Sci. 10, 1–20. https://doi.org/10.3390/app10196939

de Gennaro, B., Aprea, P., Pepe, F., Colella, C., 2007b. Cation selectivity of a Ca2+ pre-exchanged clinoptilolite tuff. Stud. Surf. Sci. Catal. 170, 2128–2133. https://doi.org/10.1016/S0167-2991(07)81110-4

de Gennaro, B., Catalanotti, L., Bowman, R.S., Mercurio, M., 2014. Anion exchange selectivity of surfactant modified clinoptilolite-rich tuff for environmental remediation. J. Colloid Interface Sci. 430, 178–183. https://doi.org/10.1016/j.jcis.2014.05.037

de Gennaro, B., Catalanotti, L., Cappelletti, P., Langella, A., Mercurio, M., Serri, C., Biondi, M., Mayol, L., 2015. Surface modified natural zeolite as a carrier for sustained diclofenac release: A preliminary feasibility study. Colloids Surfaces B Biointerfaces 130, 101–109. https://doi.org/10.1016/j.colsurfb.2015.03.052

de Gennaro, B., Colella, A., Cappelletti, P., Pansini, M., De'Gennaro, M., Colella, C., 2005. Effectiveness of clinoptilolite in removing toxic cations from water: A comparative study. Stud. Surf. Sci. Catal. 158 B, 1153–1160. https://doi.org/10.1016/s0167-2991(05)80460-4

de Gennaro, B., Mercurio, M., Cappelletti, P., Catalanotti, L., Daković, A., De Bonis, A., Grifa, C., Izzo, F., Kraković, M., Monetti, V., Langella, A., 2016. Use of surface modified natural zeolite (SMNZ) in pharmaceutical preparations. Part 2. A new approach for a fast functionalization of zeolite-rich carriers. Microporous Mesoporous Mater. 235, 42–49. https://doi.org/10.1016/j.micromeso.2016.07.043

Delkash, M., Ebrazi Bakhshayesh, B., Kazemian, H., 2015. Using zeolitic adsorbents to cleanup special wastewater streams: A review. Microporous Mesoporous Mater. 214, 224–241. https://doi.org/10.1016/j.micromeso.2015.04.039

Derouane, E.G., Fripiat, J.G., 1987. Quantum mechanical calculations on molecular sieves. 1. Properties of the Si-O-T (T = Si, Al, B) bridge in zeolites. J. Phys. Chem. 91, 145–148. https://doi.org/10.1021/j100285a032

Dimas Rivera, G.L., Martínez Hernández, A., Pérez Cabello, A.F., Rivas Barragán, E.L., Liñán Montes, A., Flores Escamilla, G.A., Sandoval Rangel, L., Suarez Vazquez, S.I., De Haro Del Río, D.A., 2020. Removal of chromate anions and immobilization using surfactant-modified zeolites. J. Water Process Eng. https://doi.org/10.1016/j.jwpe.2020.101717

Dordio, A. V., Estêvão Candeias, A.J., Pinto, A.P., Teixeira da Costa, C., Palace Carvalho, A.J., 2009. Preliminary media screening for application in the removal of clofibric acid, carbamazepine and ibuprofen by SSF-constructed wetlands. Ecol. Eng. 35, 290–302. https://doi.org/10.1016/j.ecoleng.2008.02.014

Erdem, E., Karapinar, N., Donat, R., 2004. The removal of heavy metal cations by natural zeolites. J. Colloid Interface Sci. 280, 309–314. https://doi.org/10.1016/j.jcis.2004.08.028

Esposito, S., Marocco, A., Dell'Agli, G., De Gennaro, B., Pansini, M., 2015. Relationships between the water content of zeolites and their cation population. Microporous Mesoporous Mater. 202, 36–43. https://doi.org/10.1016/j.micromeso.2014.09.041

FDA Web page, 2007. https://www.accessdata.fda.gov/scripts/cdrh/cfdocs/cfcfr/CFRSearch.cfm?fr=173.375 [WWW Document].

Flanigen, E.M., 1977. Crystal structure and chemistry of natural zeolites, in: In Mineralogy and Geology of Natural Zeolites. Mineralogical Society of America, Southern Printing Co Blacksburg, VA., pp. 19–52.

Foo, K.Y., Hameed, B.H., 2010. Insights into the modeling of adsorption isotherm systems. Chem. Eng. J. 156, 2–10. https://doi.org/10.1016/j.cej.2009.09.013

Freitas, A.M., Rivas, G., Campos-Mañas, M.C., Casas López, J.L., Agüera, A., Sánchez Pérez, J.A., 2017. Ecotoxicity evaluation of a WWTP effluent treated by solar photo-Fenton at neutral pH in a raceway pond reactor. Environ. Sci. Pollut. Res. 24, 1093–1104.

https://doi.org/10.1007/s11356-016-7101-7

Fröhlich, A.C., Foletto, E.L., Dotto, G.L., 2019. Preparation and characterization of NiFe2O4/activated carbon composite as potential magnetic adsorbent for removal of ibuprofen and ketoprofen pharmaceuticals from aqueous solutions. J. Clean. Prod. 229, 828–837. https://doi.org/10.1016/j.jclepro.2019.05.037

Ghosh, S., Badruddoza, A.Z.M., Hidajat, K., Uddin, M.S., 2013. Adsorptive removal of emerging contaminants from water using superparamagnetic Fe3O4 nanoparticles bearing aminated β-cyclodextrin. J. Environ. Chem. Eng. 1, 122–130. https://doi.org/10.1016/j.jece.2013.04.004

Glatting, G., Kletting, P., Reske, S.N., Hohl, K., Ring, C., 2007. Choosing the optimal fit function: Comparison of the Akaike information criterion and the F-test. Med. Phys. 34, 4285–4292. https://doi.org/10.1118/1.2794176

Groisman, L., Rav-Acha, C., Gerstl, Z., Mingelgrin, U., 2004. Sorption of organic compounds of varying hydrophobicities from water and industrial wastewater by long- and short-chain organoclays. Appl. Clay Sci. 24, 159–166. https://doi.org/10.1016/j.clay.2003.02.001

Gros, M., Petrović, M., Ginebreda, A., Barceló, D., 2010. Removal of pharmaceuticals during wastewater treatment and environmental risk assessment using hazard indexes. Environ. Int. 36, 15–26. https://doi.org/10.1016/j.envint.2009.09.002

Haggerty, G.M., Bowman, R.S., 1994. Sorption of Chromate and Other Inorganic Anions by Organo-Zeolite. Environ. Sci. Technol. 28, 452–458. https://doi.org/10.1021/es00052a017

Hamdaoui, O., Naffrechoux, E., 2007. Modeling of adsorption isotherms of phenol and chlorophenols onto granular activated carbon. Part I. Two-parameter models and equations allowing determination of thermodynamic parameters. J. Hazard. Mater. 147, 381–394. https://doi.org/10.1016/j.jhazmat.2007.01.021

Ho, Y.S., 2006. Review of second-order models for adsorption systems. J. Hazard. Mater. 136, 681–689. https://doi.org/10.1016/j.jhazmat.2005.12.043

Ho, Y.S., 2004. Citation review of Lagergren kinetic rate equation on adsorption reactions. Scientometrics. https://doi.org/10.1023/B:SCIE.0000013305.99473.cf

Hrenovic, J., Ivankovic, T., Sekovanic, L., Rozic, M., 2008a. Toxicity of dodecylpyridinium and cetylpyridinium clorides against phosphate-accumulating bacterium. Cent. Eur. J. Biol. 3, 143–148. https://doi.org/10.2478/s11535-008-0014-9

Hrenovic, J., Rozic, M., Sekovanic, L., Anic-Vucinic, A., 2008b. Interaction of surfactant-modified zeolites and phosphate accumulating bacteria. J. Hazard. Mater. 156, 576–582. https://doi.org/10.1016/j.jhazmat.2007.12.060

Hubbe, M., Azizian, S., Douven, S., 2019. Implications of Apparent Pseudo-Second-Order Adsorption Kinetics onto Cellulosic Materials: A Review. BioResources 14, 7582–7626.

Inglezakis, V.J., Zorpas, A.A., 2012. Handbook of natural zeolites, Handbook of Natural Zeolites. https://doi.org/10.2174/97816080526151120101

Izzo, F., Mercurio, M., de Gennaro, B., Aprea, P., Cappelletti, P., Daković, A., Germinario, C., Grifa, C., Smiljanic, D., Langella, A., 2019. Surface modified natural zeolites (SMNZs) as nanocomposite versatile materials for health and environment. Colloids Surfaces B

Biointerfaces 182, 110380. https://doi.org/10.1016/j.colsurfb.2019.110380

James, A.D., Ogden, P.H., 1979. Effect of manufacturing variables on the viscosity of aqueous di(hydrogenated tallowalkyl) dimethyl ammonium chloride. J. Am. Oil Chem. Soc. 56, 542–547. https://doi.org/10.1007/BF02680198

Jubilant SDS, 2012. Cetylpyridinium Chloride Safety Data Sheet.

Keren, Y., Borisover, M., Bukhanovsky, N., 2015. Sorption interactions of organic compounds with soils affected by agricultural olive mill wastewater. Chemosphere 138, 462–468. https://doi.org/10.1016/j.chemosphere.2015.06.085

Khalil, A.M.E., Memon, F.A., Tabish, T.A., Salmon, D., Zhang, S., Butler, D., 2020. Nanostructured porous graphene for efficient removal of emerging contaminants (pharmaceuticals) from water. Chem. Eng. J. 398, 125440. https://doi.org/10.1016/j.cej.2020.125440

Kozlowska, M., Rodziewicz, P., Kaczmarek-Kedziera, A., 2017. Structural stability of diclofenac vs. inhibition activity from ab initio molecular dynamics simulations. Comparative study with ibuprofen and ketoprofen. Struct. Chem. 28, 999–1008. https://doi.org/10.1007/s11224-016-0893-8

Kragović, M., Stojmenović, M., Petrović, J., Loredo, J., Pašalić, S., Nedeljković, A., Ristović, I., 2019. Influence of Alginate Encapsulation on Point of Zero Charge (pH pzc) and Thermodynamic Properties of the Natural and Fe(III)-Modified Zeolite. Procedia Manuf. 32, 286–293. https://doi.org/10.1016/j.promfg.2019.02.216

Krajišnik, D., Daković, A., Malenović, A., Djekić, L., Kragović, M., Dobričić, V., Milić, J., 2013a. An investigation of diclofenac sodium release from cetylpyridinium chloride-modified natural zeolite as a pharmaceutical excipient. Microporous Mesoporous Mater. 167, 94–101. https://doi.org/10.1016/j.micromeso.2012.03.033

Krajišnik, D., Daković, A., Malenović, A., Milojević-Rakić, M., Dondur, V., Radulović, Ž., Milić, J., 2013b. Investigation of adsorption and release of diclofenac sodium by modified zeolites composites. Appl. Clay Sci. 83–84, 322–326. https://doi.org/10.1016/j.clay.2013.08.011

Krajišnik, D., Daković, A., Milić, J., Marković, M., 2018. Zeolites as potential drug carriers, in: Modified Clay and Zeolite Nanocomposite Materials: Environmental and Pharmaceutical Applications. pp. 27–55. https://doi.org/10.1016/B978-0-12-814617-0.00002-5

Krajišnik, D., Daković, A., Milojević, M., Malenović, A., Kragović, M., Bogdanović, D.B., Dondur, V., Milić, J., 2011. Properties of diclofenac sodium sorption onto natural zeolite modified with cetylpyridinium chloride. Colloids Surfaces B Biointerfaces 83, 165–172. https://doi.org/10.1016/j.colsurfb.2010.11.024

Kyzas, G.Z., Fu, J., Lazaridis, N.K., Bikiaris, D.N., Matis, K.A., 2015. New approaches on the removal of pharmaceuticals from wastewaters with adsorbent materials. J. Mol. Liq. 209, 87–93. https://doi.org/10.1016/j.molliq.2015.05.025

Landry, K.A., Sun, P., Huang, C.H., Boyer, T.H., 2015. Ion-exchange selectivity of diclofenac, ibuprofen, ketoprofen, and naproxen in ureolyzed human urine. Water Res. 68, 510–521. https://doi.org/10.1016/j.watres.2014.09.056

Langella, A., Pansini, M., Cappelletti, P., De Gennaro, B., De' Gennaro, M., Colella, C., 2000.

NH4+, Cu2+, Zn2+, Cd2+ and Pb2+ exchange for Na + in a sedimentary clinoptilolite, North Sardinia, Italy. Microporous Mesoporous Mater. 37, 337–343. https://doi.org/10.1016/S1387-1811(99)00276-0

Langella, A., Pansini, M., Cerri, G., Cappelletti, P., De'Gennaro, M., 2003. Thermal behavior of natural and cation-exchanged clinoptilolite from Sardinia (Italy). Clays Clay Miner. 51, 625–633. https://doi.org/10.1346/CCMN.2003.0510605

Lemić, J., Tomašević-Čanović, M., Adamović, M., Kovačević, D., Milićević, S., 2007. Competitive adsorption of polycyclic aromatic hydrocarbons on organo-zeolites. Microporous Mesoporous Mater. 105, 317–323. https://doi.org/10.1016/j.micromeso.2007.04.014

Lewis, M.A., Wee, V.T., 1983. Aquatic safety assessment for cationic surfactants. Environ. Toxicol. Chem. 2, 105–118. https://doi.org/10.1002/etc.5620020112

Li, J., Zhan, Y., Lin, J., Jiang, A., Xi, W., 2014. Removal of bisphenol A from aqueous solution using cetylpyridinium bromide (CPB)-modified natural zeolites as adsorbents. Environ. Earth Sci. 72, 3969–3980. https://doi.org/10.1007/s12665-014-3286-6

Li, Z., Anghel, I., Bowman, R.S., 1998a. Sorption of oxyanions by surfactant-modified zeolite. J. Dispers. Sci. Technol. 19, 843–857. https://doi.org/10.1080/01932699808913218

Li, Z., Bowman, R.S., 2001. Regeneration of surfactant-modified zeolite after saturation with chromate and perchloroethylene. Water Res. 35, 322–326. https://doi.org/10.1016/S0043-1354(00)00258-X

Li, Z., Bowman, R.S., 1998. Sorption of perchloroethylene by surfactant-modified zeolite as controlled by surfactant loading. Environ. Sci. Technol. 32, 2278–2282. https://doi.org/10.1021/es971118r

Li, Z., Bowman, R.S., 1997. Counterion effects on the sorption of cationic surfactant and chromate on natural clinoptilolite. Environ. Sci. Technol. 31, 2407–2412. https://doi.org/10.1021/es9610693

Li, Z., Burt, T., Bowman, R.S., 2000. Sorption of ionizable organic solutes by surfactant-modified zeolite. Environ. Sci. Technol. 34, 3756–3760. https://doi.org/10.1021/es990743o

Li, Z., Jones, H.K., Bowman, R.S., Helferich, R., 1999. Enhanced reduction of chromate and PCE by pelletized surfactant-modified zeolite/zerovalent iron. Environ. Sci. Technol. 33, 4326–4330. https://doi.org/10.1021/es990334s

Li, Z., Roy, S.J., Zou, Y., Bowman, R.S., 1998b. Long-term chemical and biological stability of surfactant-modified zeolite. Environ. Sci. Technol. 32, 2628–2632. https://doi.org/10.1021/es970841e

Liu, X., Mäki-Arvela, P., Aho, A., Vajglova, Z., Gun'ko, V.M., Heinmaa, I., Kumar, N., Er nen, K., Salmi, T., Murzin, D.Y., 2018. Zeta potential of beta zeolites: Influence of structure, acidity, pH, temperature and concentration. Molecules 23, 1–14. https://doi.org/10.3390/molecules23040946

Lolić, A., Paíga, P., Santos, L.H.M.L.M., Ramos, S., Correia, M., Delerue-Matos, C., 2015. Assessment of non-steroidal anti-inflammatory and analgesic pharmaceuticals in seawaters of North of Portugal: Occurrence and environmental risk. Sci. Total Environ. 508, 240–250. https://doi.org/10.1016/j.scitotenv.2014.11.097

Lonappan, L., Brar, S.K., Das, R.K., Verma, M., Surampalli, R.Y., 2016. Diclofenac and its transformation products: Environmental occurrence and toxicity - A review. Environ. Int. 96, 127–138. https://doi.org/10.1016/j.envint.2016.09.014

Loos, R., Carvalho, R., António, D.C., Comero, S., Locoro, G., Tavazzi, S., Paracchini, B., Ghiani, M., Lettieri, T., Blaha, L., Jarosova, B., Voorspoels, S., Servaes, K., Haglund, P., Fick, J., Lindberg, R.H., Schwesig, D., Gawlik, B.M., 2013. EU-wide monitoring survey on emerging polar organic contaminants in wastewater treatment plant effluents. Water Res. 47, 6475–6487. https://doi.org/10.1016/j.watres.2013.08.024

Loos, R., Gawlik, B.M., Locoro, G., Rimaviciute, E., Contini, S., Bidoglio, G., 2009. EU-wide survey of polar organic persistent pollutants in European river waters. Environ. Pollut. 157, 561–568. https://doi.org/10.1016/j.envpol.2008.09.020

Loos, R., Locoro, G., Comero, S., Contini, S., Schwesig, D., Werres, F., Balsaa, P., Gans, O., Weiss, S., Blaha, L., Bolchi, M., Gawlik, B.M., 2010. Pan-European survey on the occurrence of selected polar organic persistent pollutants in ground water. Water Res. 44, 4115–4126. https://doi.org/10.1016/j.watres.2010.05.032

Margot, J., Kienle, C., Magnet, A., Weil, M., Rossi, L., de Alencastro, L.F., Abegglen, C., Thonney, D., Chèvre, N., Schärer, M., Barry, D.A., 2013. Treatment of micropollutants in municipal wastewater: Ozone or powdered activated carbon? Sci. Total Environ. 461–462, 480–498. https://doi.org/10.1016/j.scitotenv.2013.05.034

Marković, M., Daković, A., Krajišnik, D., Kragović, M., Milić, J., Langella, A., de Gennaro, B., Cappelletti, P., Mercurio, M., 2016. Evaluation of the surfactant/phillipsite composites as carriers for diclofenac sodium. J. Mol. Liq. 222, 711–716. https://doi.org/10.1016/j.molliq.2016.07.127

Marković, M., Daković, A., Rottinghaus, G.E., Kragović, M., Petković, A., Krajišnik, D., Milić, J., Mercurio, M., de Gennaro, B., 2017a. Adsorption of the mycotoxin zearalenone by clinoptilolite and phillipsite zeolites treated with cetylpyridinium surfactant. Colloids Surfaces B Biointerfaces 151, 324–332. https://doi.org/10.1016/j.colsurfb.2016.12.033

Marković, M., Daković, A., Rottinghaus, G.E., Petković, A., Kragović, M., Krajišnik, D., Milić, J., 2017b. Ochratoxin A and zearalenone adsorption by the natural zeolite treated with benzalkonium chloride. Colloids Surfaces A Physicochem. Eng. Asp. 529, 7–17. https://doi.org/10.1016/j.colsurfa.2017.05.054

Mercurio, M., Izzo, F., Langella, A., Grifa, C., Germinario, C., Daković, A., Aprea, P., Pasquino, R., Cappelletti, P., Graziano, F.S., De Gennaro, B., 2018. Surface-modified phillipsite-rich tuff from the Campania region (southern Italy) as a promising drug carrier: An ibuprofen sodium salt trial. Am. Mineral. 103, 700–710. https://doi.org/10.2138/am-2018-6328

Ming, D.W., Dixon, J.B., 1987. Quantitative determination of clinoptilolite in soils by a cation-exchange capacity method. Clays Clay Miner. 35, 463–468. https://doi.org/10.1346/CCMN.1987.0350607

Mirzaei, N., Hadi, M., Gholami, M., Fard, R.F., Aminabad, M.S., 2016. Sorption of acid dye by surfactant modificated natural zeolites. J. Taiwan Inst. Chem. Eng. 59, 186–194. https://doi.org/10.1016/j.jtice.2015.07.010

Misaelides, P., 2011. Application of natural zeolites in environmental remediation: A short review. Microporous Mesoporous Mater. 144, 15–18.

https://doi.org/10.1016/j.micromeso.2011.03.024

Mumpton, F.A., 1977. Natural zeolites, in: In Mineralogy and Geology of Natural Zeolites. pp. 1–17.

Nouryon, 2020. Arquad 2HT-75, Product Data Sheet.

Oaks, J.L., Meteyer, C.U., Rideout, B.A., Shivaprasad, H.L., Gilbert, M., Virani, M., Watson, R.T., Khan, A.A., 2004. Diagnostic investigation of vulture mortality: the anti-inflammatory drug diclofenac is associated with visceral gout. Raptor worldwide. Proc. 6th world Conf. birds prey owls 241–3.

Okumura, O., Ohbu, K., Yokoi, K., Yamada, K., Saika, D., 1983. A study on the adsorption of dialkyldimethyl ammonium chloride. J. Am. Oil Chem. Soc. 60, 1699–1704. https://doi.org/10.1007/BF02662437

Onyango, M.S., Kittinya, J., Hadebe, N., Ojijo, V.O., Ochieng, A., 2011. Sorpcija melanoidina na površinski modifikovanom zeolitu. Chem. Ind. Chem. Eng. Q. 17, 385–395. https://doi.org/10.2298/CICEQ110125025O

Pabalan, R.T., Bertetti, F.P., 2001. Cation-exchange properties of natural zeolites, in: Reviews in Mineralogy and Geochemistry. pp. 453–517. https://doi.org/10.2138/rmg.2001.45.14

Passaglia, E., Sheppard, R.A., 2001. The crystal chemistry of zeolites, in: Reviews in Mineralogy and Geochemistry. pp. 68–116. https://doi.org/10.2138/rmg.2001.45.2

Pavelić, K., Hadžija, M., 2003. Handbook of zeolite science and technology. pp. 1141–1172.

Pavelić, K., Hadžija, M., Bedrica, L., Pavelić, J., Crossed D signikić, I., Katić, M., Kralj, M., Bosnar, M.H., Kapitanović, S., Poljak-Blaži, M., Križanac, Š., Stojković, R., Jurin, M., Subotić, B., Čolić, M., 2000. Natural zeolite clinoptilolite: New adjuvant in anticancer therapy. J. Mol. Med. 78, 708–720. https://doi.org/10.1007/s001090000176

Payra, P., Dutta, P., 2003. Zeolites: A Primer, in: Handbook of Zeolite Science and Technology, 2(2). pp. 1–19.

Pérez, L., Pinazo, A., Pons, R., Infante, M., 2014. Gemini surfactants from natural amino acids. Adv. Colloid Interface Sci. 205, 134–155. https://doi.org/10.1016/j.cis.2013.10.020

Petrovic, M., Eljarrat, E., Lopez De Alda, M.J., Barceló, D., 2004. Endocrine disrupting compounds and other emerging contaminants in the environment: A survey on new monitoring strategies and occurrence data. Anal. Bioanal. Chem. 378, 549–562. https://doi.org/10.1007/s00216-003-2184-7

Plazinski, W., Rudzinski, W., Plazinska, A., 2009. Theoretical models of sorption kinetics including a surface reaction mechanism: A review. Adv. Colloid Interface Sci. 152, 2–13. https://doi.org/10.1016/j.cis.2009.07.009

Pletnev, M.Y., 2001. Chemistry of Surfactantants, in: Studies in Interface Science. pp. 1–97.

Płuciennik-Koropczuk, E., 2015. Non-Steroid Anti-Infflamatory Drugs in Municipal Wastewater and Surface Waters/ Niesteroidowe Leki Przeciwzaplane W Ściekach Mieskich I Wodach Powierzchniowych. Civ. Environ. Eng. Reports 14, 63–74. https://doi.org/10.1515/ceer-2014-0026

Rathi, B.S., Kumar, P.S., Show, P.L., 2020. A review on effective removal of emerging contaminants from aquatic systems: Current trends and scope for further research. J.

Hazard. Mater. 124413. https://doi.org/10.1016/j.jhazmat.2020.124413

Reeve, P.J., Fallowfield, H.J., 2018. Natural and surfactant modified zeolites: A review of their applications for water remediation with a focus on surfactant desorption and toxicity towards microorganisms. J. Environ. Manage. 205, 253–261. https://doi.org/10.1016/j.jenvman.2017.09.077

Reeve, P.J., Fallowfield, H.J., 2017. The toxicity of cationic surfactant HDTMA-Br, desorbed from surfactant modified zeolite, towards faecal indicator and environmental microorganisms. J. Hazard. Mater. 339, 208–215. https://doi.org/10.1016/j.jhazmat.2017.06.022

Ricciotti, E., Fitzgerald, G.A., 2011. Prostaglandins and inflammation. Arterioscler. Thromb. Vasc. Biol. 31, 986–1000. https://doi.org/10.1161/ATVBAHA.110.207449

Rivera-Utrilla, J., Sánchez-Polo, M., Ferro-García, M.Á., Prados-Joya, G., Ocampo-Pérez, R., 2013. Pharmaceuticals as emerging contaminants and their removal from water. A review. Chemosphere 93, 1268–1287. https://doi.org/10.1016/j.chemosphere.2013.07.059

Rowe, R.C., Sheskey, P.J., Weller, P.J., 2006. Handbook of pharmaceutical excipients, Sixth. ed. Pharmaceutical press, London.

Sánchez-Borges, M., Caballero-Fonseca, F., Capriles-Hulett, A., González-Aveledo, L., 2010. Hypersensitivity reactions to nonsteroidal anti-inflammatory drugs: An update. Pharmaceuticals 3, 10–18. https://doi.org/10.3390/ph3010010

Sarioglu, M., 2005. Removal of ammonium from municipal wastewater using natural Turkish (Dogantepe) zeolite. Sep. Purif. Technol. 41, 1–11. https://doi.org/10.1016/j.seppur.2004.03.008

Sarkar, B., Xi, Y., Megharaj, M., Krishnamurti, G.S.R., Rajarathnam, D., Naidu, R., 2010. Remediation of hexavalent chromium through adsorption by bentonite based Arquad®2HT-75 organoclays. J. Hazard. Mater. 183, 87–97. https://doi.org/10.1016/j.jhazmat.2010.06.110

Sauvé, S., Desrosiers, M., 2014. A review of what is an emerging contaminant. Chem. Cent. J. 8, 1–7. https://doi.org/10.1186/1752-153X-8-15

Schulze-Makuch, D., Pillai, S.D., Guan, H., Bowman, R., Couroux, E., Hielscher, F., Totten, J., Espinosa, I.Y., Kretzschmar, T., 2002. Surfactant-modified zeolite can protect drinking water wells from viruses and bacteria. Eos (Washington. DC). 83. https://doi.org/10.1029/2002EO000128

Serri, C., De Gennaro, B., Catalanotti, L., Cappelletti, P., Langella, A., Mercurio, M., Mayol, L., Biondi, M., 2016. Surfactant-modified phillipsite and chabazite as novel excipients for pharmaceutical applications? Microporous Mesoporous Mater. 224, 143–148. https://doi.org/10.1016/j.micromeso.2015.11.023

Serri, C., de Gennaro, B., Quagliariello, V., Iaffaioli, R.V., De Rosa, G., Catalanotti, L., Biondi, M., Mayol, L., 2017. Surface modified zeolite-based granulates for the sustained release of diclofenac sodium. Eur. J. Pharm. Sci. 99, 202–208. https://doi.org/10.1016/j.ejps.2016.12.019

Sigma-Aldrich ARQ SDS, 2019. Arquad® 2HT-75 Safety Data Sheet. Mater. Saf. Data Sheet.

Sigma-Aldrich CPyCl SDS, 2019. Cetylpyridinum chloride.

Singh, K.P., Singh, A.K., Singh, U.V., Verma, P., 2012. Optimizing removal of ibuprofen from water by magnetic nanocomposite using Box-Behnken design. Environ. Sci. Pollut. Res. 19, 724–738. https://doi.org/10.1007/s11356-011-0611-4

Smiljanić, D., de Gennaro, B., Izzo, F., Langella, A., Daković, A., Germinario, C., Rottinghaus, G.E., Spasojević, M., Mercurio, M., 2020. Removal of emerging contaminants from water by zeolite-rich composites: A first approach aiming at diclofenac and ketoprofen. Microporous Mesoporous Mater. 298. https://doi.org/10.1016/j.micromeso.2020.110057

Smiljanić, D., Gennaro, B. De, Galzerano, B., Germinario, C., Izzo, F., Rottinghaus, G.E., Langella, A., 2021. Accepted, currently in the publising process: Removal of Non-Steroidal Anti-inflammatory drugs from water by zeolite-rich composites : the interference of inorganic anions on the ibuprofen and naproxen adsorption. J. Environ. Manage.

Smiljanić, D., Mercurio, M., Izzo, F., de Gennaro, B., Daković, A., Germinario, C., Grifa, C. and, Langella, A., 2018. Book of Abstracts, in: ZEOLITE 2018 - 10th International Conference on the Occurrence, Properties and Utilization of Natural Zeolites. pp. 185–186. https://doi.org/10.23919/eumc.2018.8541769

Smith, J. V., 1984. Definition of a zeolite. Zeolites 4, 309–310. https://doi.org/10.1016/0144-2449(84)90003-4

Sousa, J.C.G., Ribeiro, A.R., Barbosa, M.O., Pereira, M.F.R., Silva, A.M.T., 2018. A review on environmental monitoring of water organic pollutants identified by EU guidelines. J. Hazard. Mater. 344, 146–162. https://doi.org/10.1016/j.jhazmat.2017.09.058

Spiess, A.-N., Neumeyer, N., 2010. An evaluation of R2 as an inadequate measure for nonlinear models in pharmacological and biochemical research: a Monte Carlo approach. BMC Pharmacol. 10, 6. https://doi.org/https://doi.org/10.1186/1471-2210-10-6

Streit, A.F.M., Collazzo, G.C., Druzian, S.P., Verdi, R.S., Foletto, E.L., Oliveira, L.F.S., Dotto, G.L., 2021. Adsorption of ibuprofen, ketoprofen, and paracetamol onto activated carbon prepared from effluent treatment plant sludge of the beverage industry. Chemosphere 262. https://doi.org/10.1016/j.chemosphere.2020.128322

Sullivan, E.J., Carey, J.W., Bowman, R.S., 1998a. Thermodynamics of cationic surfactant sorption onto natural clinoptilolite. J. Colloid Interface Sci. 206, 369–380. https://doi.org/10.1006/jcis.1998.5764

Sullivan, E.J., Hunter, D.B., Bowman, R.S., 1998b. Fourier transform Raman spectroscopy of sorbed HDTMA and the mechanism of chromate sorption to surfactant-modified clinoptilolite. Environ. Sci. Technol. 32, 1948–1955. https://doi.org/10.1021/es9708981

Sullivan, E.J., Hunter, D.B., Bowman, R.S., 1997. Topological and thermal properties of surfactant-modified clinoptilolite studied by tapping-mode™ atomic force microscopy and high-resolution thermogravimetric analysis. Clays Clay Miner. 45, 42–53. https://doi.org/10.1346/CCMN.1997.0450105

Sun, K., Shi, Y., Wang, X., Li, Z., 2017. Sorption and retention of diclofenac on zeolite in the presence of cationic surfactant. J. Hazard. Mater. 323, 584–592. https://doi.org/10.1016/j.jhazmat.2016.08.026

Tehrani Bagha, A.R., Bahrami, H., Movassagh, B., Arami, M., Menger, F.M., 2007. Interactions of gemini cationic surfactants with anionic azo dyes and their inhibited effects

on dyeability of cotton fabric. Dye. Pigment. 72, 331–338. https://doi.org/10.1016/j.dyepig.2005.09.011

Terzić, S., Senta, I., Ahel, M., Gros, M., Petrović, M., Barcelo, D., Müller, J., Knepper, T., Martí, I., Ventura, F., Jovančić, P., Jabučar, D., 2008. Occurrence and fate of emerging wastewater contaminants in Western Balkan Region. Sci. Total Environ. 399, 66–77. https://doi.org/10.1016/j.scitotenv.2008.03.003

Tiedeken, E.J., Tahar, A., McHugh, B., Rowan, N.J., 2017. Monitoring, sources, receptors, and control measures for three European Union watch list substances of emerging concern in receiving waters – A 20 year systematic review. Sci. Total Environ. 574, 1140–1163. https://doi.org/10.1016/j.scitotenv.2016.09.084

Tomašević-Čanović, M., Daković, A., Rottinghaus, G., Matijašević, S., Duričić, M., 2003. Surfactant modified zeolites-new efficient adsorbents for mycotoxins. Microporous Mesoporous Mater. 61, 173–180. https://doi.org/10.1016/S1387-1811(03)00365-2

Tomul, F., Arslan, Y., Kabak, B., Trak, D., Kendüzler, E., Lima, E.C., Tran, H.N., 2020. Peanut shells-derived biochars prepared from different carbonization processes: Comparison of characterization and mechanism of naproxen adsorption in water. Sci. Total Environ. 726. https://doi.org/10.1016/j.scitotenv.2020.137828

Torabian, A., Kazemian, H., Seifi, L., Bidhendi, G.N., Azimi, A.A., Ghadiri, S.K., 2010. Removal of petroleum aromatic hydrocarbons by surfactant-modified natural zeolite: The effect of surfactant. Clean - Soil, Air, Water 38, 77–83. https://doi.org/10.1002/clen.200900157

Tosun, I., 2012. Ammonium removal from aqueous solutions by clinoptilolite: Determination of isotherm and thermodynamic parameters and comparison of kinetics by the double exponential model and conventional kinetic models. Int. J. Environ. Res. Public Health 9, 970–984. https://doi.org/10.3390/ijerph9030970

Turk Sekulic, M., Boskovic, N., Slavkovic, A., Garunovic, J., Kolakovic, S., Pap, S., 2019. Surface functionalized adsorbent for emerging pharmaceutical removal: Adsorption performance and mechanisms. Process Saf. Environ. Prot. 125, 50–63. https://doi.org/10.1016/j.psep.2019.03.007

Vieno, N., Sillanpää, M., 2014. Fate of diclofenac in municipal wastewater treatment plant - A review. Environ. Int. 69, 28–39. https://doi.org/10.1016/j.envint.2014.03.021

Wang, S., Peng, Y., 2010. Natural zeolites as effective adsorbents in water and wastewater treatment. Chem. Eng. J. 156, 11–24. https://doi.org/10.1016/j.cej.2009.10.029

Wongrakpanich, S., Wongrakpanich, A., Melhado, K., Rangaswami, J., 2018. A comprehensive review of non-steroidal anti-inflammatory drug use in the elderly. Aging Dis. 9, 143–150. https://doi.org/10.14336/AD.2017.0306

Yang, Y., Ok, Y.S., Kim, K.H., Kwon, E.E., Tsang, Y.F., 2017. Occurrences and removal of pharmaceuticals and personal care products (PPCPs) in drinking water and water/sewage treatment plants: A review. Sci. Total Environ. 596–597, 303–320. https://doi.org/10.1016/j.scitotenv.2017.04.102

Zarghi and Arfaei, 2001. Selective COX-2 inhibitors. Iran. J. Pharm. Res. 10, 655–683. https://doi.org/10.1097/00000446-200104000-00024

Zhan, Y., Lin, J., Qiu, Y., Gao, N., Zhu, Z., 2011. Adsorption of humic acid from aqueous

solution on bilayer hexadecyltrimethyl ammonium bromide-modified zeolite. Front. Environ. Sci. Eng. China 5, 65–75. https://doi.org/10.1007/s11783-010-0277-z

Zhao, H.W., Viraraghavan, T., 2004. Analysis of the performance of an anaerobic digestion system at the Regina wastewater treatment plant. Bioresour. Technol. 95, 301–307. https://doi.org/10.1016/j.biortech.2004.02.023

Zhu, L., Chen, B., Shen, X., 2000. Sorption of phenol, p-nitrophenol, and aniline to dual-cation organobentonites from water. Environ. Sci. Technol. 34, 468–475. https://doi.org/10.1021/es990177x

Zhu, L., Ren, X., Yu, S., 1998. Use of cetyltrimethylammonium bromide-bentonite to remove organic contaminants of varying polar character from water. Environ. Sci. Technol. 32, 3374–3378. https://doi.org/10.1021/es980353m